Experimental status of two photon exchange effects

Michael Kohl <kohlm@jlab.org> *

Hampton University, Hampton, VA 23668
Jefferson Laboratory, Newport News, VA 23606

*Presently supported by DOE DE-SC0013941 and NSF PHY-1505934+1436680

Outline

- **Proton form factors in the context of one-photon exchange (OPE)**
- **The limit of OPE or:**
  - **What is G_E^p ?**
  - **What is the nature of lepton scattering?**
- **Two-photon exchange (TPE): New observables**
- **Current and future experiments to probe TPE**
  ➔ OLYMPUS & more

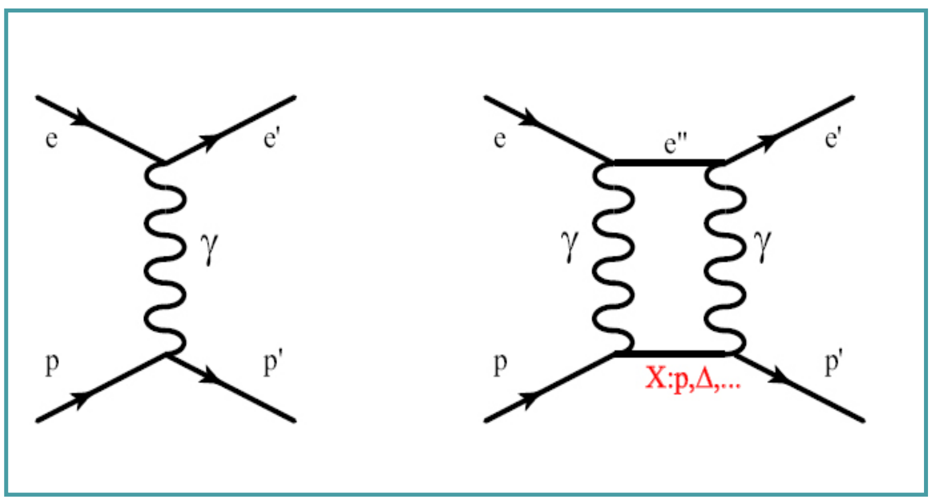

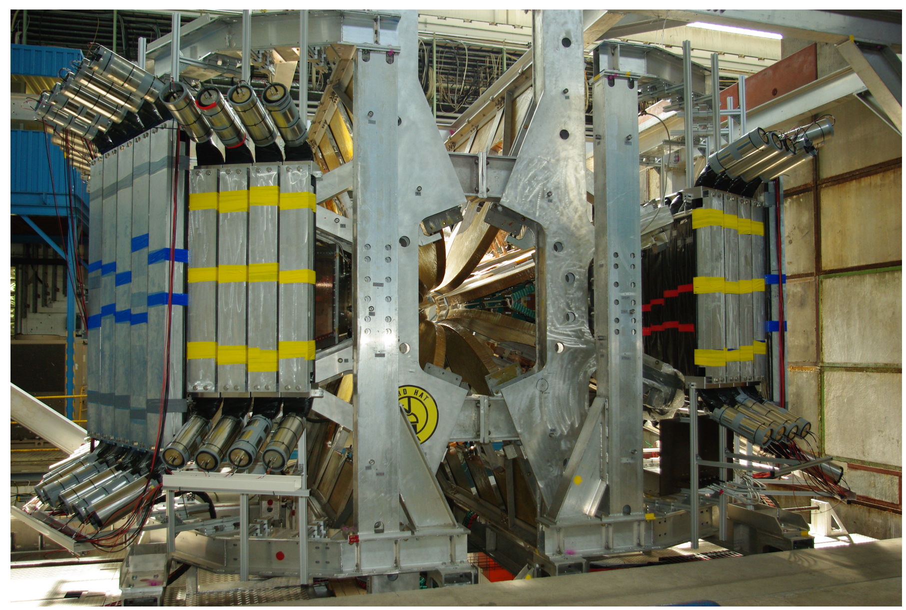

OLYMPUS @ DESY

Nucleon elastic form factors …

- Fundamental quantities
- Defined in context of single-photon exchange

- Describe internal structure of the nucleons
- Related to spatial distribution of charge and magnetism

- Rigorous tests of nucleon models
- Determined by quark structure of the nucleon
- Role of orbital angular momentum and diquark correlation
- Ultimately calculable by Lattice-QCD
- Input to nuclear structure and parity violation experiments

G. Miller,
PRC68, 022201 (2003)

50 years of ever increasing activity

- Considerable progress in experiment and theory over last two decades
- New techniques / polarization experiments
- Unexpected results

Proton form factor and TPE experiments

Recoil polarization and polarized target (Jlab)

E04-108 – high-Q^2 recoil polarization (Gep-III)	– published (2010)
E04-019 – ε dependence of recoil pol. (2-Gamma)	– published (2011)
E08-007 – part I: low-Q^2 recoil polarization	– published (2011)
E08-007 – part II: low-Q^2 polarized target	– analysis in progress
E07-003 – high-Q^2 polarized target (SANE)	– to be published
E12-07-109 – high Q^2 recoil pol. (GEp-SBS)	– proposed

Unpolarized cross sections (Jlab)

E12-07-108 – high-Q^2 unpolarized (GMp)	– running
E05-017 – high-Q^2 Rosenbluth (Super-Rosen)	– analysis in progress

Positron-electron comparisons

Novosibirsk/VEPP-3	– published (2015)
CLAS/Jlab	– published (2015)
OLYMPUS/DESY	– analysis in progress

Proton radius measurements

PSI / (muonic hydrogen Lamb shift, HFS)	– published (2010, 2013)
MAMI / A1 (e-scattering)	– published (2010)
MAMI / A1 (ISR)	– analysis in progress
Jlab / PRad (e-scattering)	– running
PSI / MUSE ($e^{\pm}$, $\mu^{\pm}$ scattering)	– proposed

Hadronic structure and EM interaction

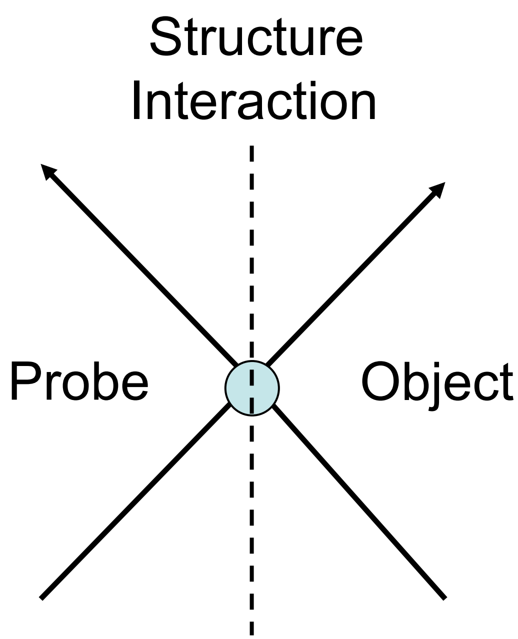

Factorization!

$$|\text{Form factor}|^2 = \frac{\sigma(\text{structured object})}{\sigma(\text{pointlike object})}$$

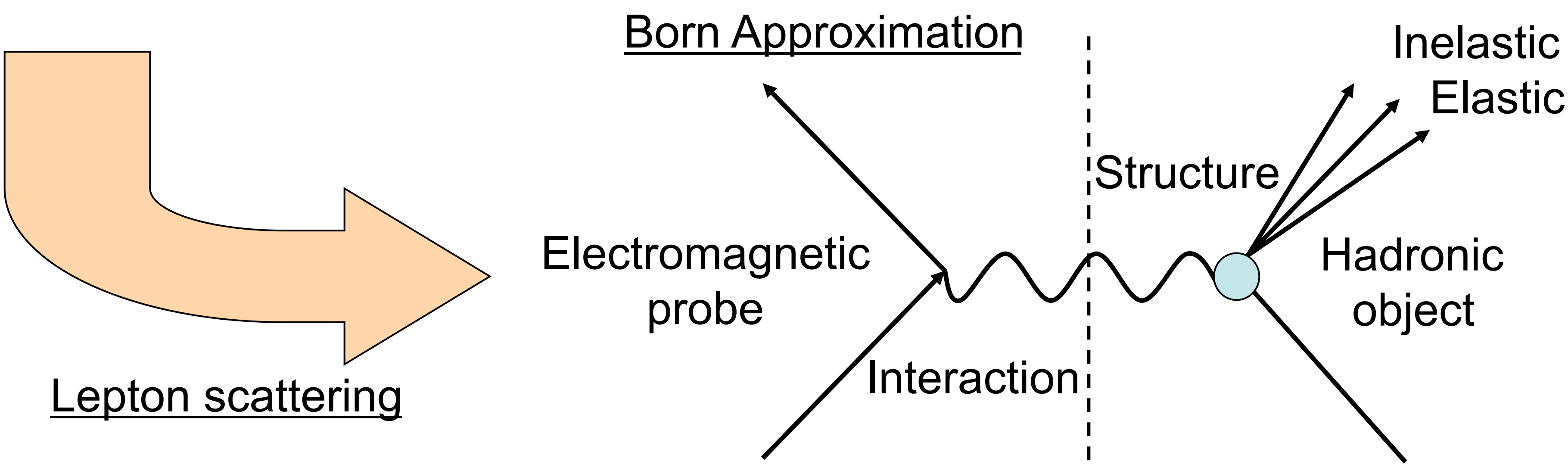

One-Photon Exchange Approximation

The beginnings

Robert Hofstadter
Nobel prize 1961

ep-elastic
finite size of the proton
$R_p \sim 0.8$ fm

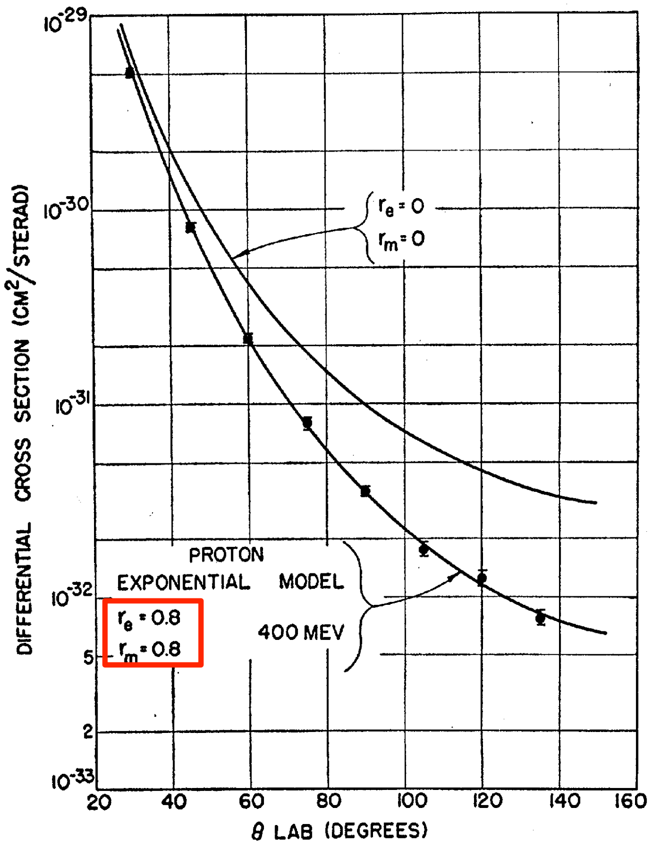

FIG. 26. Typical angular distribution for elastic scattering of 400-Mev electrons against protons. The solid line is a theoretical curve for a proton of finite extent. The model providing the theoretical curve is an exponential with rms radii = 0.80×10^{-13} cm.

R. Hofstadter, Rev. Mod. Phys. 56 (1956) 214

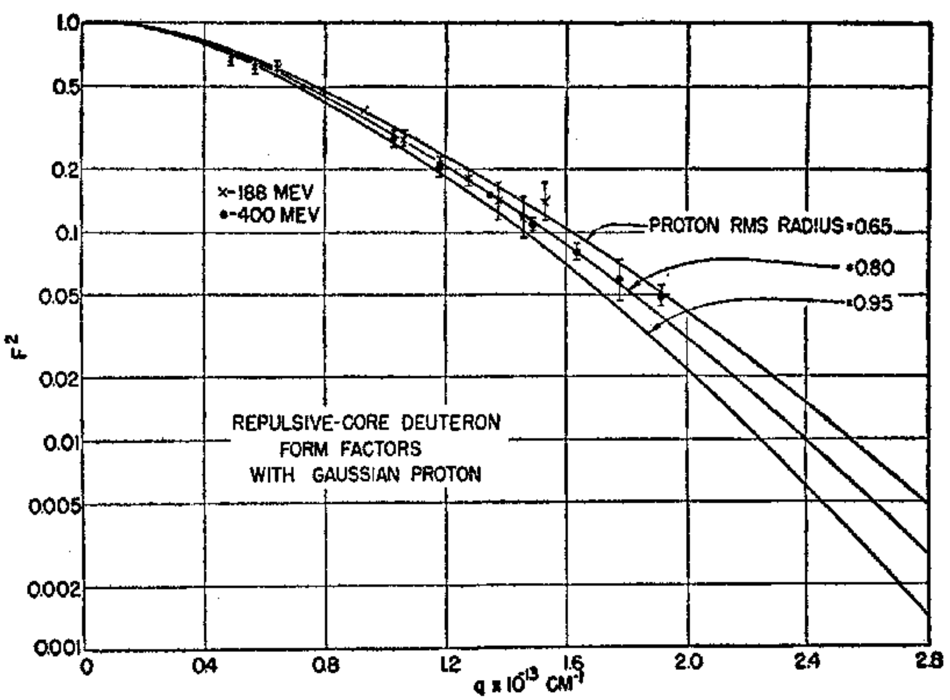

FIG. 31. Introduction of a finite proton core allows the experimental data to be fitted with conventional form factors (McIntyre).

ed-elastic
Finite size + nuclear structure

Form factors from Rosenbluth method

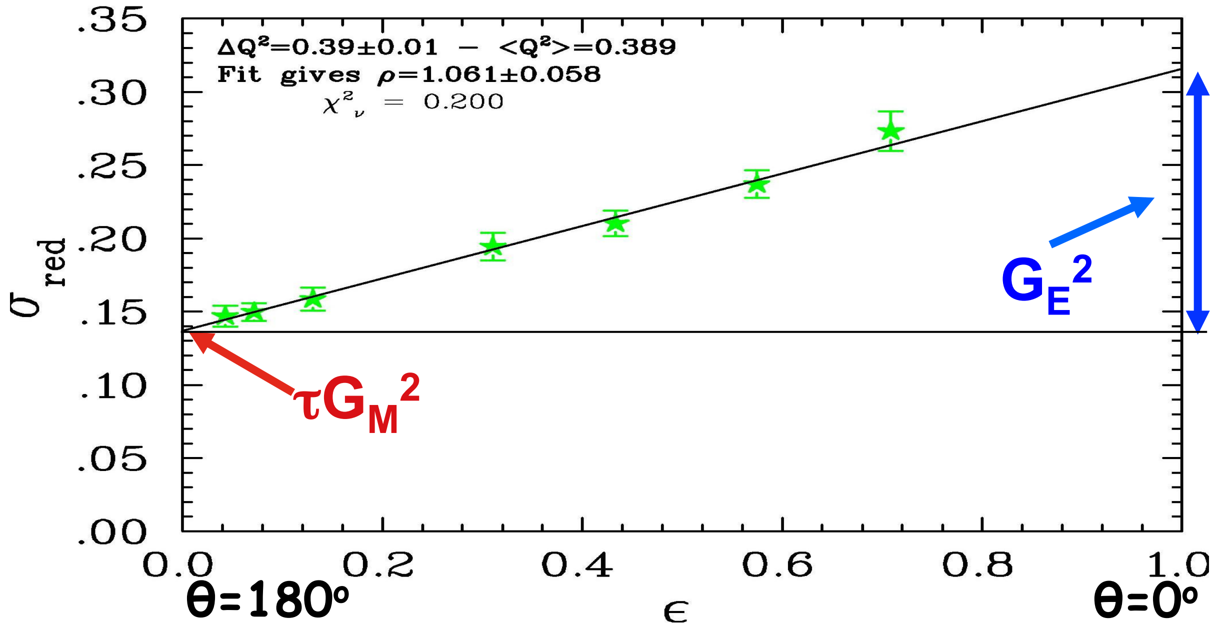

$\sigma_{red} = \varepsilon G_E^2 + \tau G_M^2$

➔Determine

$|G_E|$, $|G_M|$, $|G_E/G_M|$

- In One-photon exchange, form factors are related to radiatively corrected elastic electron-proton scattering cross section

$$\frac{d\sigma/d\Omega}{(d\sigma/d\Omega)_{Mott}} = S_0 = A(Q^2) + B(Q^2)\tan^2\frac{\theta}{2}$$

$$= \frac{G_E^2(Q^2) + \tau G_M^2(Q^2)}{1+\tau} + 2\tau G_M^2(Q^2)\tan^2\frac{\theta}{2}$$

$$= \frac{\epsilon\, G_E^2 + \tau G_M^2}{\epsilon\,(1+\tau)}, \qquad \epsilon = \left[1 + 2(1+\tau)\tan^2\frac{\theta}{2}\right]^{-1}$$

G^p_E and G^p_M from unpolarized data

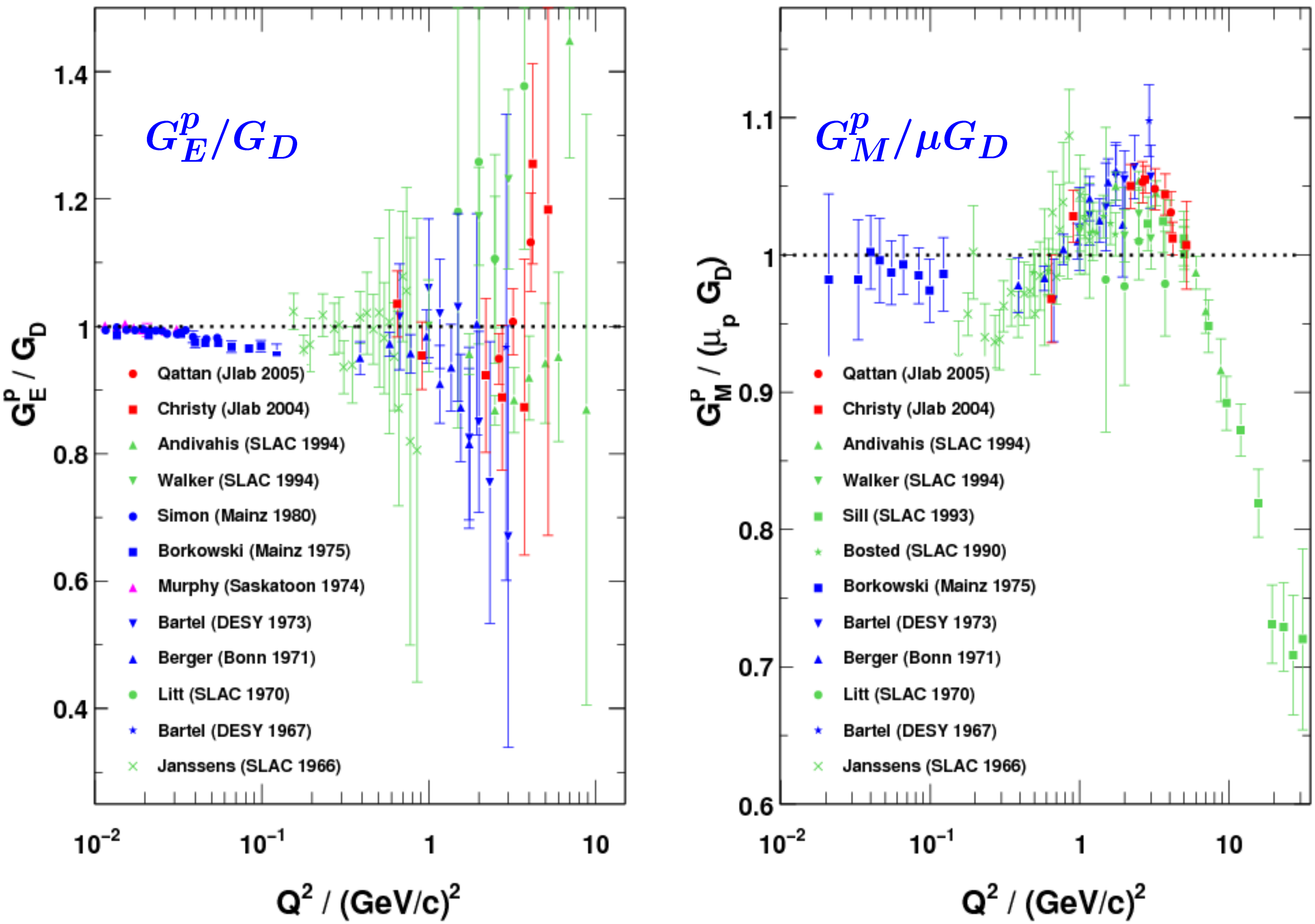

G^p_E and G^p_M from unpolarized data

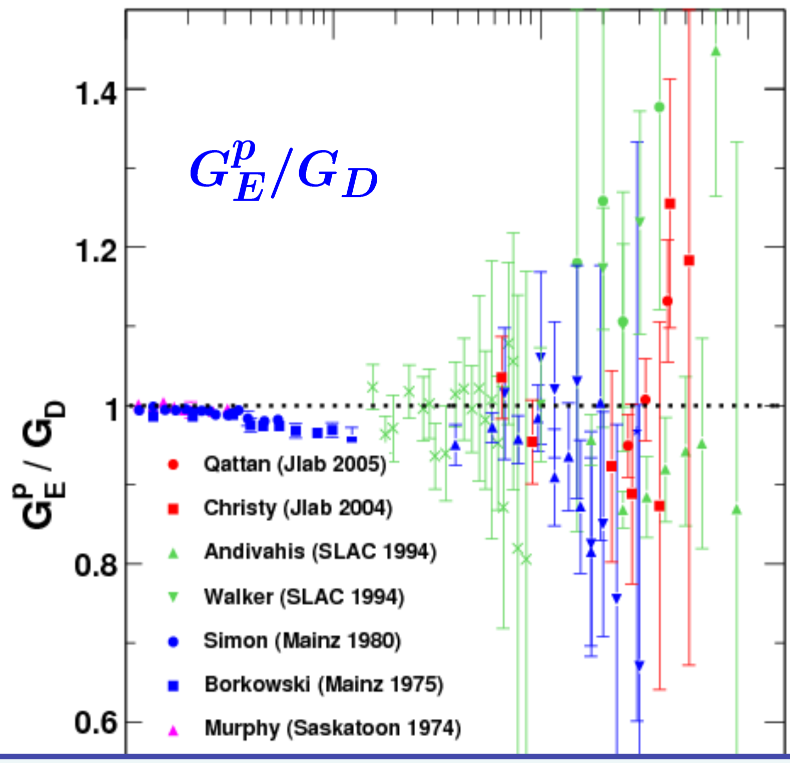

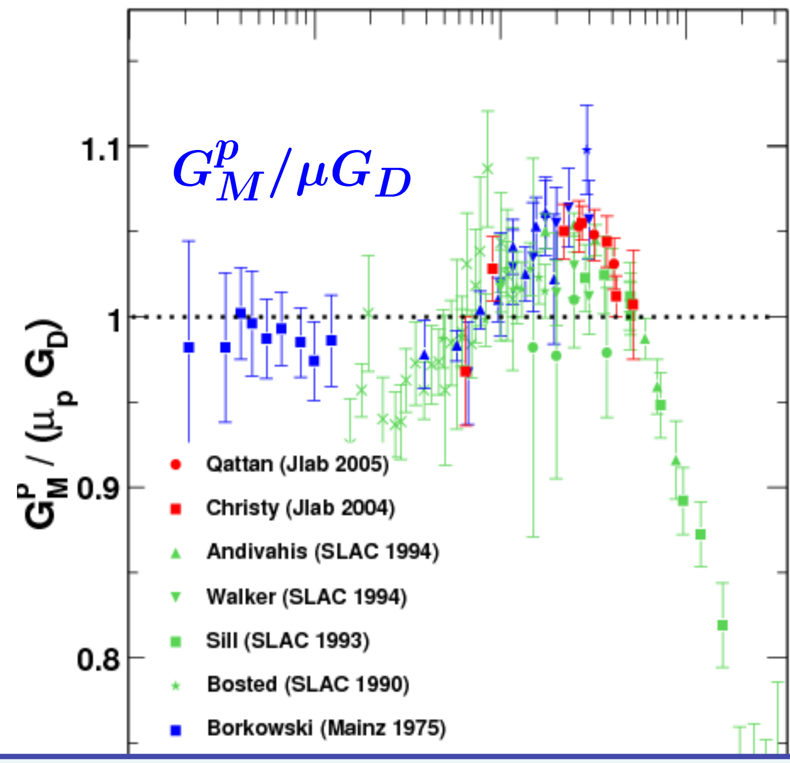

- $G(Q^2) \overset{\text{Fourier}}{\longleftrightarrow} \rho(r)$ **charge and magnetization density (Breit fr.)**
- **Dipole form factor** $G_D = \frac{1}{\left(1+\frac{Q^2}{0.71}\right)^2} \quad \longleftrightarrow \quad \rho_D(r) = \rho_0\, \mathrm{e}^{-\sqrt{0.71}r}$
- $G^p_E \approx G^p_M/\mu_p \approx G^n_M/\mu_n \approx G_D$ **within 10% for $Q^2 < 10\ (\mathrm{GeV}/c)^2$**

Nucleon form factors and polarization

- **Double polarization in elastic ep scattering:**
  Recoil polarization or (vector) polarized target

  $^1\mathrm{H}(\vec{e},e'\vec{p})$, $^1\vec{\mathrm{H}}(\vec{e},e'p)$

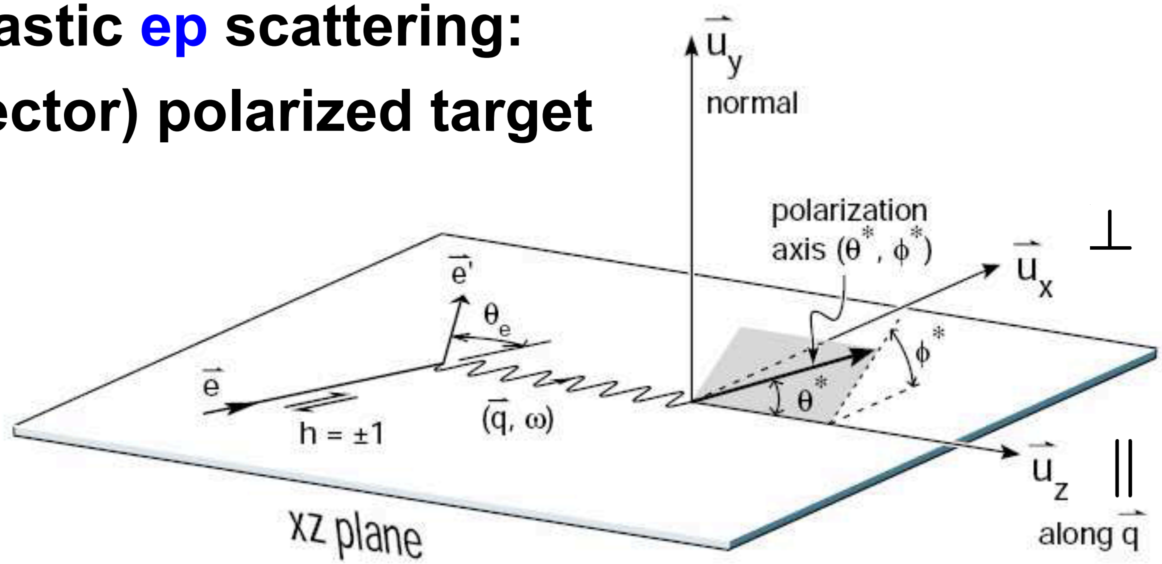

- **Polarized cross section**

$$\sigma = \sigma_0 \left(1 + P_e \vec{P}_p \cdot \vec{A}\right)$$

- **Double polarization observable = spin correlation**

$$-\sigma_0\, \vec{P}_p \cdot \vec{A} = \sqrt{2\tau\epsilon(1-\epsilon)}\, G_E G_M \sin\theta^* \cos\phi^* + \tau\sqrt{1-\epsilon^2}\, {G_M}^2 \cos\theta^*$$

- **Asymmetry ratio ("Super ratio")**

$$\frac{P_\perp}{P_\parallel} = \frac{A_\perp}{A_\parallel} \propto \frac{G_E}{G_M}$$

  independent of
  polarization or analyzing power

Dombey (1969)
Donnelly and Raskin (1986)

Polarized targets

UVA / "SLAC"-Target:
Dynamic Nuclear Polarization

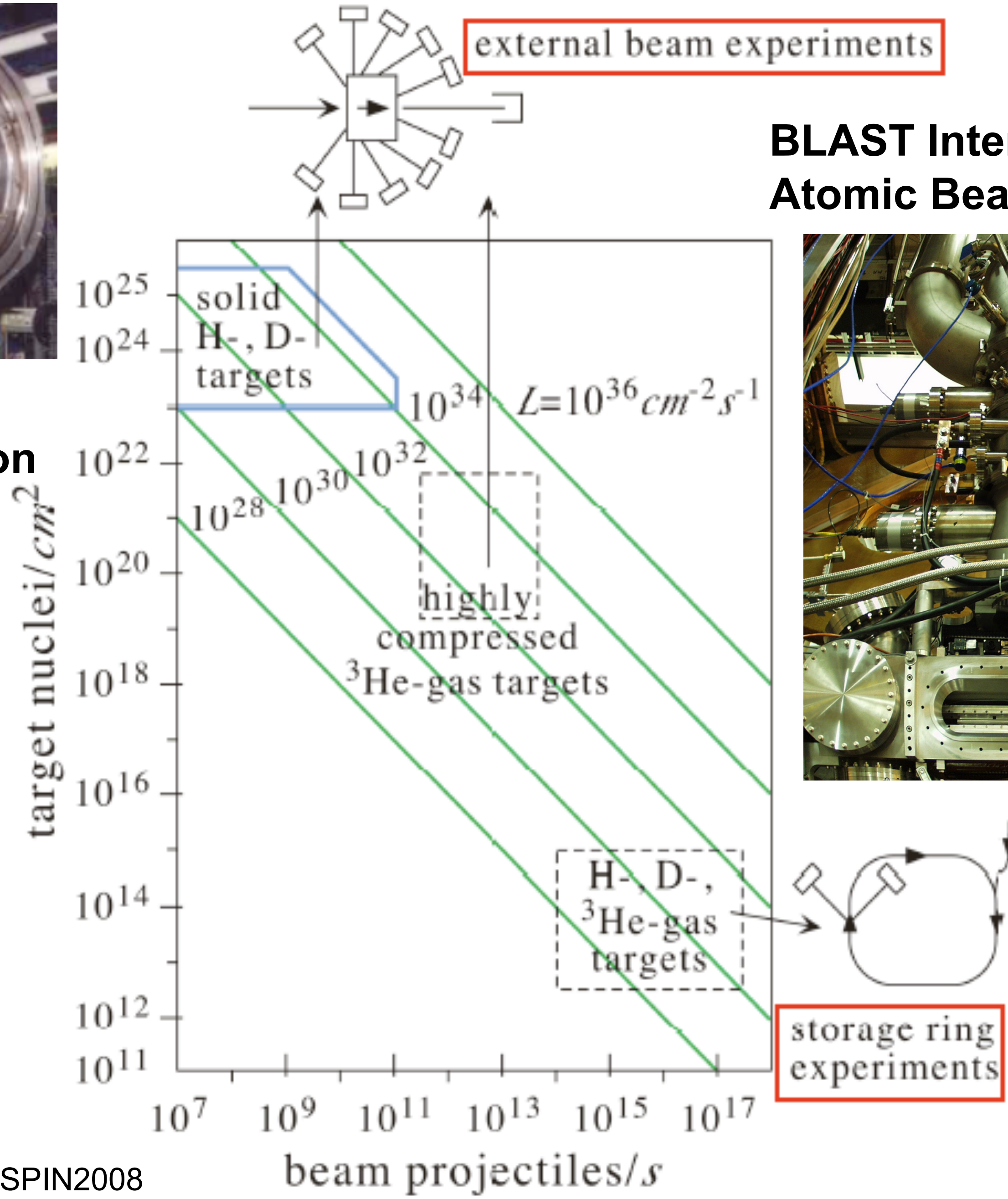

BLAST Internal Target:
Atomic Beam Source

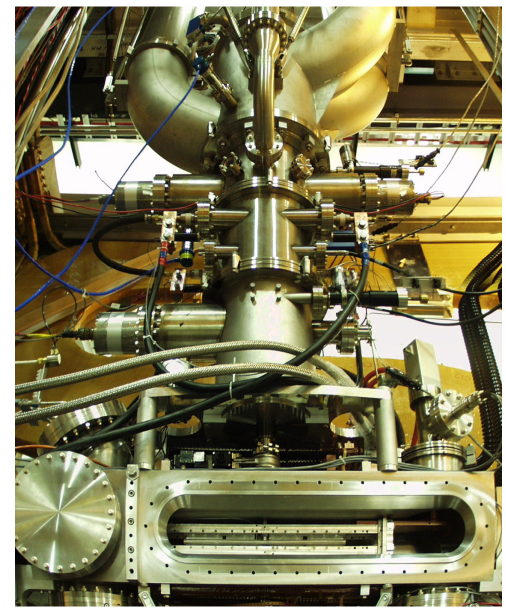

Limited luminosity for polarized hydrogen/ deuterium targets

Very precise at low to moderately high Q^2

from W. Meyer, SPIN2008

Recoil polarization technique

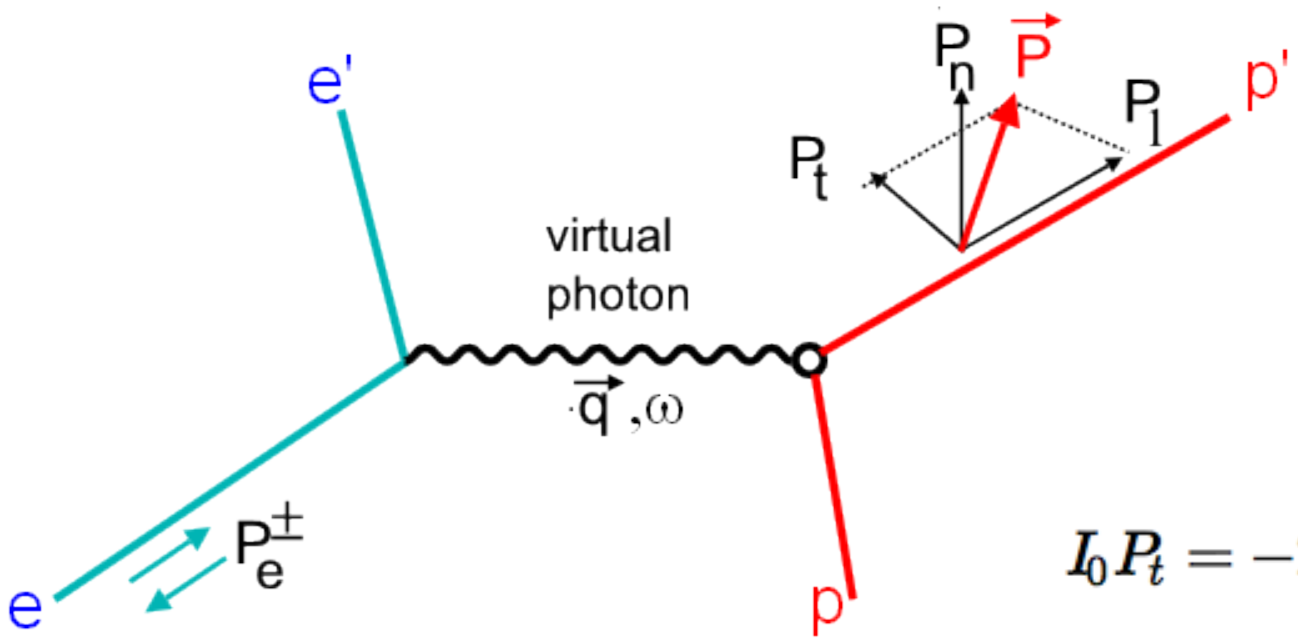

$$I_0 P_t = -2\sqrt{\tau(1+\tau)} G_E G_M \tan\frac{\theta_e}{2}$$

$$I_0 P_\ell = \frac{1}{M}(E_e + E_e')\sqrt{\tau(1+\tau)} G_M^2 \tan^2\frac{\theta_e}{2}$$

$$\frac{G_E}{G_M} = -\frac{P_t}{P_\ell}\frac{(E_e + E_e')}{2M_p}\tan\left(\frac{\theta_e}{2}\right)$$

$$I_0 \propto G_E^2 + \frac{\tau}{\epsilon} G_M^2$$

<u>Applicable to protons and neutrons</u>

Akhiezer and Rekalo (1968+1974)
Arnold, Carlson and Gross (1981)

Recoil polarization technique

- Pioneered at MIT-Bates
- Pursued in Halls A and C, and MAMI A1
- In preparation for Jlab @ 12 GeV

V. Punjabi *et al.*, Phys. Rev. C 71, 05520 (2005)

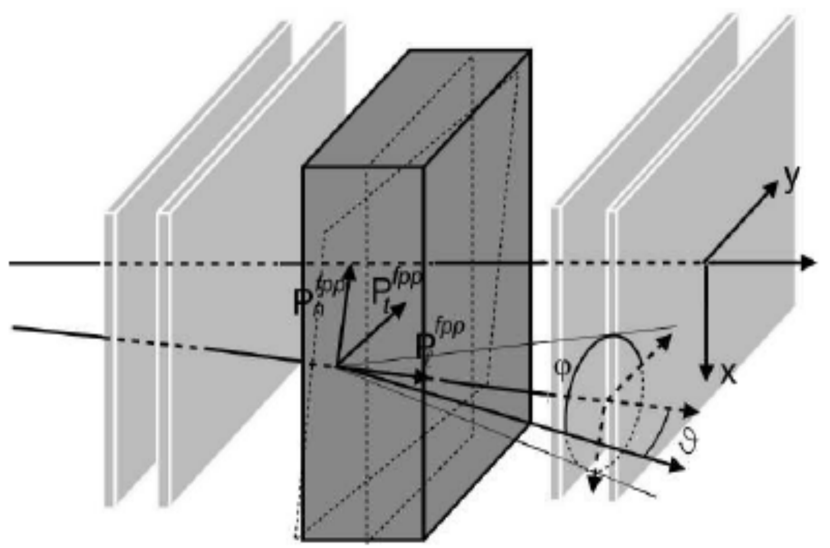

FIG. 9: Schematic of the polarimeter chambers and analyzer, showing a non-central trajectory; ϑ is the polar angle, and φ is the azimuthal angle from the y-direction counterclockwise.

Focal-plane polarimeter
Secondary scattering of polarized proton from unpolarized analyzer

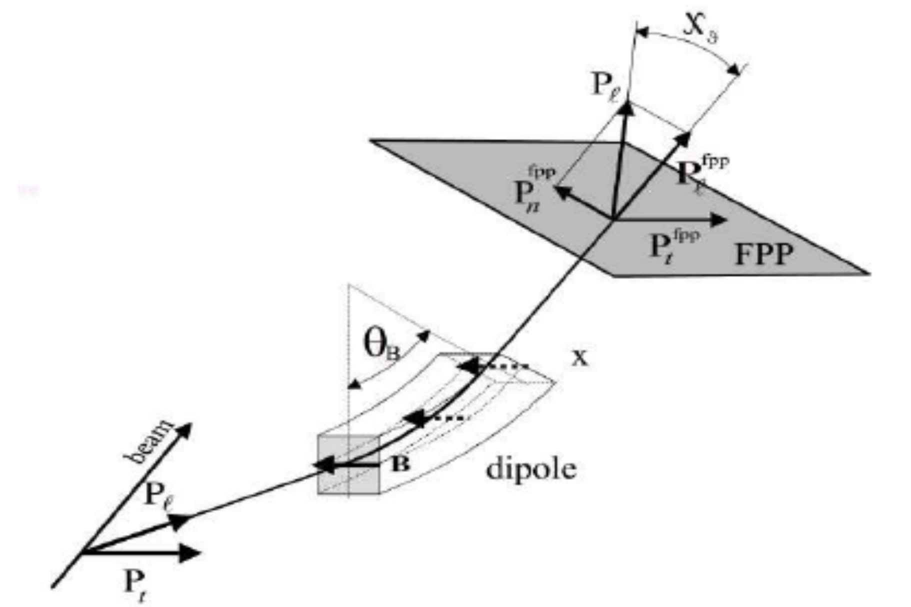

FIG. 15: Schematic drawing showing the precession by angle χ_θ of the P_ℓ component of the polarization in the dipole of the HRS.

Spin transfer formalism to account for spin precession through spectrometer

Proton form factor ratio

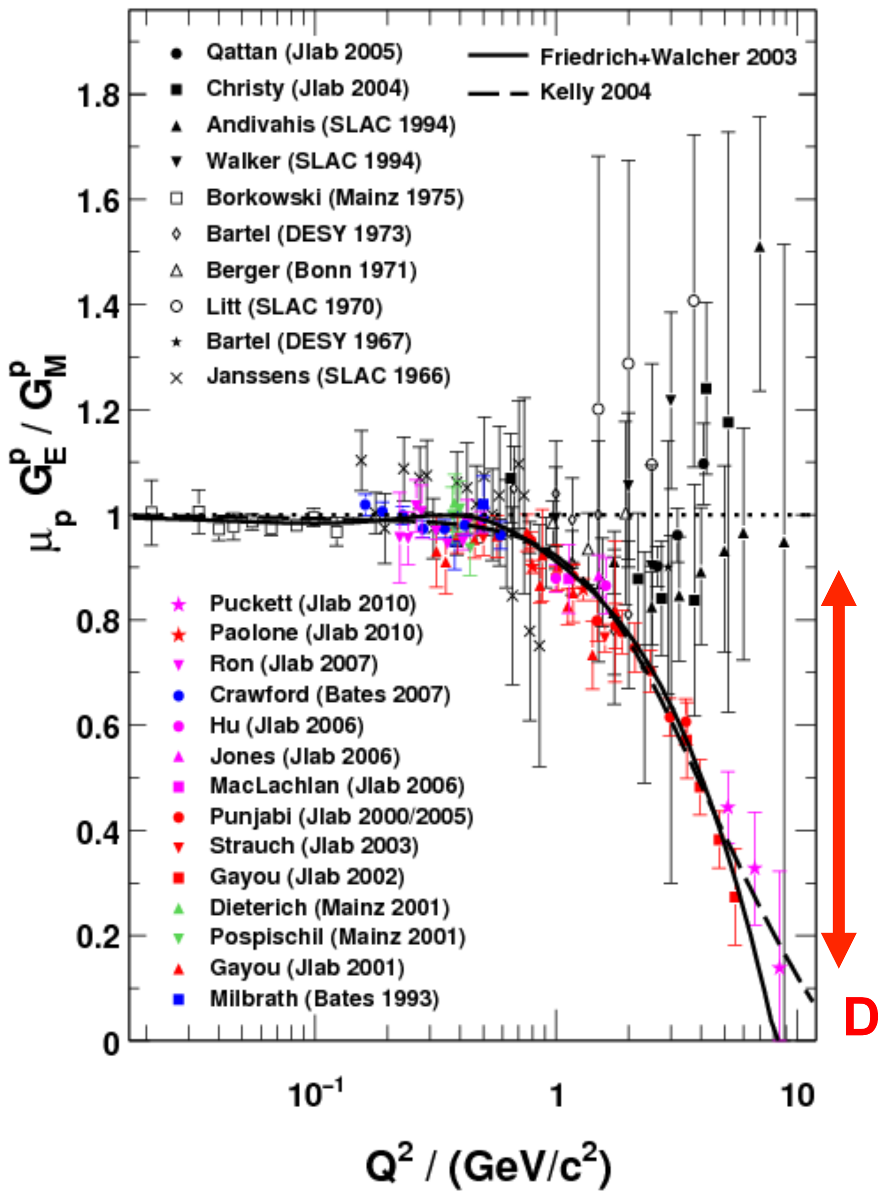

Dramatic discrepancy!

Jefferson Lab 2000–

- All Rosenbluth data from SLAC and Jlab in agreement
- Dramatic discrepancy between Rosenbluth and recoil polarization technique
- Multi-photon exchange considered best candidate

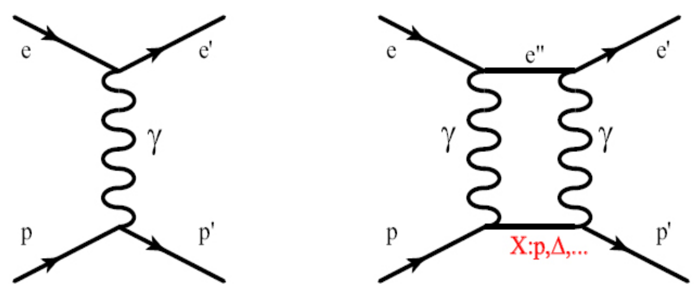

>800 citations

Proton form factor ratio

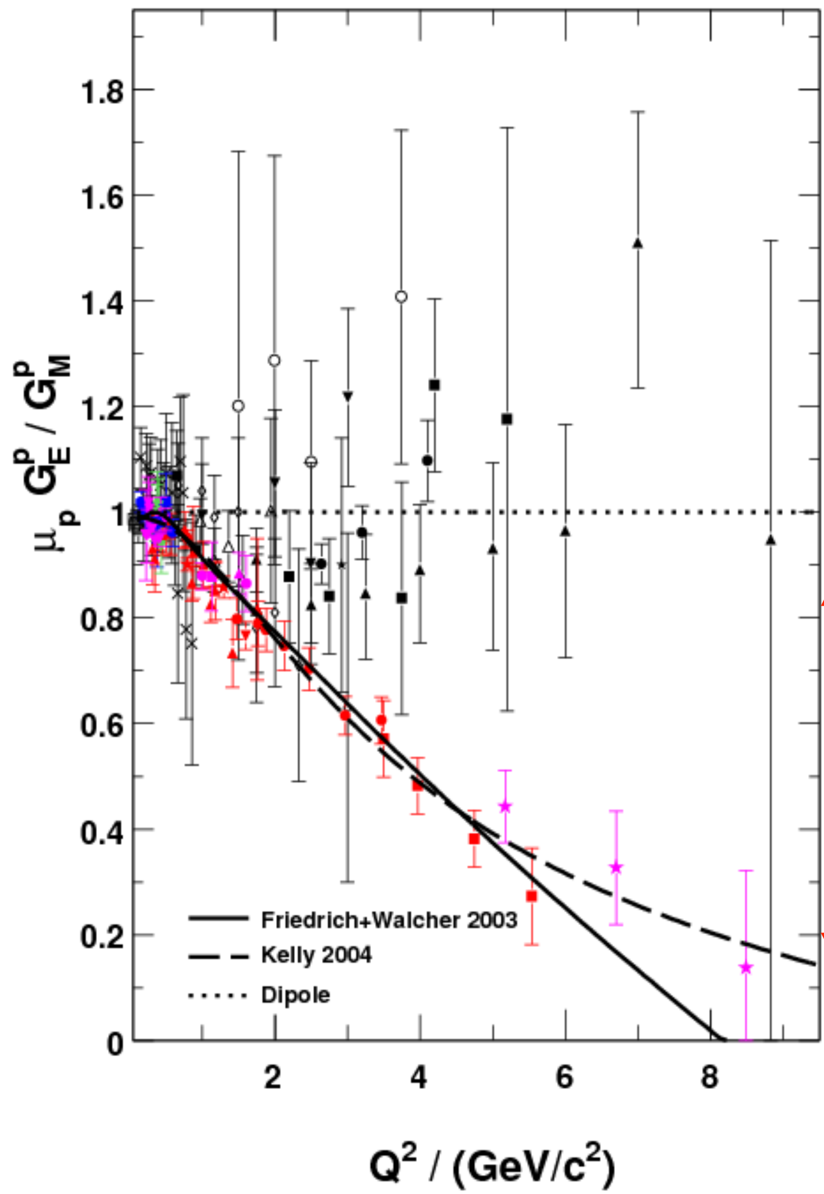

Jefferson Lab 2000–

- All Rosenbluth data from SLAC and Jlab in agreement
- Dramatic discrepancy between Rosenbluth and recoil polarization technique
- Multi-photon exchange considered best candidate

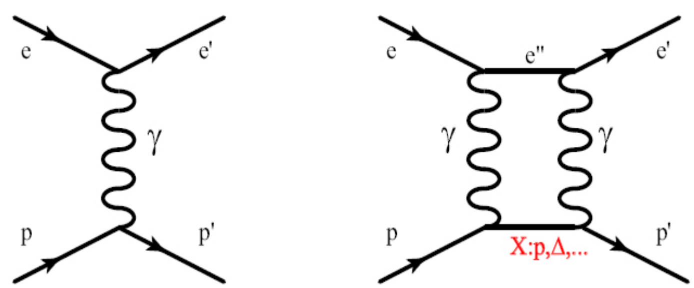

Dramatic discrepancy!

>800 citations

Another look

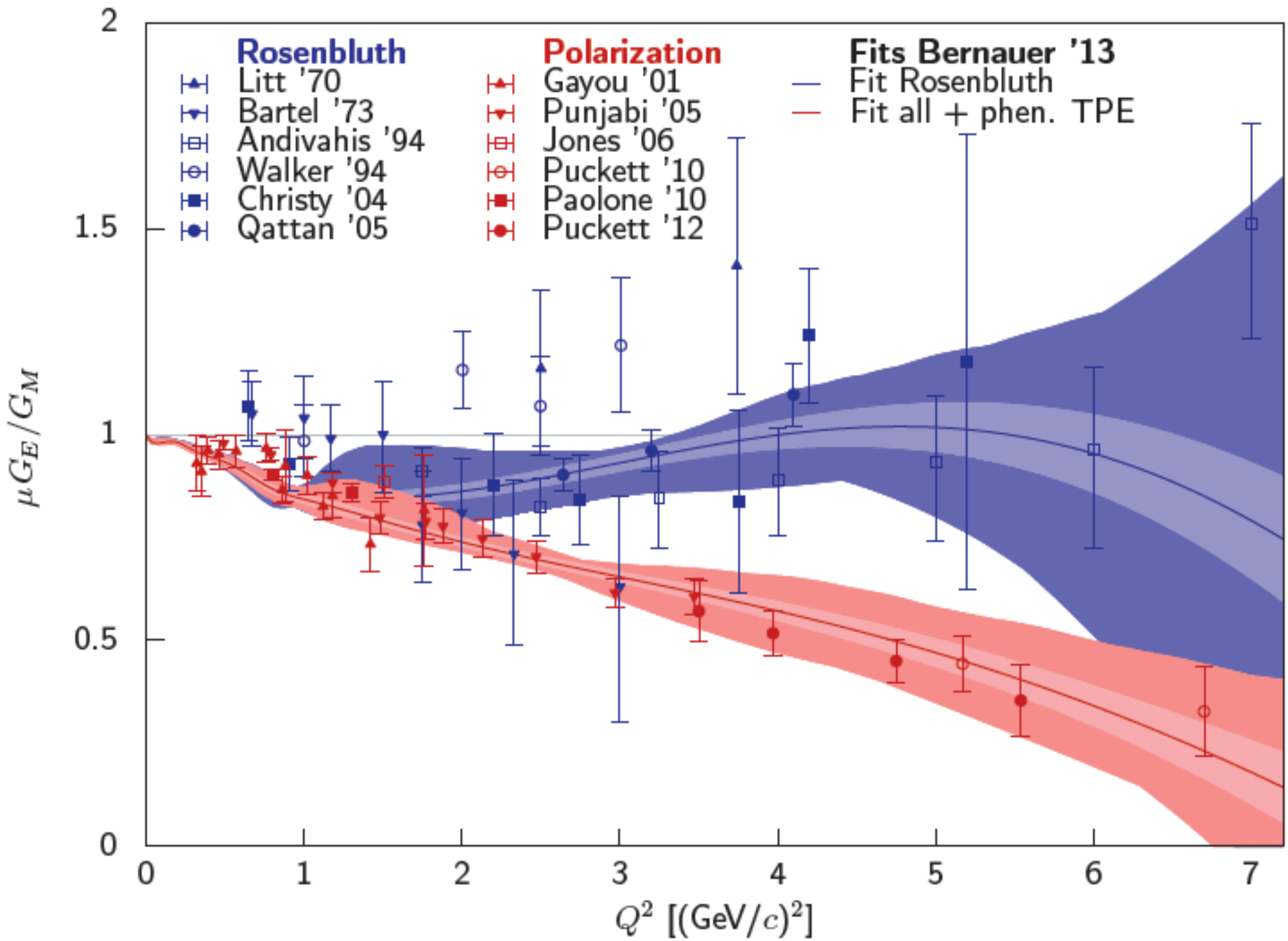

No discrepancy below Q^2 = 2 (GeV/c)^2 !

Polarized target data at high Q^2

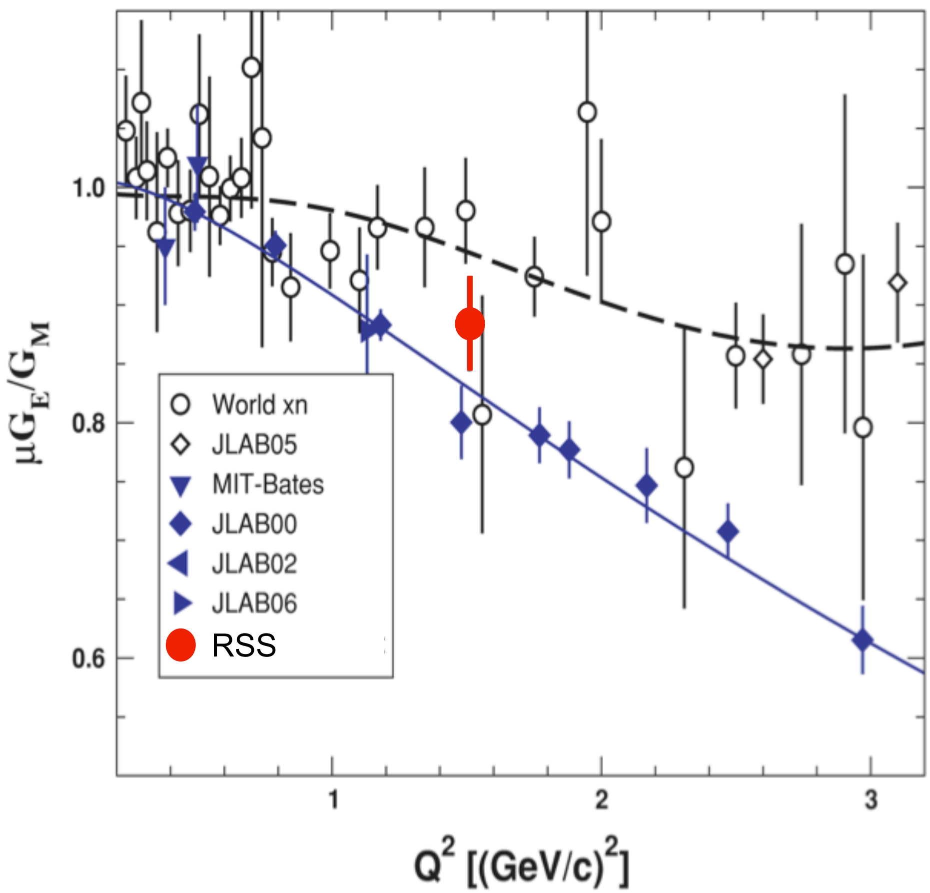

Polarized Target:
Independent verification of recoil polarization result is crucial

Polarized internal target / low Q^2: **BLAST**
Q^2<0.65 (GeV/c)^2 not high enough to see deviation from scaling

RSS /Hall C: $Q^2 \approx 1.5$ (GeV/c)^2

M.K. Jones *et al.*, PRC74, 035201 (2006)

Polarized target data at high Q^2

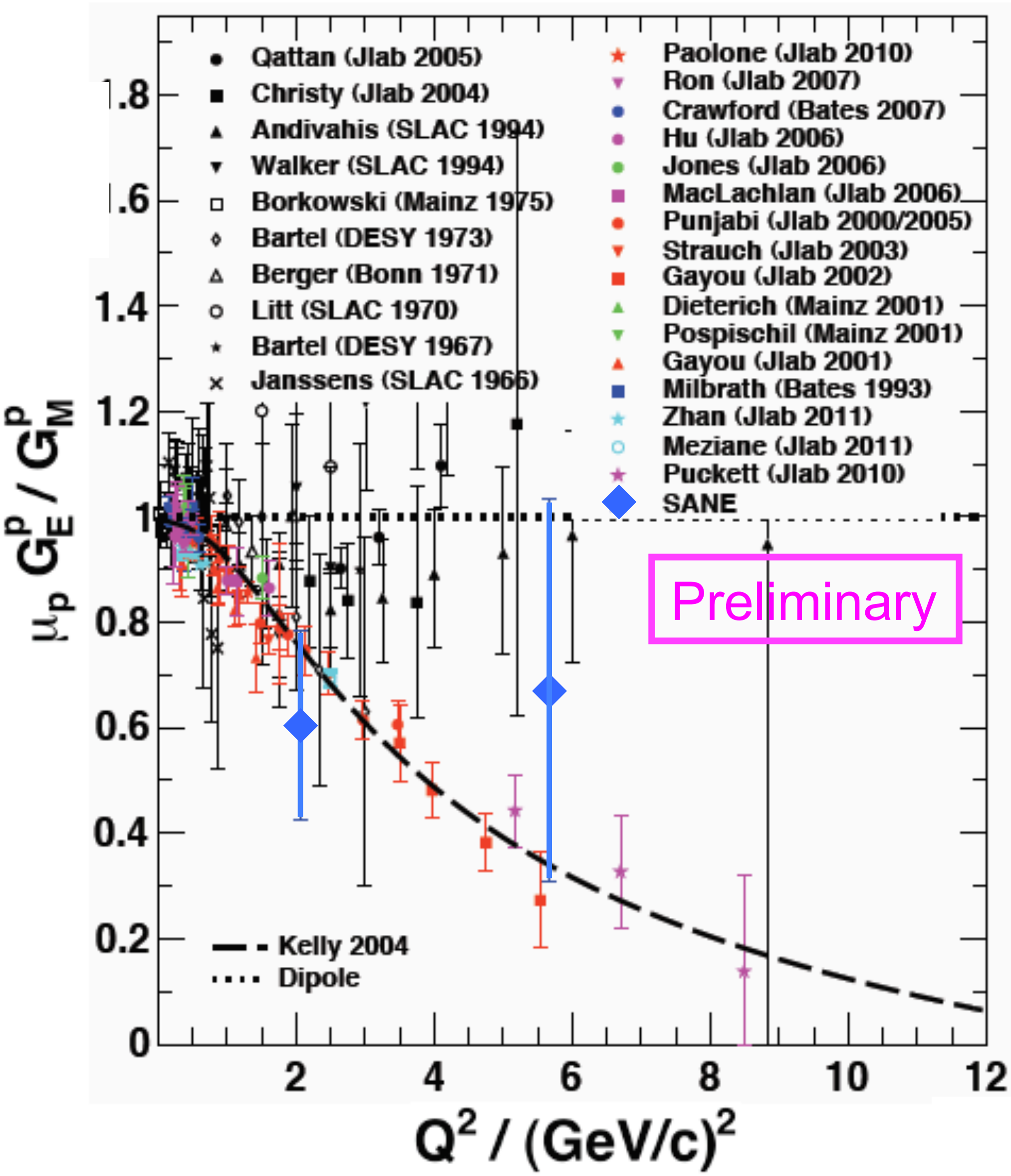

A. Liyanage, M.K. *et al.*, to be published

Polarized Target:
Independent verification of recoil polarization result is crucial

Polarized internal target / low Q^2: **BLAST**
Q^2<0.65 (GeV/c)^2 not high enough to see deviation from scaling

RSS /Hall C: $Q^2 \approx 1.5$ (GeV/c)^2

SANE/Hall C: completed March 2009
BigCal electron detector
Recoil protons in HMS parasitically
G_E/G_M at $Q^2 \approx$ 2.1 and 5.7 (GeV/c)^2

Decline of G_E/G_M has been confirmed!

Future precision measurements at high Q^2 are feasible

Effect of two-photon exchange

J. Arrington, P. Blunden, W. Melnitchouk, Prog. Part. Nucl. Phys. 66, 782 (2011)

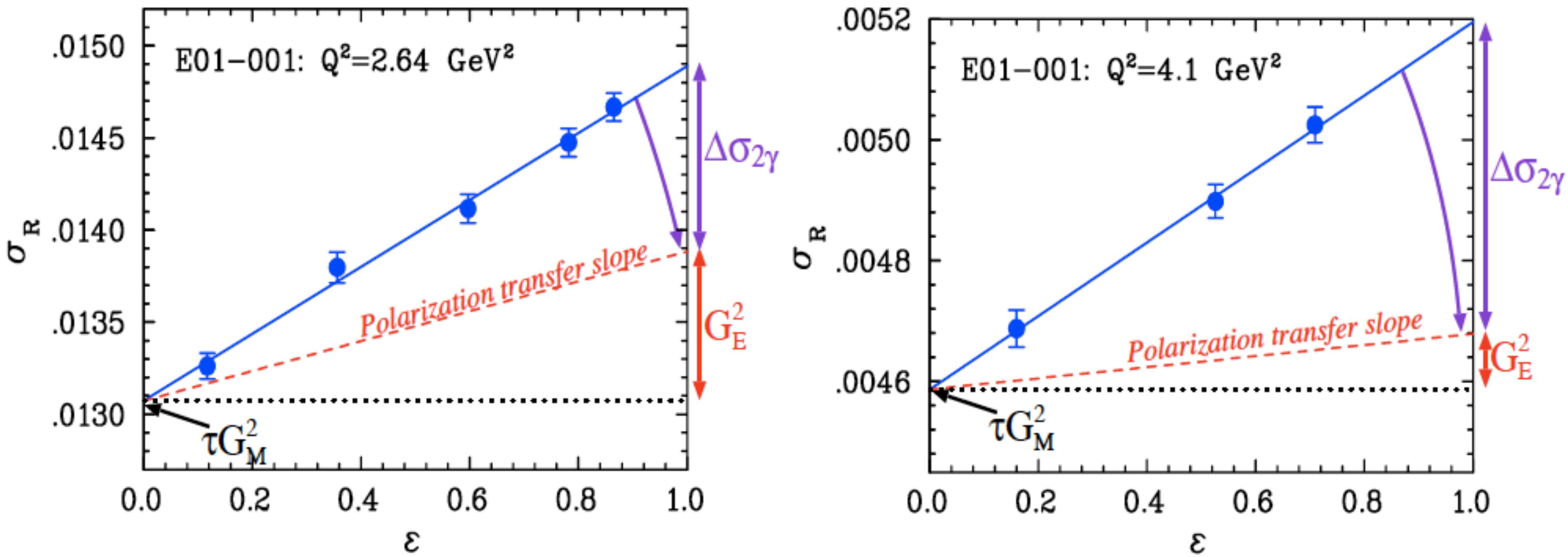

by construction, theorists sought mechanism that affects the “slope” in the Rosenbluth plot (ε-dependence)

At high Q^2 , the contribution of G_E to the cross section is of similar order as the TPE effect (few %)

Two-photon exchange: exp. evidence

Two-photon exchange theoretically suggested

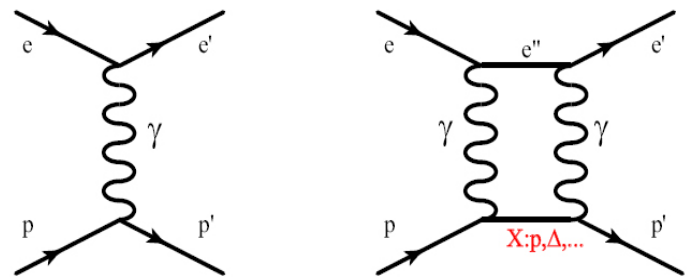

TPE can explain form factor discrepancy

J. Arrington, W. Melnitchouk, J.A. Tjon,
Phys. Rev. C 76, 035205 (2007)

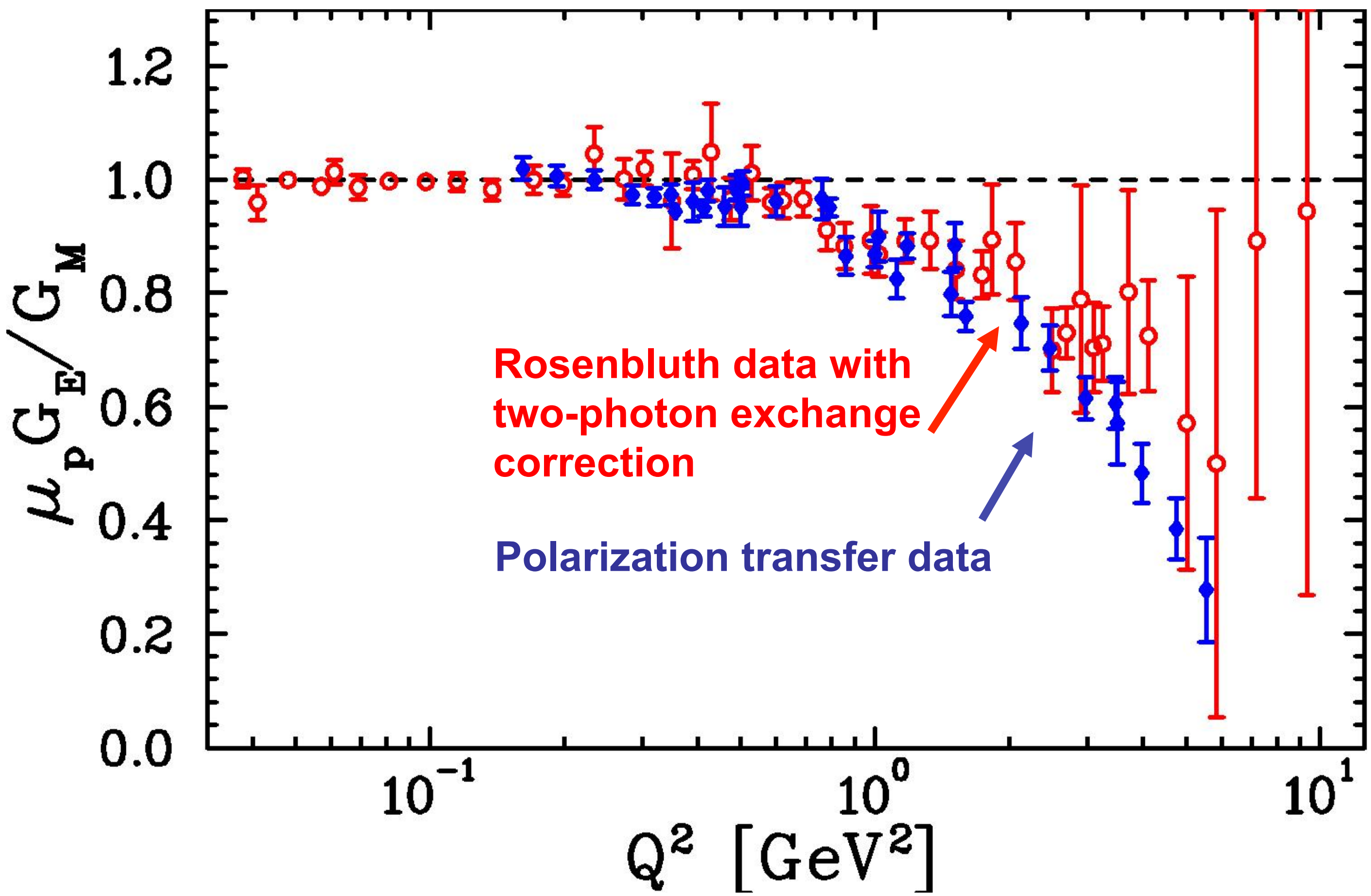

Elastic ep scattering beyond OPE

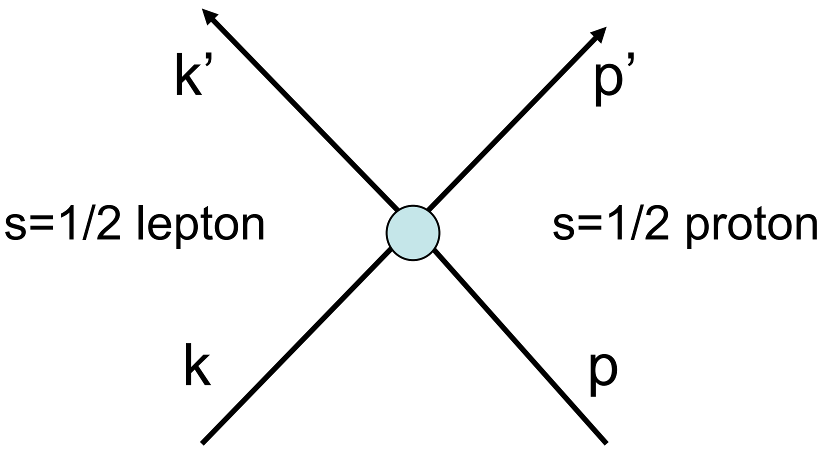

$$P \equiv \frac{p+p'}{2}, \qquad K \equiv \frac{k+k'}{2}$$

Kinematical invariants :

$$\begin{aligned} Q^2 &= -(p-p')^2 \\ \nu &= K \cdot P = (s-u)/4 \end{aligned}$$

Next-to Born approximation:

$$T^{non-flip}_{h'\lambda'_N, h\lambda_N} = \frac{e^2}{Q^2} \bar{u}(k', h') \gamma_\mu u(k, h)$$

$$\times \quad \bar{u}(p', \lambda'_N) \left(\tilde{G}_M \gamma^\mu - \tilde{F}_2 \frac{P^\mu}{M} + \tilde{F}_3 \frac{\gamma.K P^\mu}{M^2} \right) u(p, \lambda_N)$$

($m_e = 0$)

The T-matrix still factorizes, however a new response term F_3 is generated by TPE

Born-amplitudes are modified in presence of TPE; modifications ~α^3

$$\begin{aligned} \tilde{G}_M(\nu, Q^2) &= G_M(Q^2) + \delta\tilde{G}_M \\ \tilde{F}_2(\nu, Q^2) &= F_2(Q^2) + \delta\tilde{F}_2 \\ \tilde{F}_3(\nu, Q^2) &= 0 + \delta\tilde{F}_3 \end{aligned}$$

$$\tilde{G}_E \equiv \tilde{G}_M - (1+\tau)\,\tilde{F}_2$$

$$\tilde{G}_E(\nu, Q^2) = G_E(Q^2) + \delta\tilde{G}_E$$

New amplitudes are complex!

Inherited from M. Vanderhaeghen

Imaginary part: Single-spin asymmetries

spin of beam OR target NORMAL to scattering plane

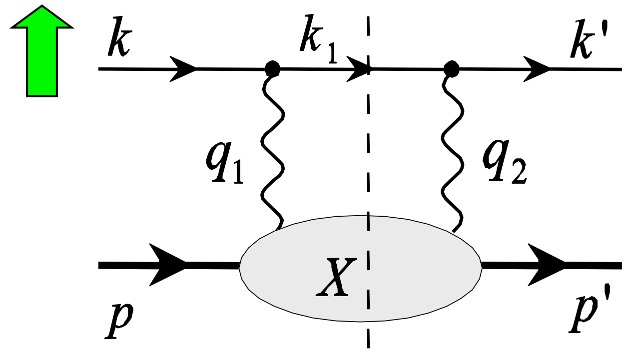

$$s = (k+p)^2$$

on-shell intermediate state ($M_X = W$)

$$A_n = -\frac{1}{(2\pi)^3}\frac{e^2(1-\varepsilon)}{8Q^2}\int_{M^2}^{s} dW^2 \frac{|\vec{k}_1|^2}{4\sqrt{s}}\int d\Omega_{k1}\frac{1}{Q_1^2 Q_2^2}\,\mathcal{I}\left(L_{\alpha\mu\nu}H^{\alpha\mu\nu}\right)$$

E.g. target normal spin asymmetry

$$A_n = \sqrt{\frac{2\varepsilon(1+\varepsilon)}{\tau}}\frac{1}{\sigma_R}\left\{-G_M\,\mathcal{I}\left(\delta\tilde{G}_E + \frac{\nu}{M^2}\tilde{F}_3\right) + G_E\,\mathcal{I}\left(\delta\tilde{G}_M + \left(\frac{2\varepsilon}{1+\varepsilon}\right)\frac{\nu}{M^2}\tilde{F}_3\right)\right\},$$

⇧Beam: PVES at Bates, MAMI and Jlab;

⇧Target: (Quasi-)elastic: E05-015: ^{3}He⇧(e,e'), E08-005: ^{3}He⇧(e,e'n)
Deep inelastic: E07-013; HERMES p⇧(e,e')

Inherited from M. Vanderhaeghen

Beam-normal single spin asymmetry

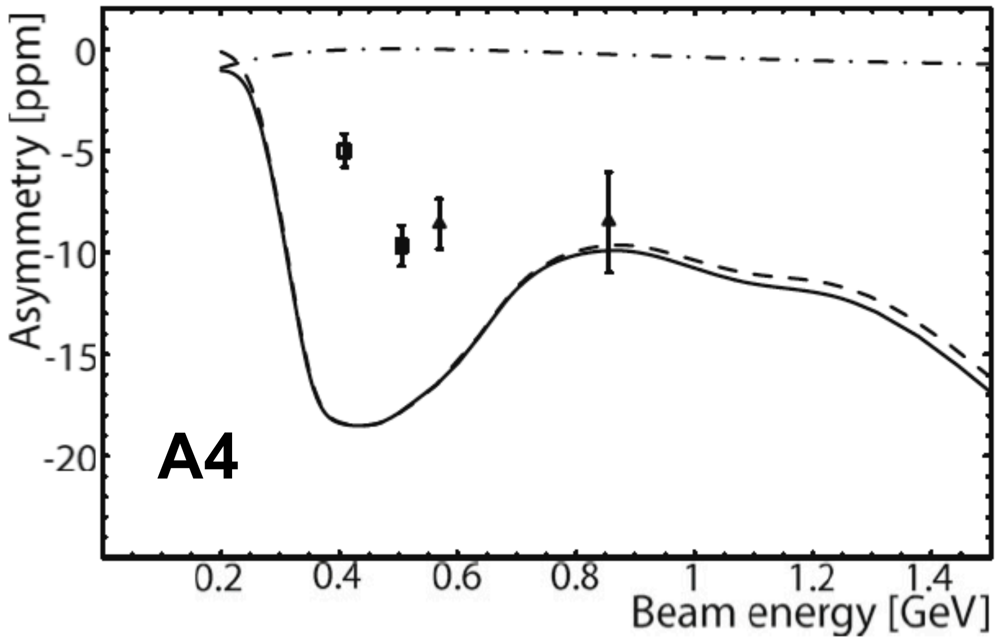

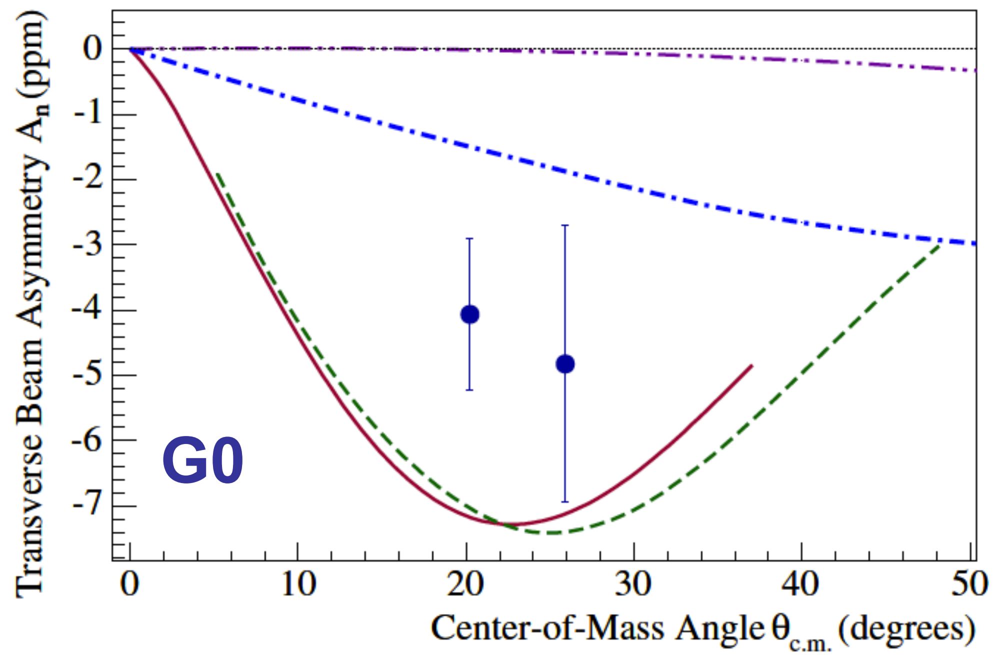

F. Maas *et al.*, PRL 99, 092301 (2005);
S. Baunack, EPJ ST198, 343 (2011)

D. Armstrong *et al.*, PRL 99, 092301 (2007)

p(e⇧,e') at forward angles

Qweak (preliminary):

A_n= (−5.35±0.07±0.15) ppm

B.P. Waidyawansa, PAVI2014, arXiv:1604.04602

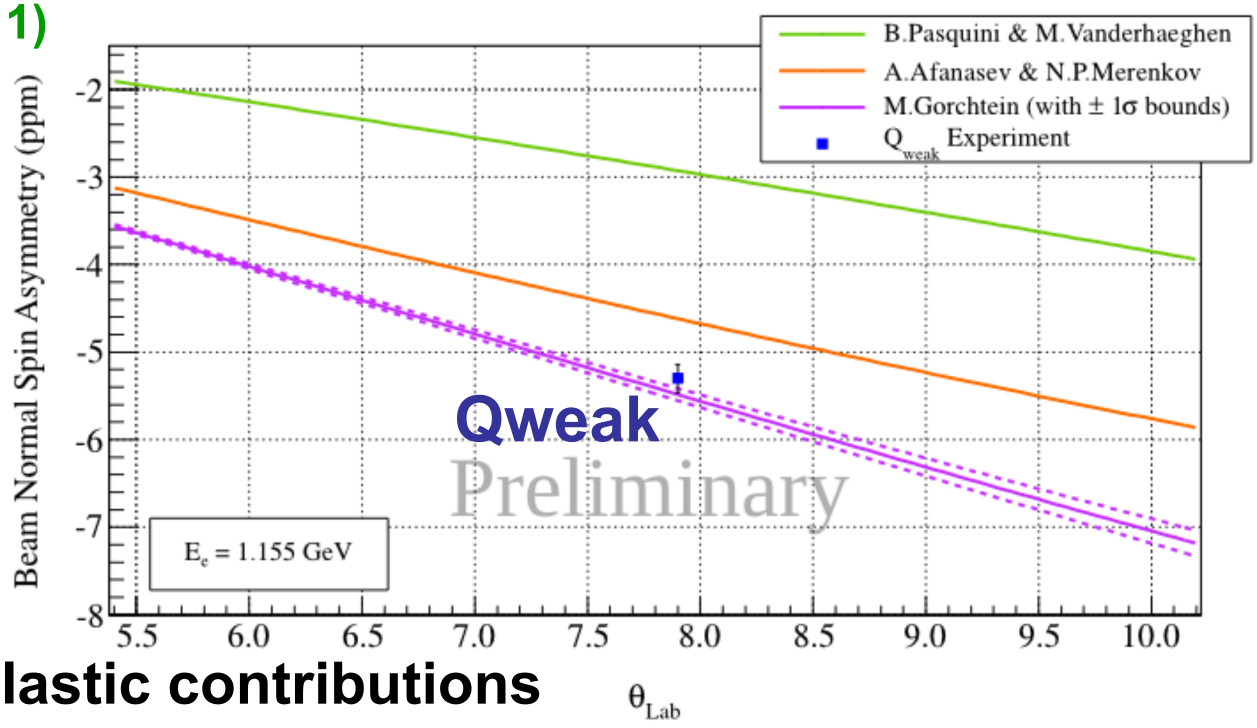

BNSSA's dominated by inelastic contributions

Beam-normal single spin asymmetry

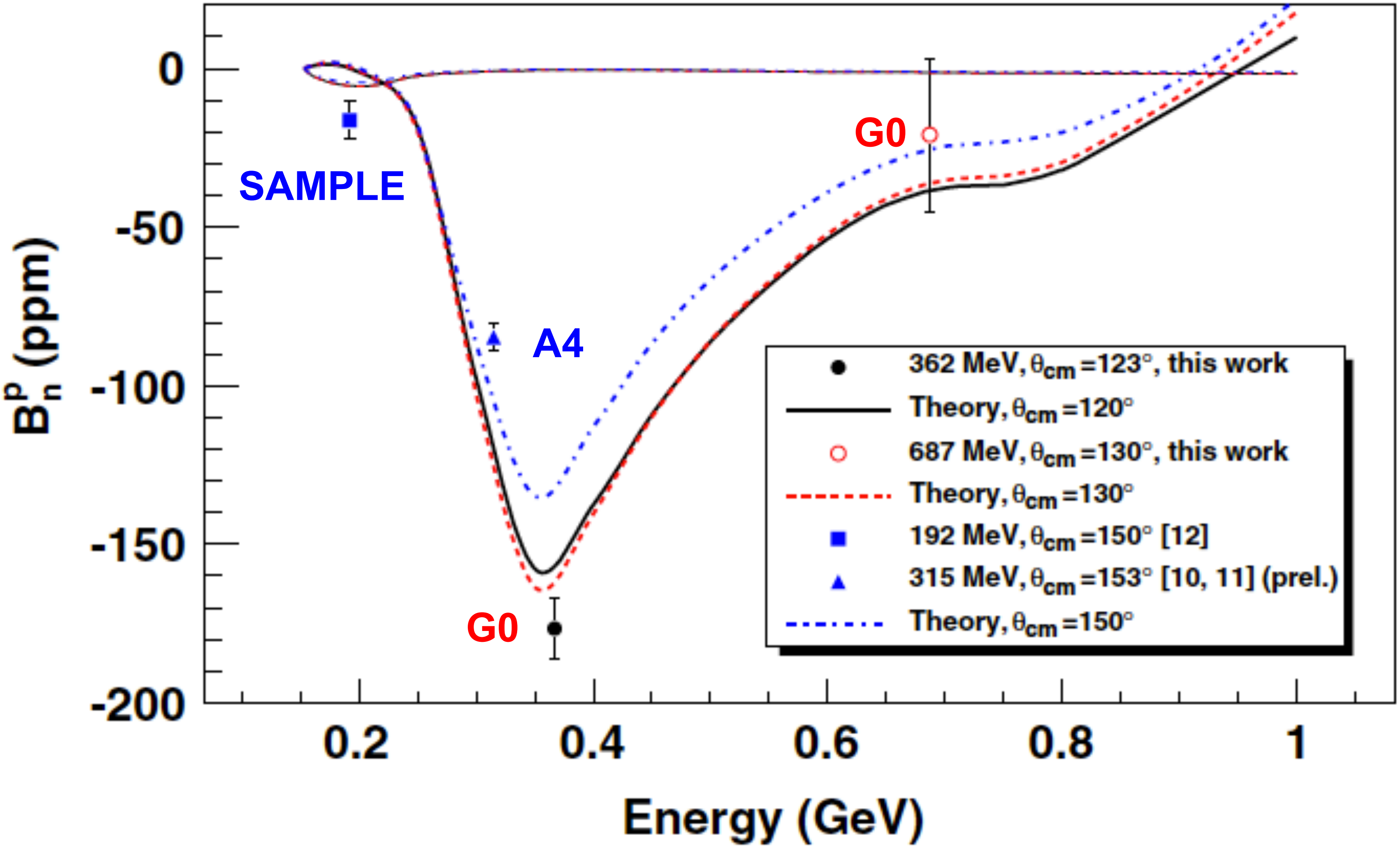

p(e⇧,e') at backward angles:

G0 bwd: D. Androic *et al.*, PRL 107, 022501 (2011)
A4 bwd: S. S. Baunack, EPJ ST198, 343 (2011)
SAMPLE: S. Wells *et al.*, PRC 63, 064001 (2001)

BNSSA's dominated by inelastic contributions

Target-normal single spin asymmetry

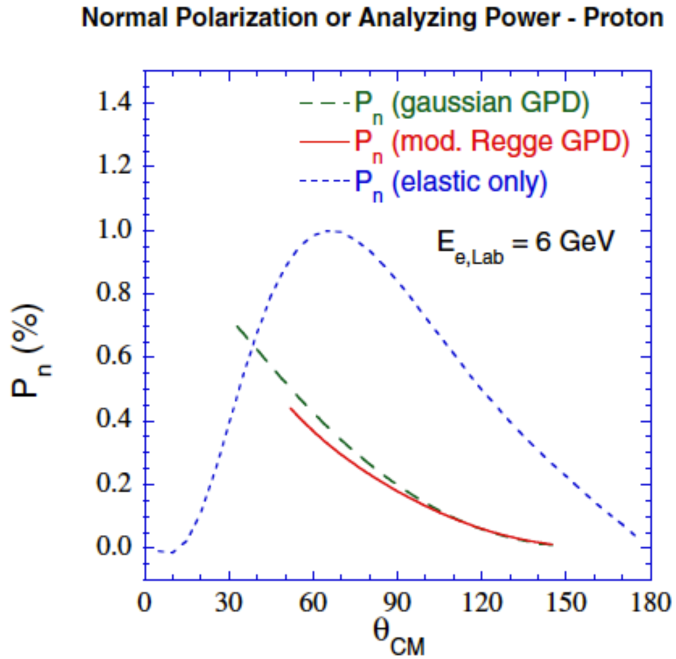

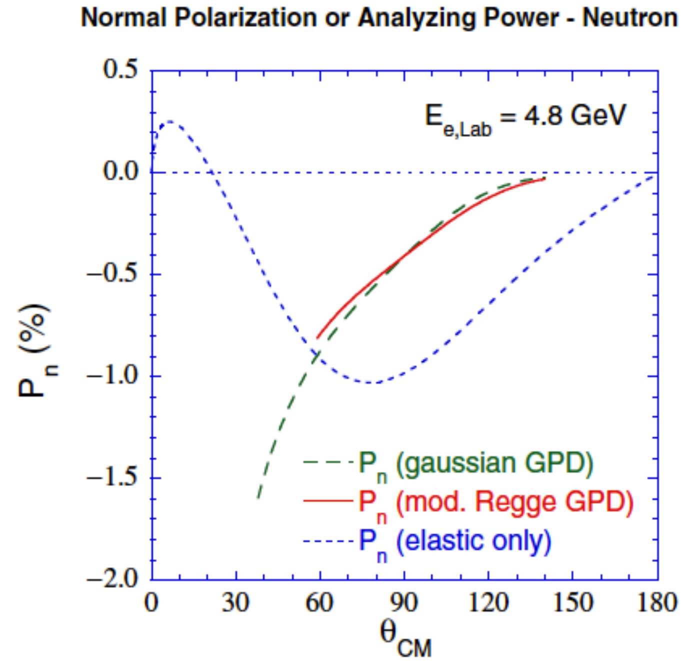

A. Afanasev *et al.*,
PRD 72, 013008 (2005)
(elastic)
%-level asymmetries
opposite sign for p&n

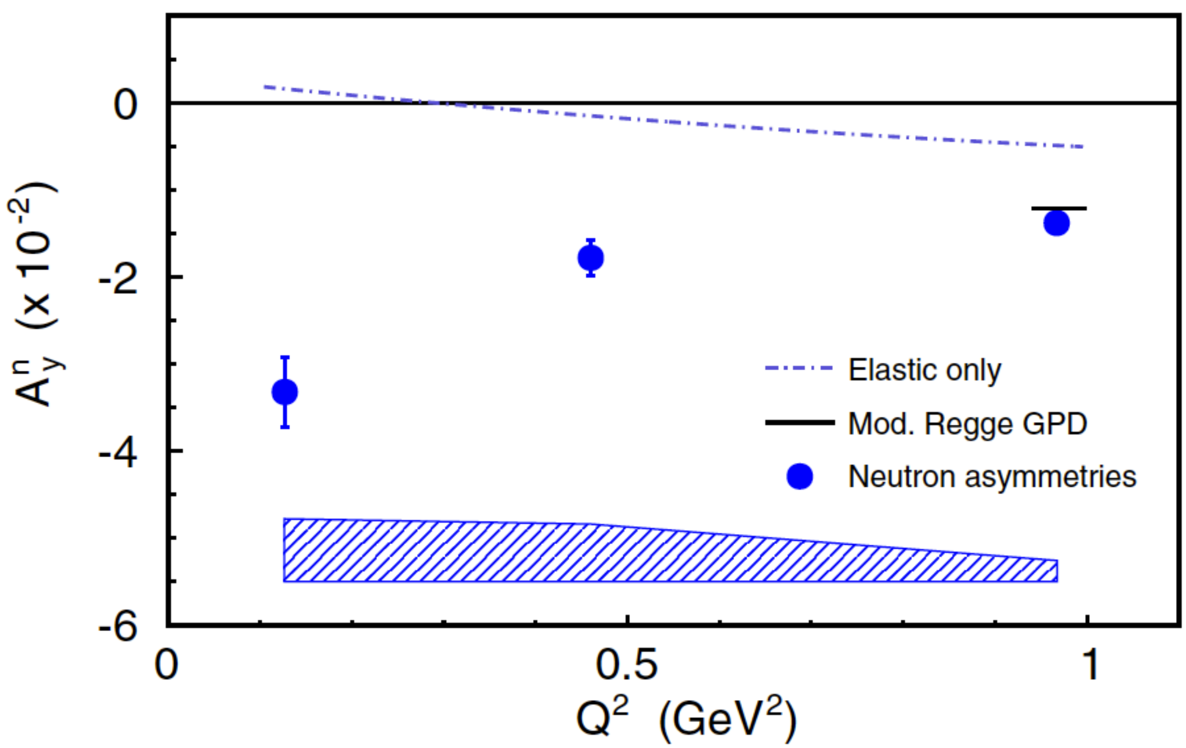

^{3}He⇧(e,e'): E05-015 (quasielastic)

Y.-W. Zhang *et al.*,
PRL 115, 172502 (2015)

Theory:
Y.C. Chen *et al.*,
PRL 93, 122301 (2004)

Further:

^{3}He⇧(e,e'n): E08-005 (quasielastic)

Target-normal single spin asymmetry

^{3}He⇧(e,e')X: E07-013 (DIS)

J. Katich *et al.*, PRL 113, 022502 (2014)

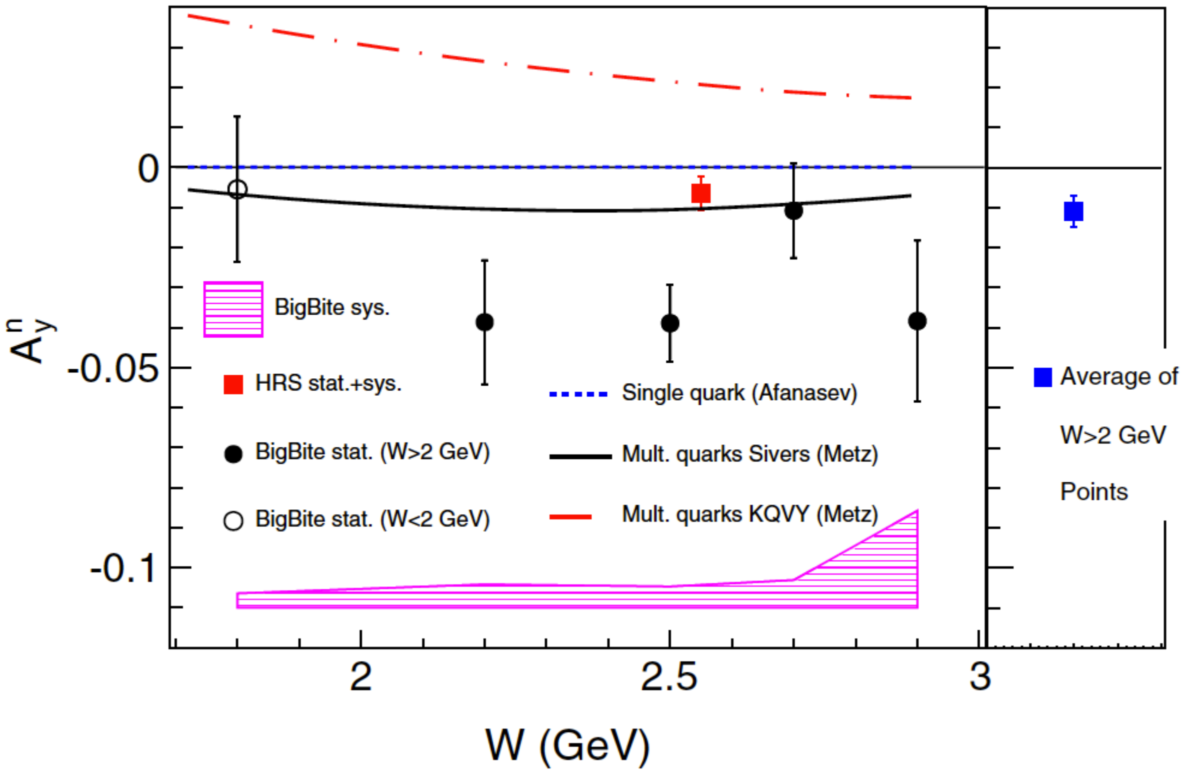

p⇧(e,e')X: HERMES (DIS)

A. Airapetian *et al.*, PLB 682, 351 (2010)

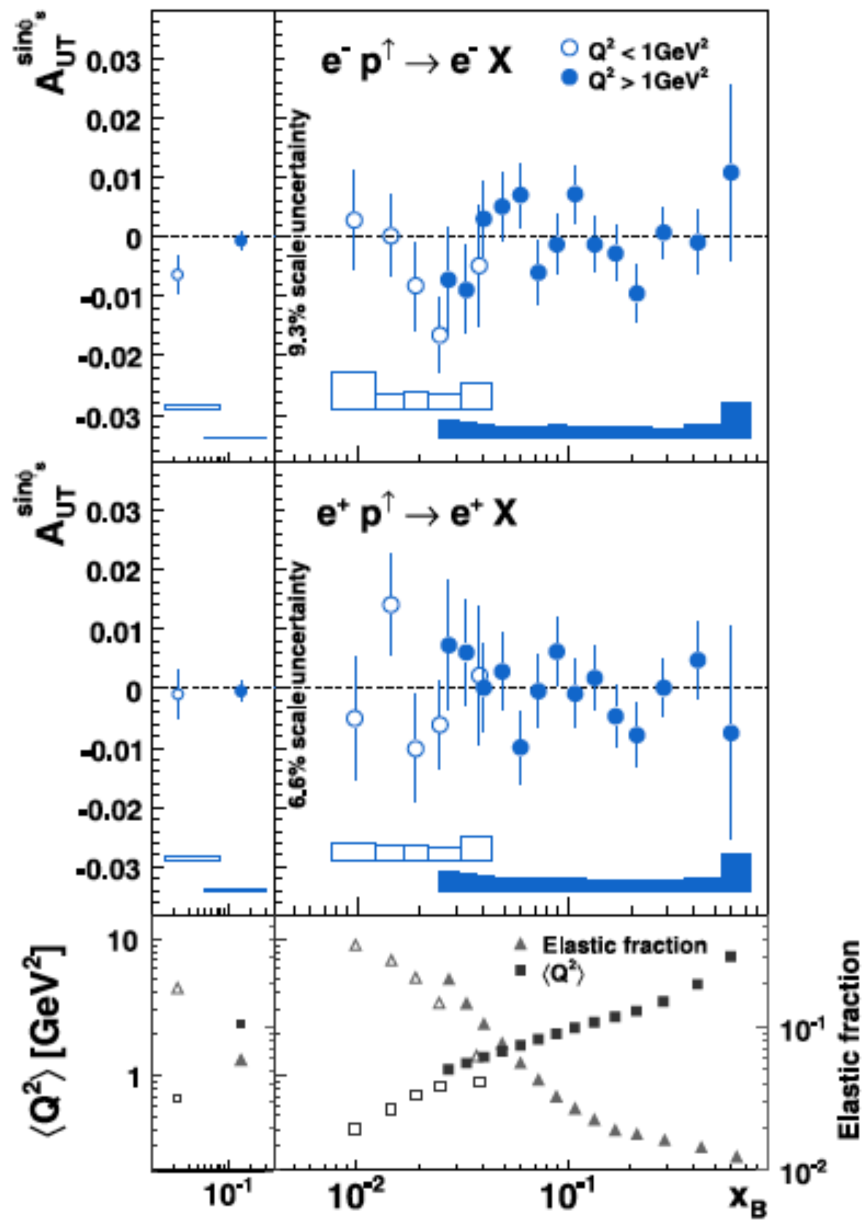

Single-quark: 10^{-4}-level asymmetries

A. Afanasev *et al.*, PRD77, 014028 (2008)

Multi-quark: %-level asymmetries

A. Metz *et al.*, PRD 86, 094039 (2012)

Observables involving real part of TPE

$$P_t = -\sqrt{\frac{2\varepsilon(1-\varepsilon)}{\tau}}\frac{G_M^2}{d\sigma_{red}}\left\{R + R\frac{\Re\left(\delta\tilde{G}_M\right)}{G_M} + \frac{\Re\left(\delta\tilde{G}_E\right)}{G_M} + Y_{2\gamma}\right\}$$

$$P_l = \sqrt{(1+\varepsilon)(1-\varepsilon)}\frac{G_M^2}{d\sigma_{red}}\left\{1 + 2\frac{\Re(\delta\tilde{G}_M)}{G_M} + \frac{2}{1+\varepsilon}\varepsilon Y_{2\gamma}\right\}$$

$$\frac{P_t}{P_l} = -\sqrt{\frac{2\varepsilon}{(1+\varepsilon)\tau}}\left\{R - R\frac{\Re\left(\delta\tilde{G}_M\right)}{G_M} + \frac{\Re\left(\delta\tilde{G}_E\right)}{G_M} + 2\left(1 - R\frac{2\varepsilon}{1+\varepsilon}\right)Y_{2\gamma}\right\}$$

E04-019 (Two-gamma)

$$d\sigma_{red}/G_M^2 = 1 + \frac{\varepsilon R^2}{\tau} + 2\frac{\Re(\delta\tilde{G}_M)}{G_M} + 2R\frac{\varepsilon\Re(\delta\tilde{G}_E)}{\tau G_M} + 2\left(1+\frac{R}{\tau}\right)\varepsilon Y_{2\gamma}$$

e^+/e^- x-section ratio
CLAS,VEPP3,OLYMPUS

Rosenbluth non-linearity
E05-017

$$\Re(\tilde{G}_E) = G_E(Q^2) + \Re(\delta\tilde{G}_E(Q^2,\varepsilon))$$

$$\Re(\tilde{G}_M) = G_M(Q^2) + \Re(\delta\tilde{G}_M(Q^2,\varepsilon))$$

$$R = G_E/G_M \qquad Y_{2\gamma} = 0 + \sqrt{\frac{\tau(1+\tau)(1+\varepsilon)}{1-\varepsilon}}\frac{\Re(\tilde{F}_3(Q^2,\varepsilon))}{G_M}$$

Born Approximation | **Beyond Born Approximation**

P.A.M. Guichon and M.Vanderhaeghen, Phys.Rev.Lett. 91, 142303 (2003)

M.P. Rekalo and E. Tomasi-Gustafsson, E.P.J. A 22, 331 (2004)

Slide idea:
L. Pentchev

Jefferson Lab E04-019 (Two-gamma)

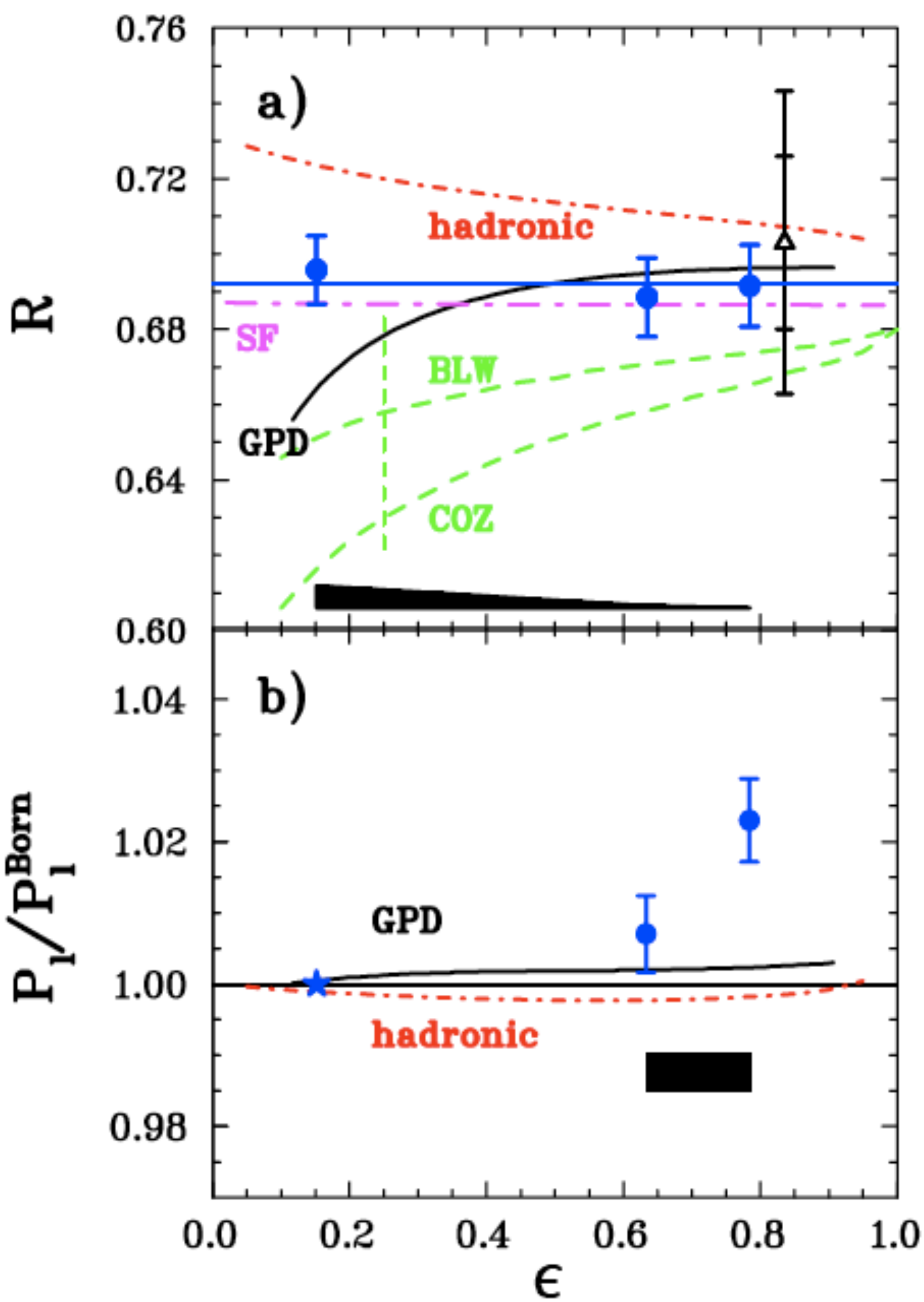

Jlab – Hall C
Q^2 = 2.5 (GeV/c)^2

G_E/G_M from P_t/P_l constant vs. ε

➔ **no effect in P_t/P_l**
➔ **some effect in P_l**

Expect larger effect in e+/e-!

M. Meziane *et al.*, hep-ph/1012.0339v2
Phys. Rev. Lett. 106, 132501 (2011)

Empirical extraction of TPE amplitudes

J. Guttmann, N. Kivel, M. Meziane, and M. Vanderhaeghen, EPJA 47, 77 (2011)

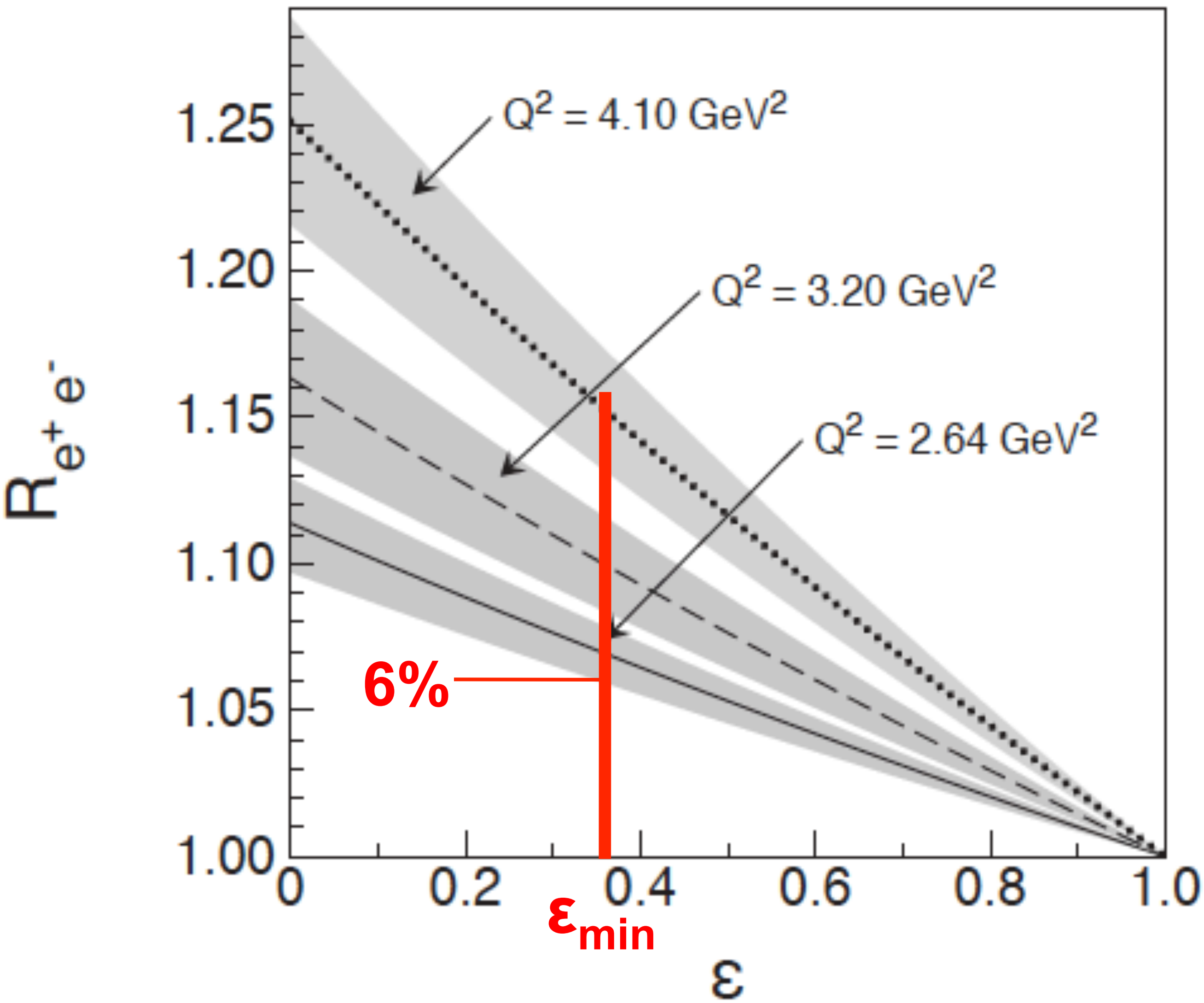

grows with Q^2!

Expect ~6% effect for OLYMPUS@2.0GeV

$\varepsilon_{min} > 0.35$, $Q^2 < 2.2\ (GeV/c)^2$

Lepton-proton elastic scattering

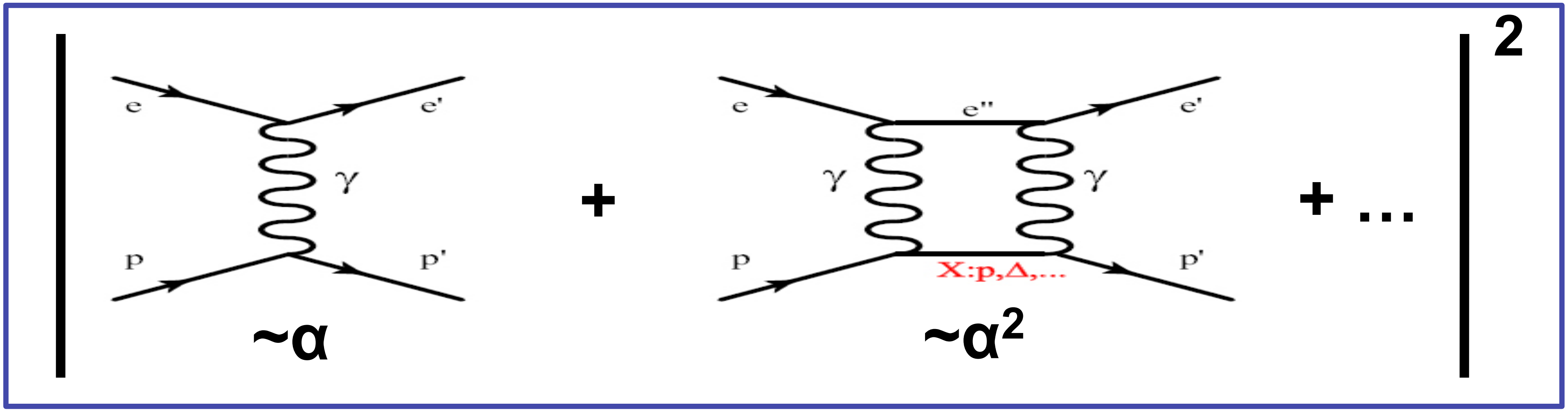

- Interference term depends on lepton charge sign (C-odd)

$$\sigma_{e^\pm p} = |\mathcal{M}_{1\gamma}|^2 \pm 2\Re\{\mathcal{M}^\dagger_{1\gamma}\mathcal{M}_{2\gamma}\} + \cdots$$

- e^+/e^- ratio deviates from unity by two-photon contribution

$$\frac{\sigma_{e^+p}}{\sigma_{e^-p}} \approx 1 + 4\frac{\Re\{\mathcal{M}^\dagger_{1\gamma}\mathcal{M}_{2\gamma}\}}{|\mathcal{M}_{1\gamma}|^2}$$

Comparison of e^+/e^- experiments

- **VEPP-3 @ Novosibirsk: E_{beam} = 1.6, 1.0 (and 0.6) GeV**
- **CLAS @ JLAB : E_{beam} = 0.5 – 4.0 GeV continuous**
- **OLYMPUS @ DESY: E_{beam} = 2.0 GeV**

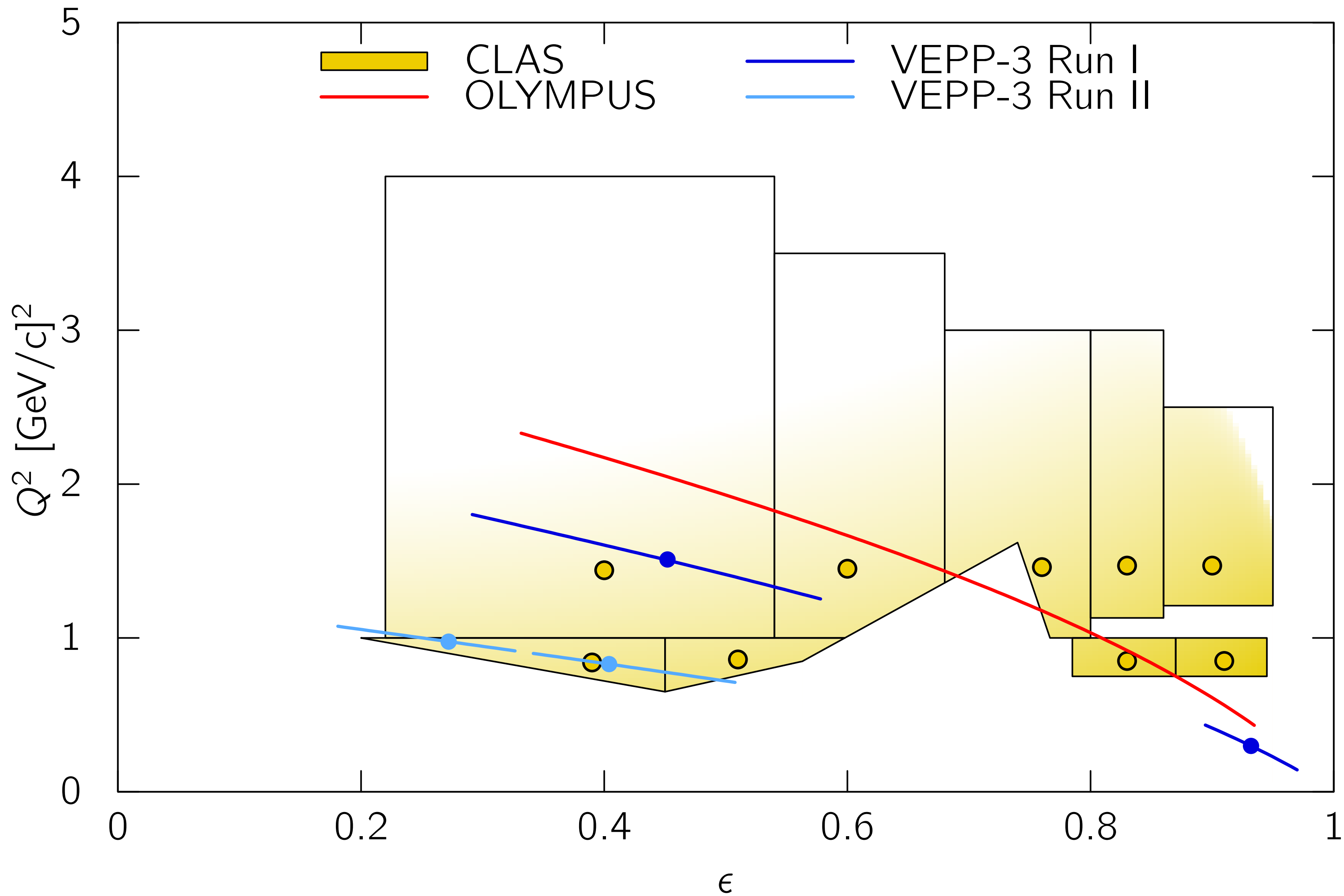

Comparison of e^+/e^- experiments

	VEPP–3 Novosibirsk	OLYMPUS DESY	EG5 CLAS JLab
beam energy	3 fixed	1 fixed	wide spectrum
equality of $e^\pm$ beam energy	measured	measured	reconstructed
e^+/e^- swapping frequency	half-hour	24 hours	simultaneously
e^+/e^- lumi monitor	elastic low-Q^2	elastic low-Q^2, Möller/Bhabha	from simulation
energy of scattered $e^\pm$	EM-calorimeter	mag. analysis	mag. analysis
proton PID	$\Delta E/E$, TOF	mag. analysis, TOF	mag. analysis, TOF
e^+/e^- detector acceptance	identical	big difference	big difference
luminosity	1.0×10^{32}	2.0×10^{33}	2.5×10^{32}
beam type	storage ring	storage ring	secondary beam
target type	internal H target	internal H target	liquid H target
data taken	2009, 2011-12	2012	2011
published	2015	not yet	2015

TPE experiments: Novosibirsk/VEPP-3

Run I (2009)
E=1.6 GeV

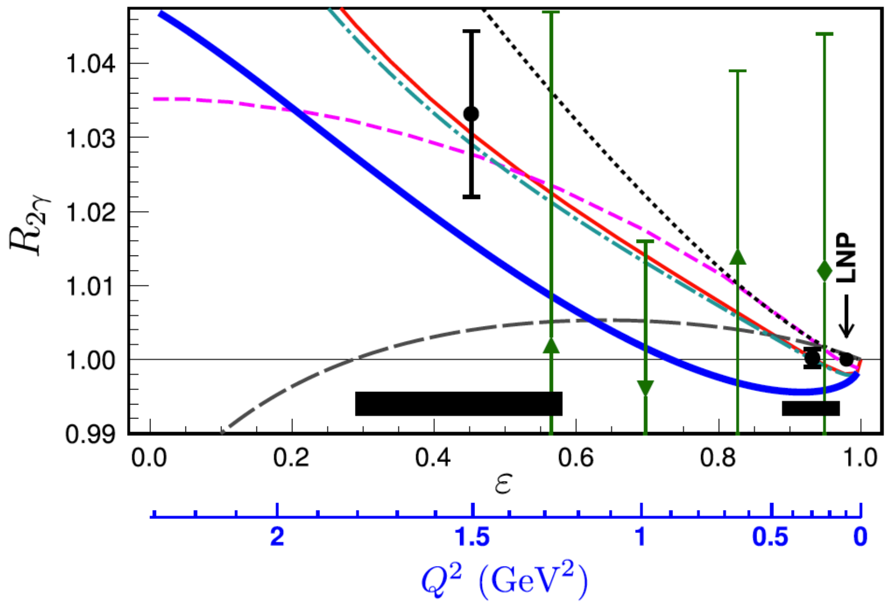

Run II (2011/12)
E=1.0 GeV

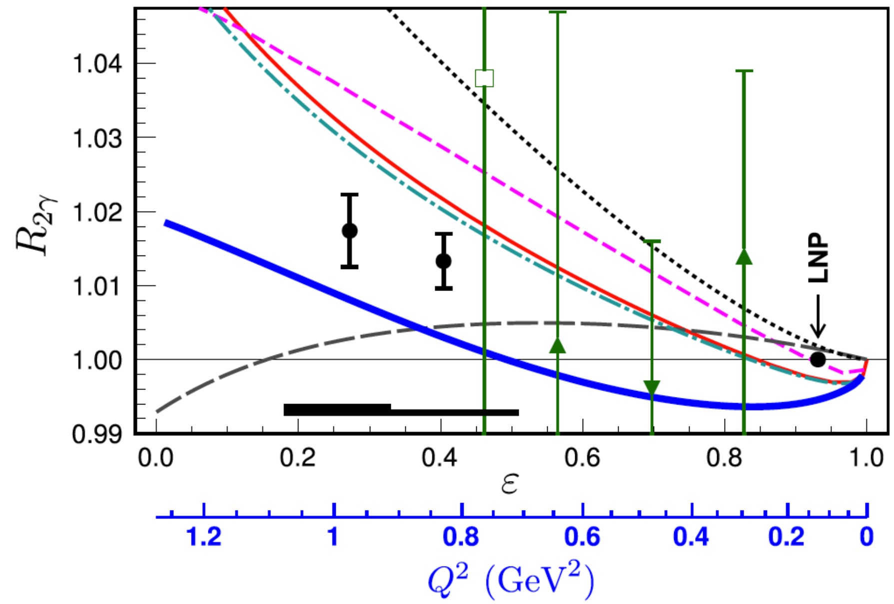

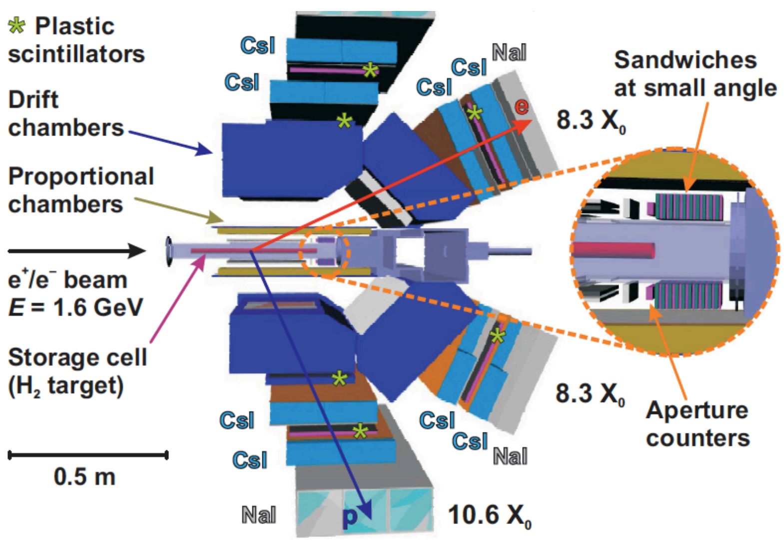

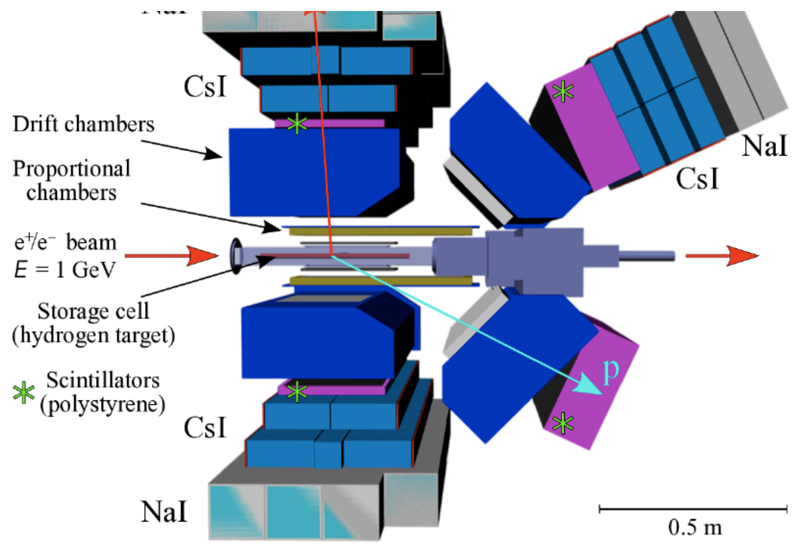

I.A. Rachek *et al.*, PRL 114, 062005 (2015)

TPE experiments: CLAS (E04-116)

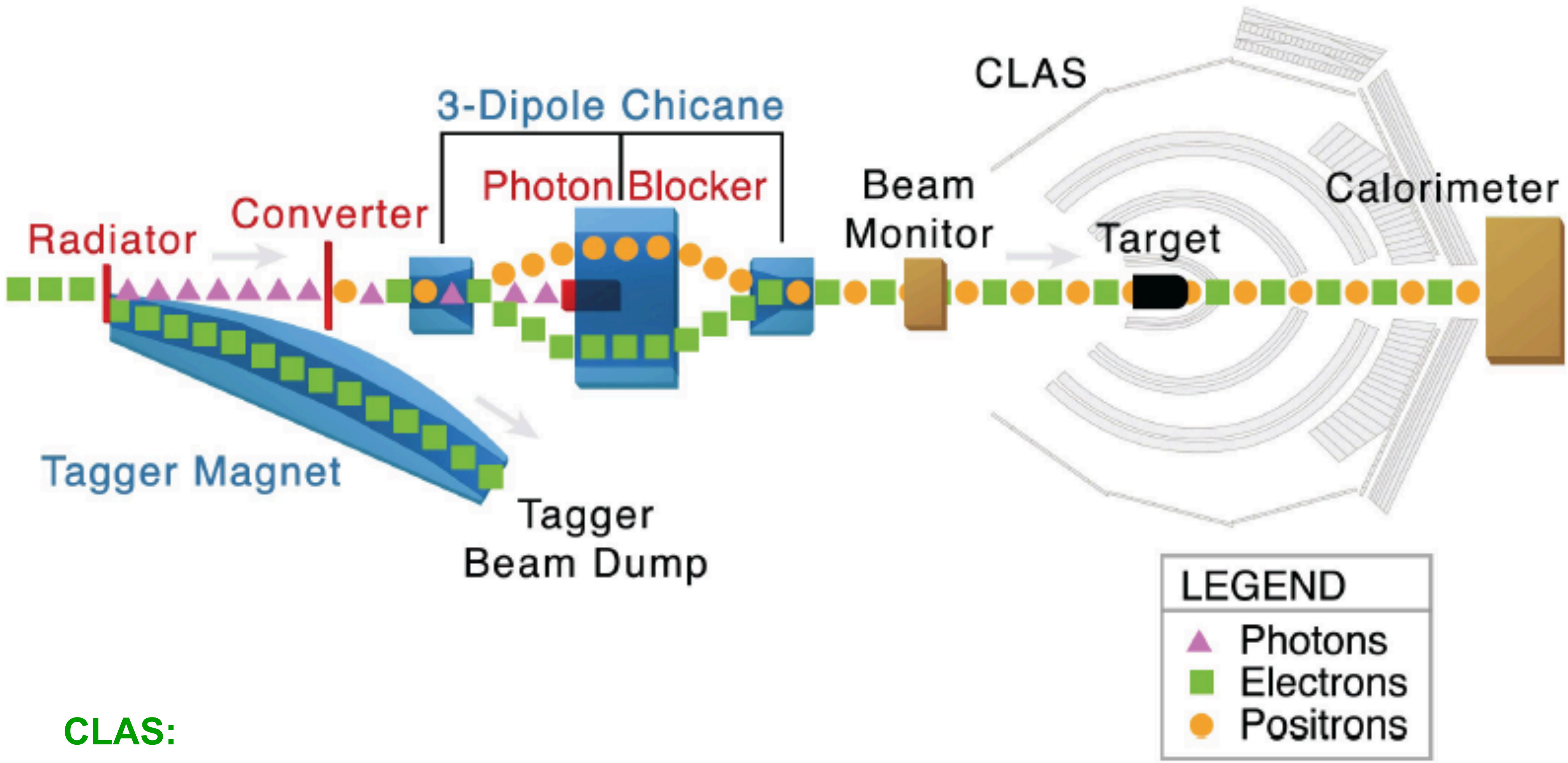

CLAS:
D. Rimal *et al.*, arXiv:1603.00315v1
D. Adikaram *et al.*, PRL 114, 062003 (2015)

TPE experiments: CLAS (E04-116)

ε dependence

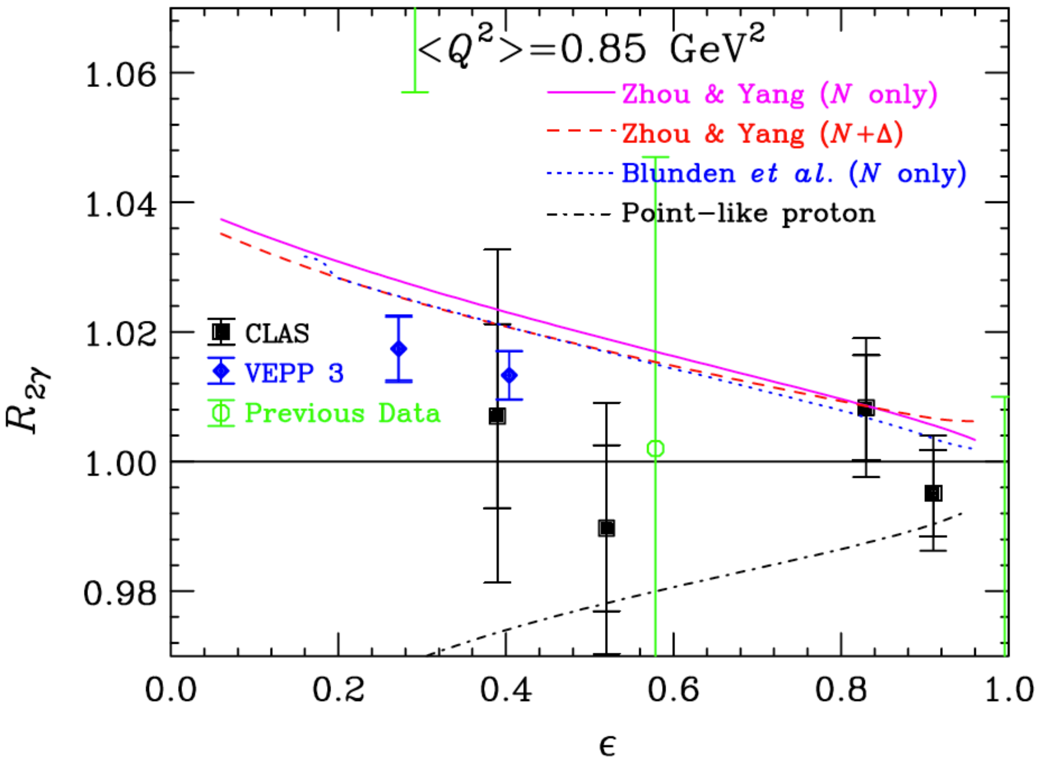

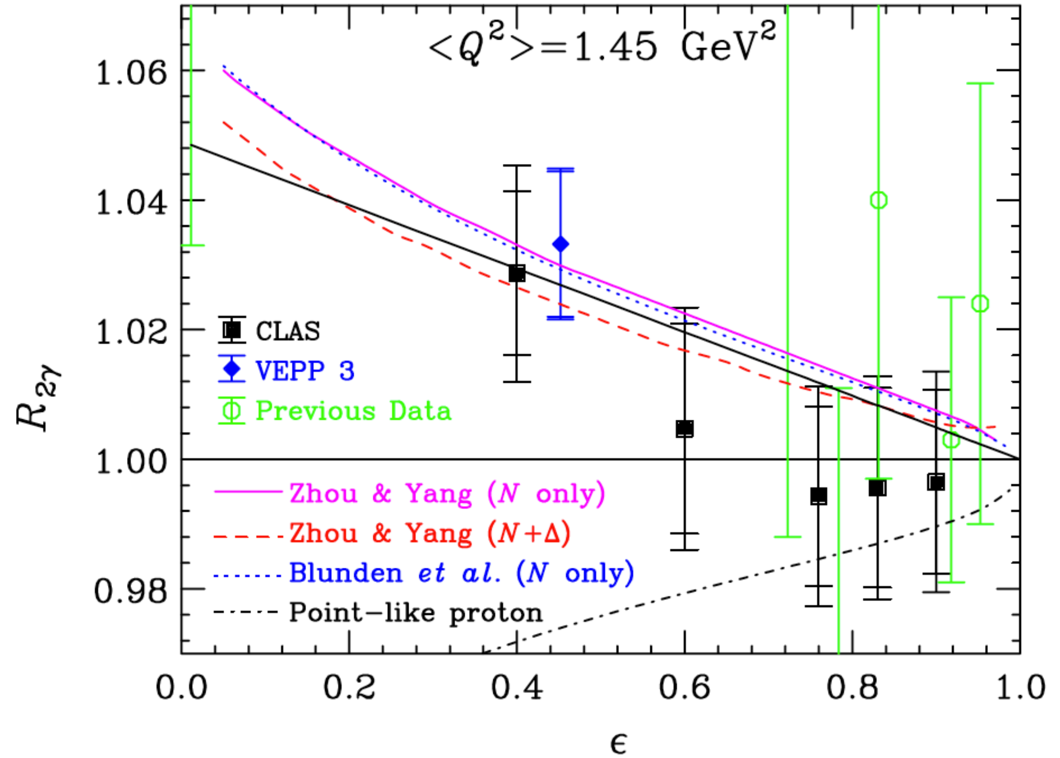

CLAS:
D. Rimal *et al.*, arXiv:1603.00315v1
D. Adikaram *et al.*, PRL 114, 062003 (2015)

VEPP-3:
I.A. Rachek *et al.*, PRL 114, 062005 (2015)

CLAS result consistent with "standard" TPE prescription
… however, limited precision

TPE experiments: CLAS (E04-116)

Q^2 dependence

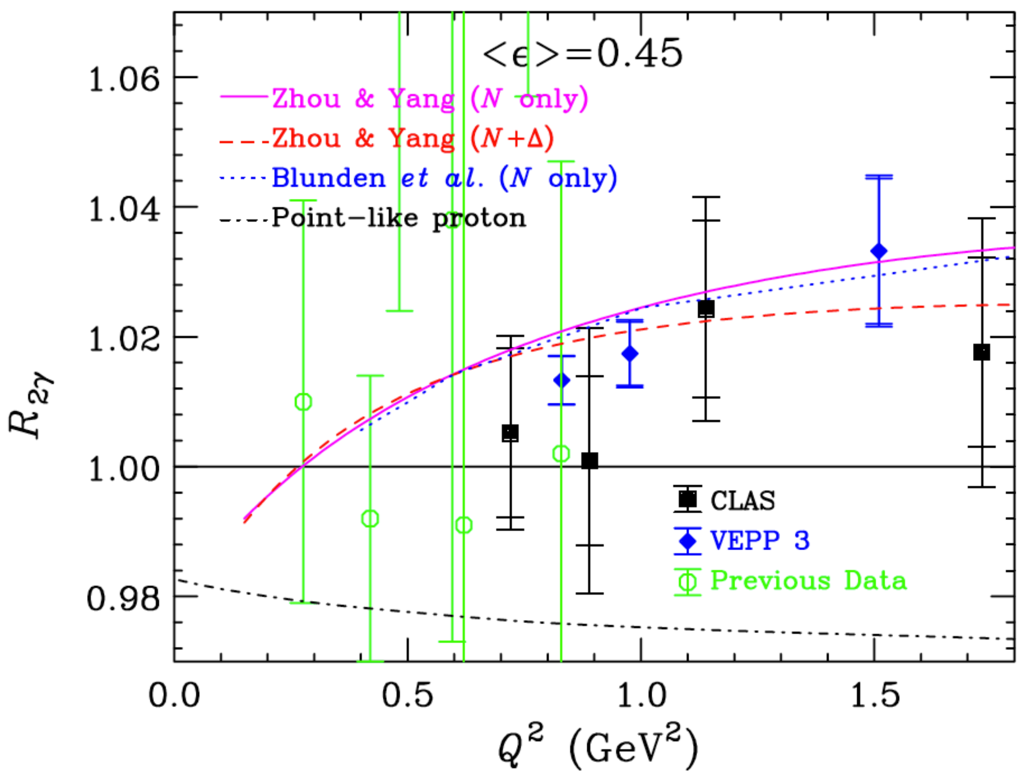

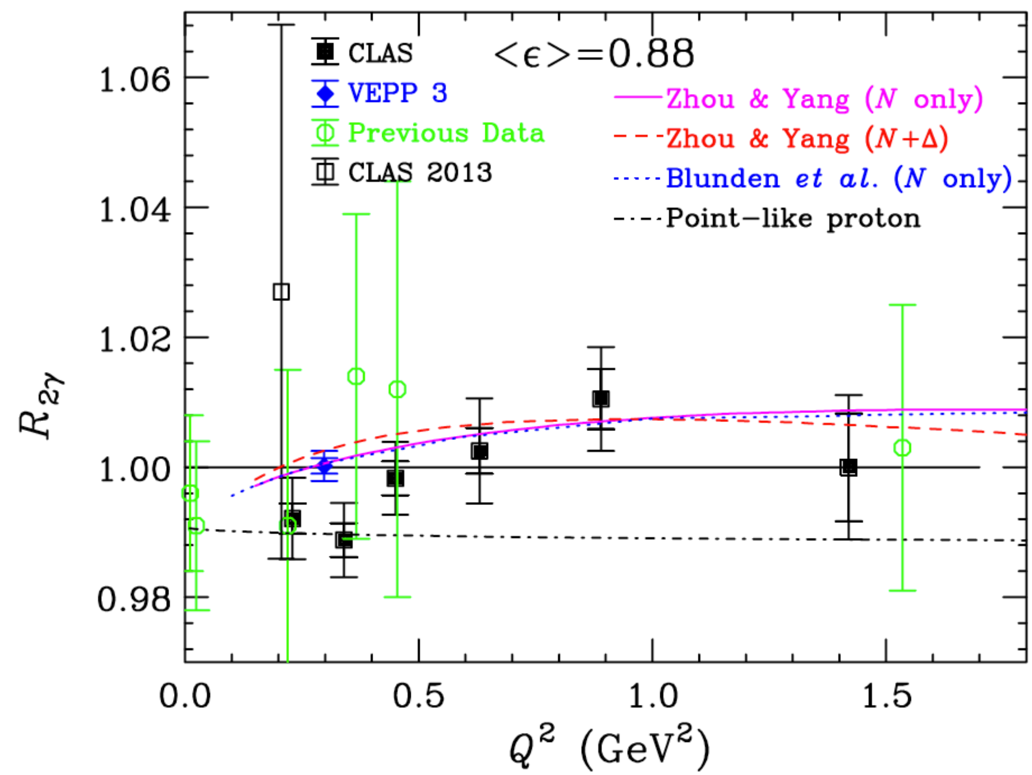

CLAS:
D. Rimal *et al.*, arXiv:1603.00315v1
D. Adikaram *et al.*, PRL 114, 062003 (2015)

VEPP-3:
I.A. Rachek *et al.*, PRL 114, 062005 (2015)

CLAS result consistent with "standard" TPE prescription
… however, limited precision

Projected results for OLYMPUS

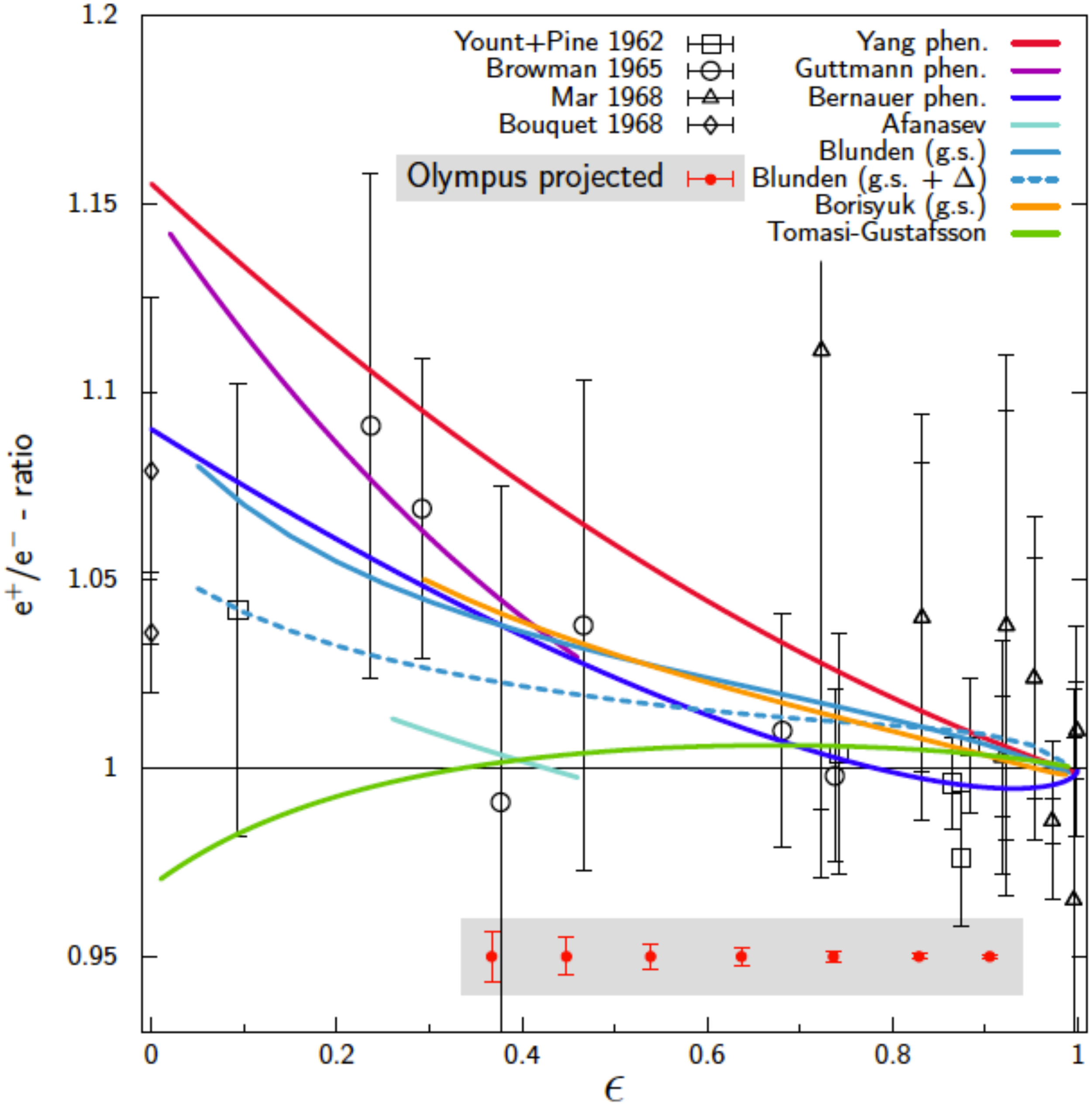

Data from 1960's

Many theoretical predictions with little constraint

OLYMPUS:

- **E= 2.0 GeV**
- **$0.4 < Q^2/(GeV/c)^2 < 2.2$**
- **Acquire 3.6 fb^{-1} for <1% projected uncertainties**

Data taking completed in 2012

OLYMPUS @ DORIS/DESY

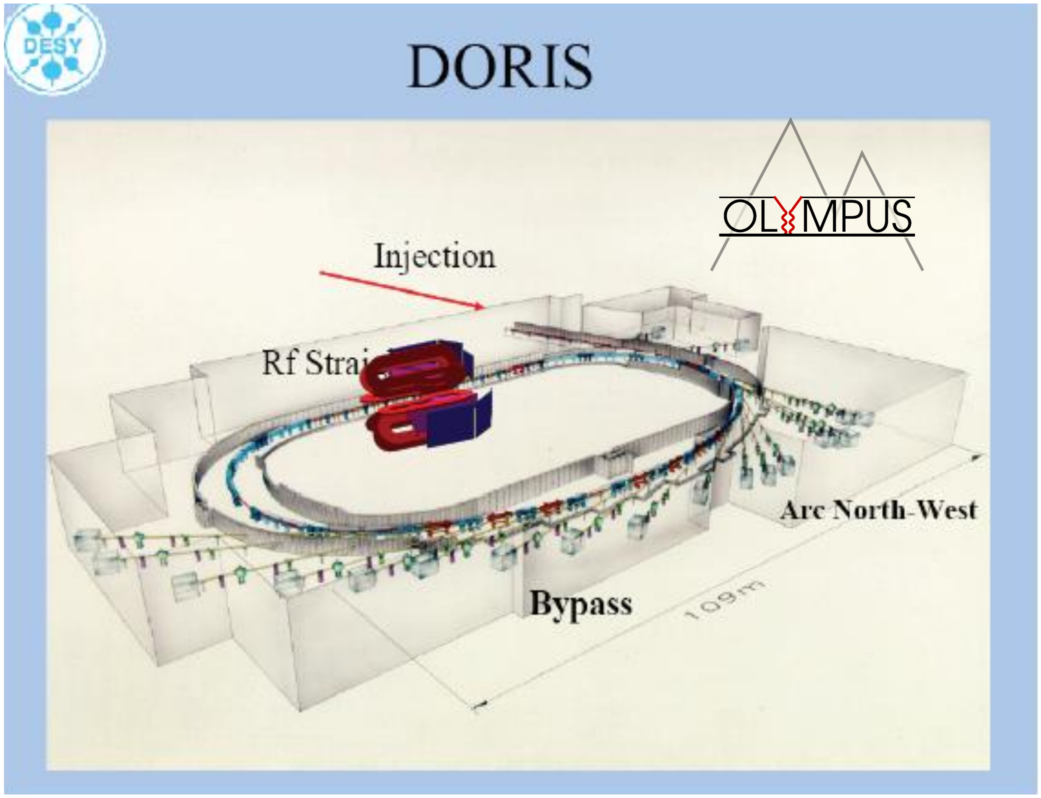

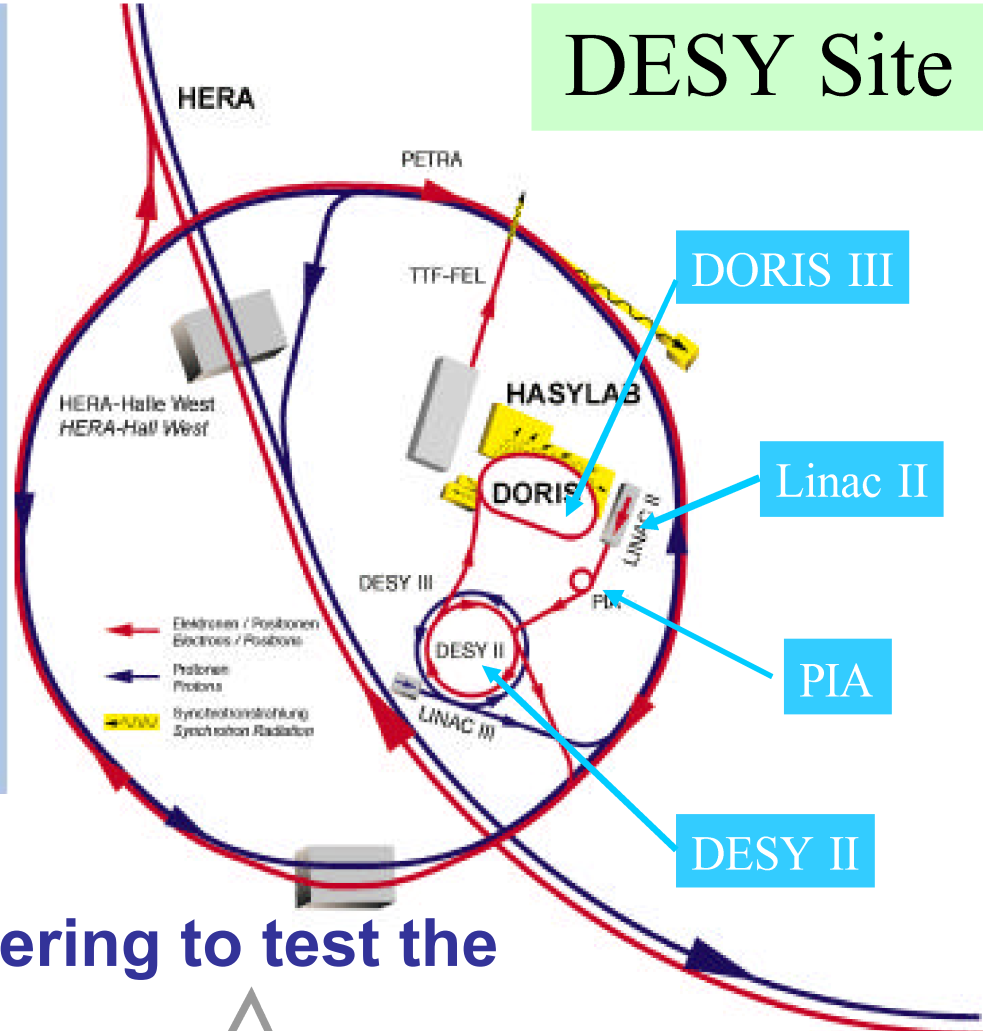

pOsitron-proton and
eLectron-proton elastic scattering to test the
hYpothesis of
Multi-
Photon exchange
Using
DoriS

The OLYMPUS experiment

- Electrons/positrons (100mA) in 2.0–4.5 GeV storage ring
  DORIS at DESY, Hamburg, Germany
- Unpolarized internal hydrogen target (buffer system)
  $3x10^{15}$ at/cm^2 @ 100 mA $\rightarrow$ L = $2x10^{33}$ / (cm^{2}s)
- Large acceptance detector for e-p in coincidence
  BLAST detector from MIT-Bates available
- Redundant monitoring of luminosity
  Pressure, temperature, flow, current measurements
  Small-angle elastic scattering at high epsilon / low Q^2
  Symmetric Moller/Bhabha scattering

- Measure ratio of positron-proton to electron-proton unpolarized elastic scattering to 1% stat.+sys.

OLYMPUS kinematics at 2.0 GeV

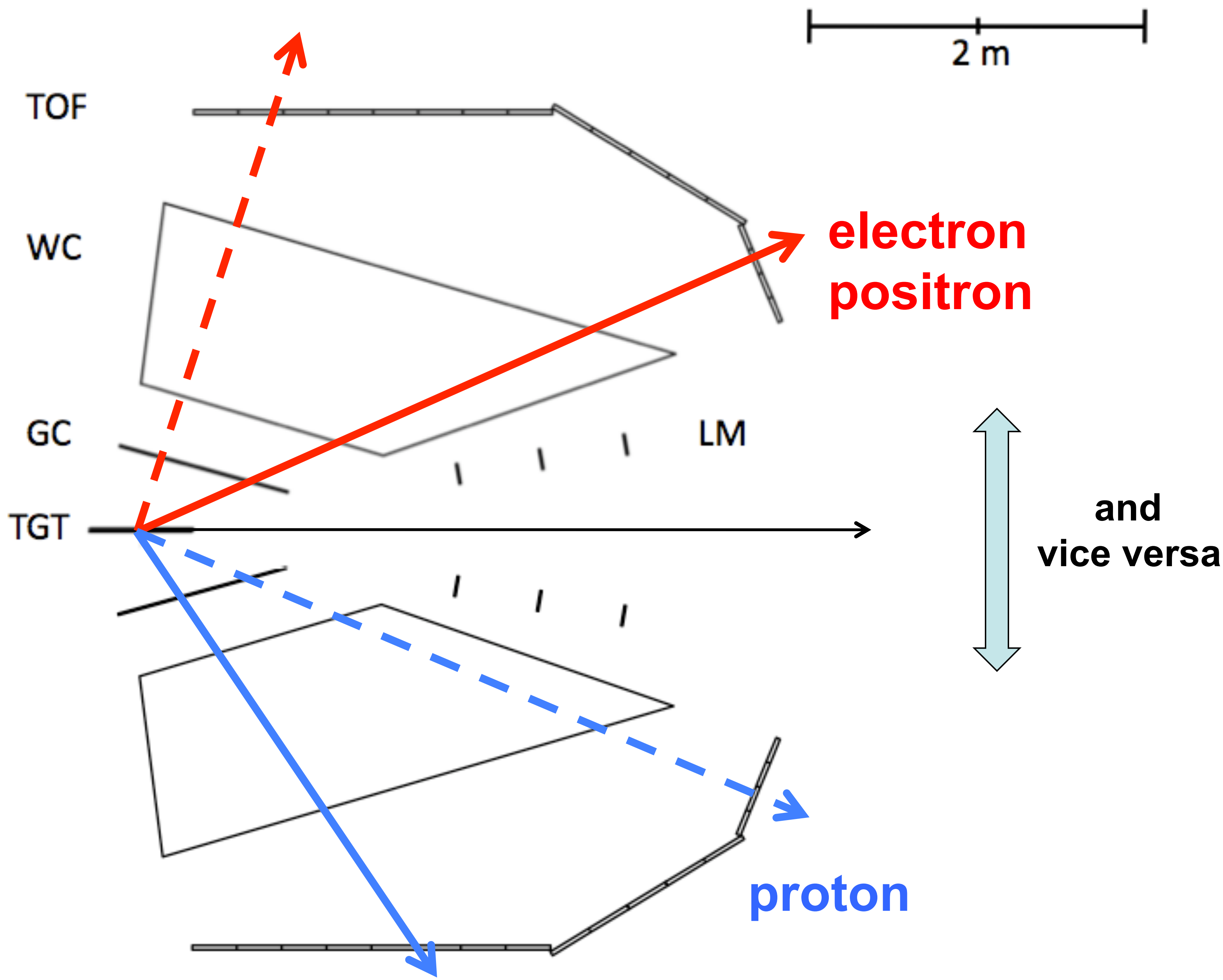

The designed OLYMPUS detector

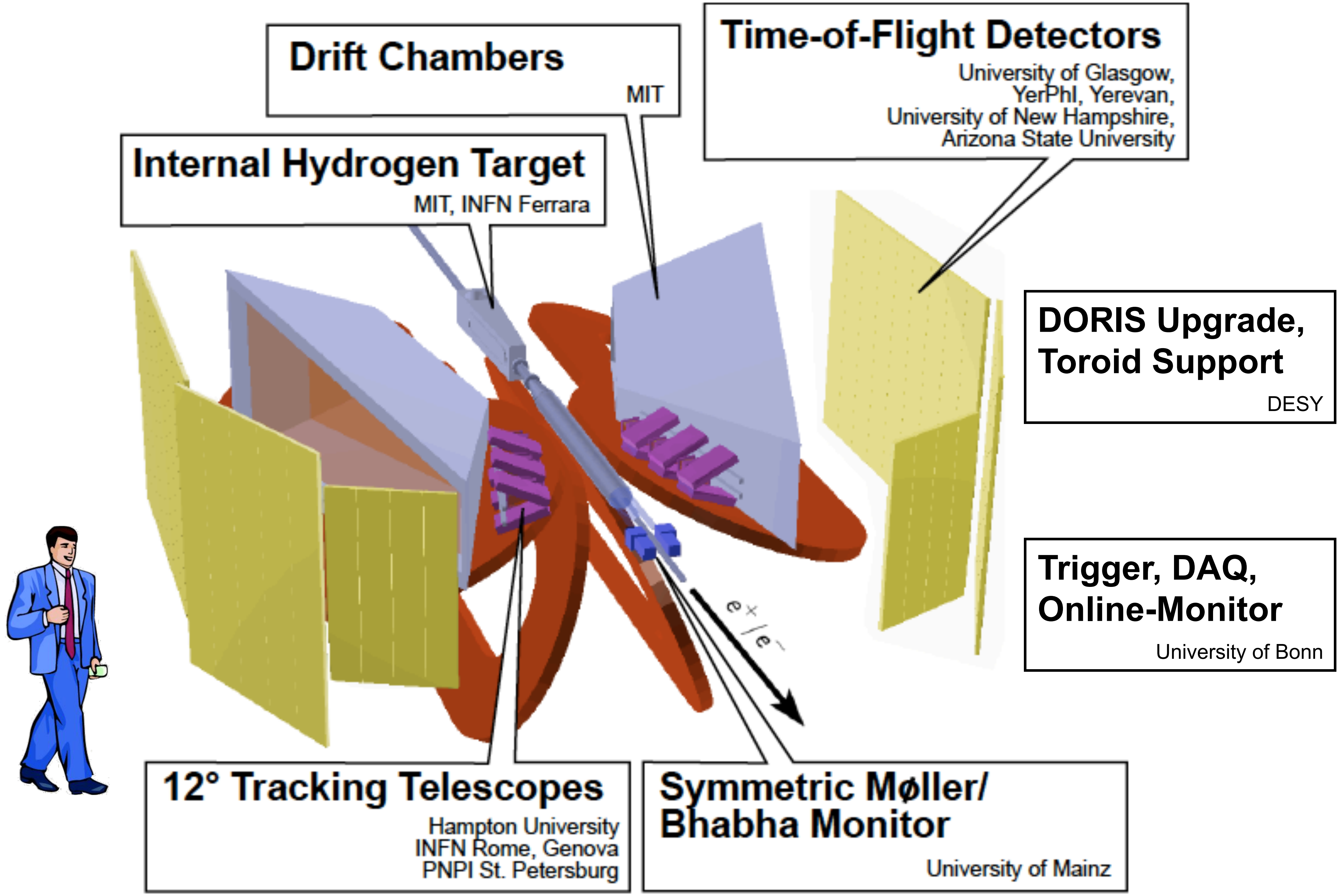

based on a figure by R. Russell

The realized OLYMPUS detector

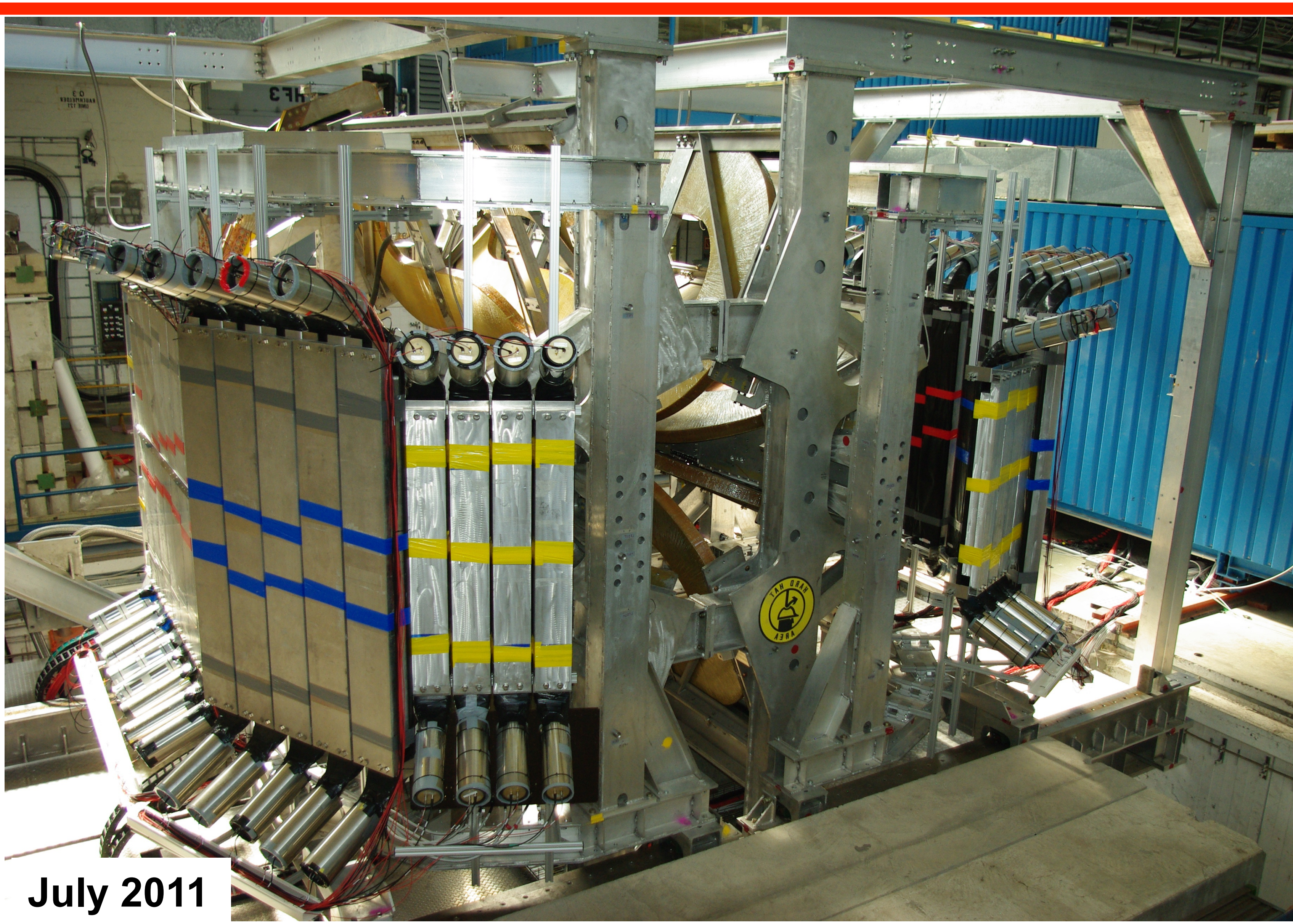

July 2011

"The OLYMPUS Experiment", R. Milner *et al*., NIMA 741, 1 (2014)

"Measurement and tricubic interpolation of the magnetic field for the OLYMPUS experiment", J. Bernauer *et al*., arXiv:1603.06510

Target and vacuum system

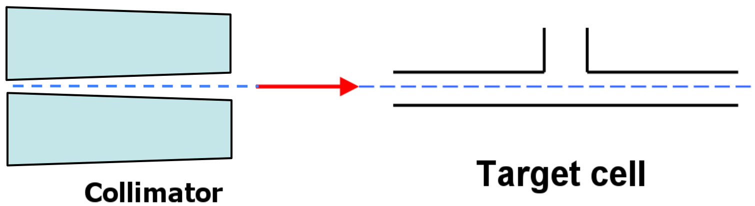

MIT
INFN Ferrara

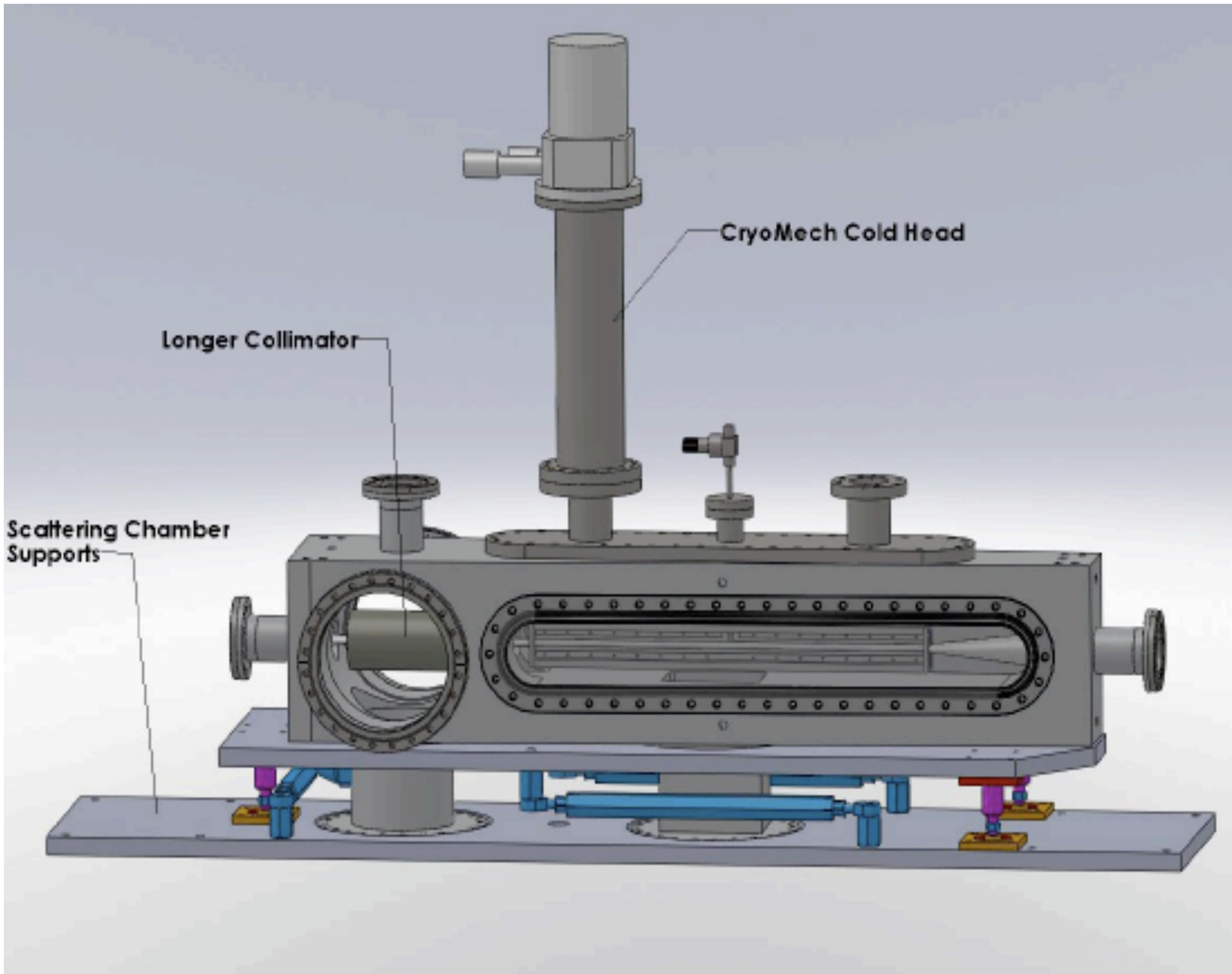

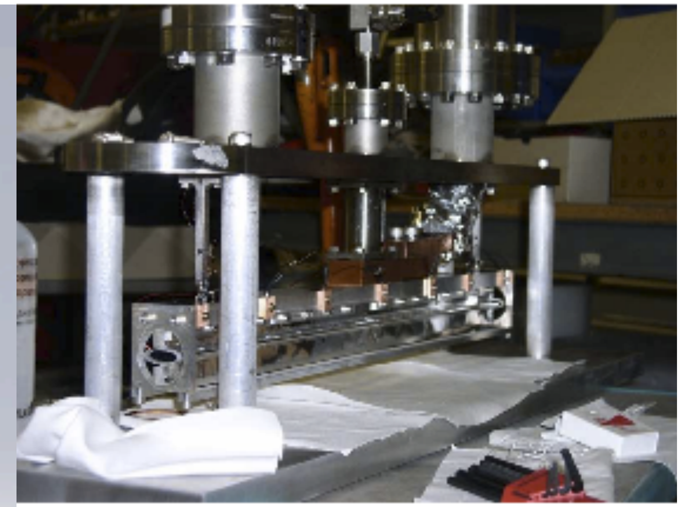

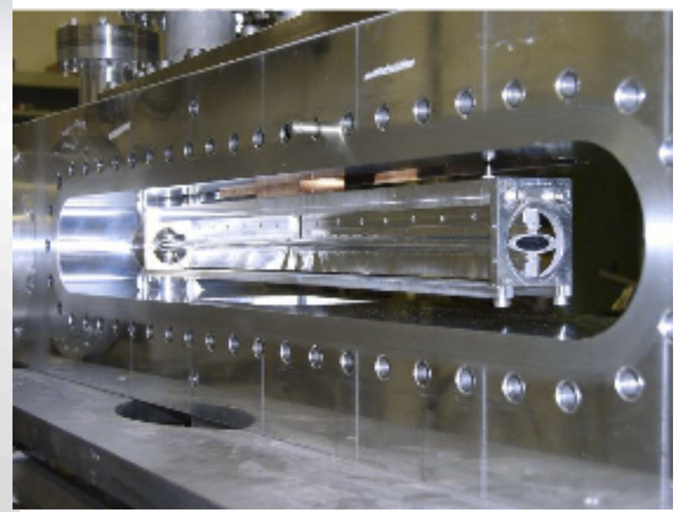

Designed and built in 2010
Very stable operation

"The OLYMPUS Internal Hydrogen Target", J.C. Bernauer *et al.*, NIMA 755, 20 (2014)

Timeline of OLYMPUS

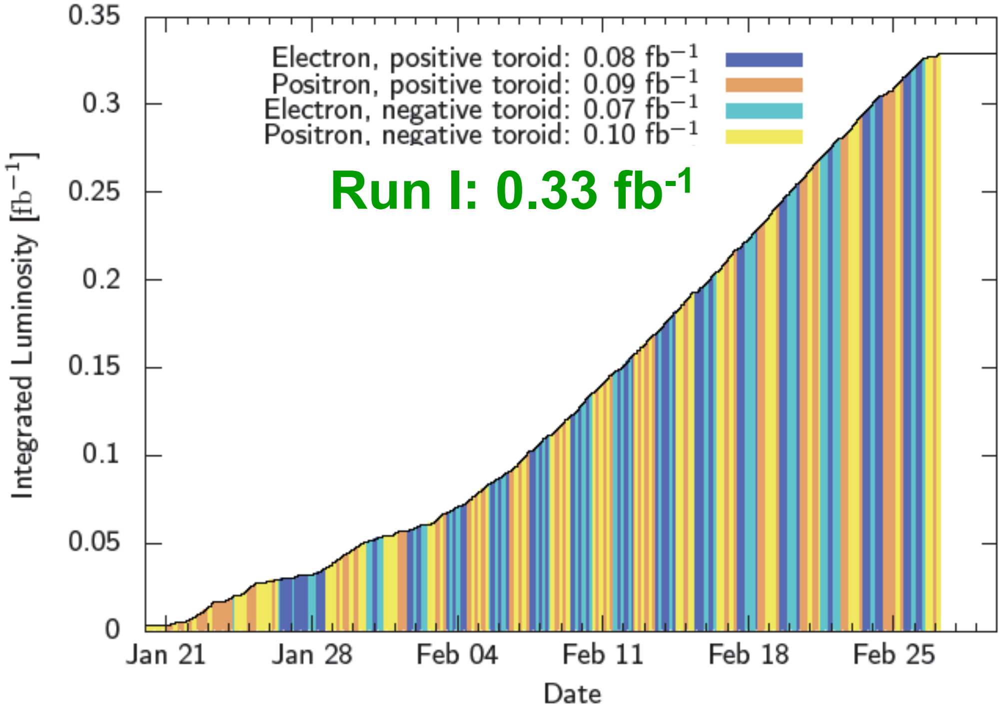

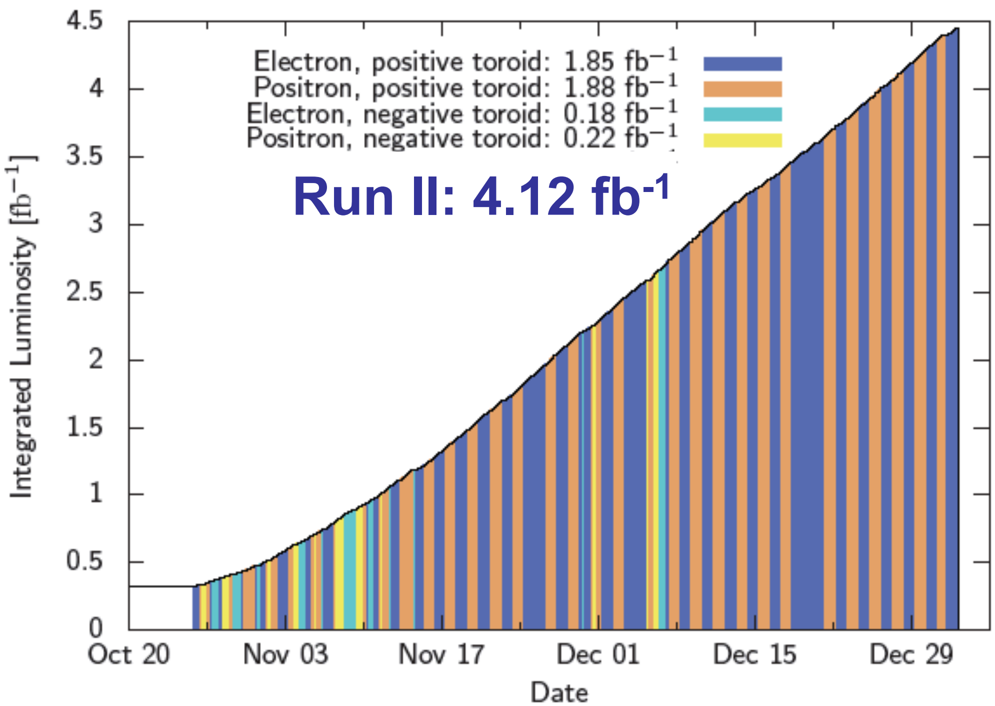

- 2007 Letter of Intent
- 2008 Proposal
- 2009 Technical review
- 2010 Approval and funding
- Summer 2010 BLAST transfer
- Spring 2011 Target test run
- Summer 2011 Detector installed
- Fall 2011 Commissioning

First run Jan 30 – Feb 27, 2012
… acquired < 0.3 fb^{-1}

- Summer 2012 Repairs and upgrades

Second run Oct 24, 2012 – Jan 2, 2013
… acquired > 4.0 fb^{-1}

- Smooth performance of machine, target, detector
- Spring 2013 Survey & field mapping
- Analysis progressing – framework, calibrations, tracking, simulations
- **Expect results by summer 2016**

Analysis framework

ROOT based C++ analysis framework ("cooker")
with plug-ins and recipes **(J. Bernauer)**
and full MC integration

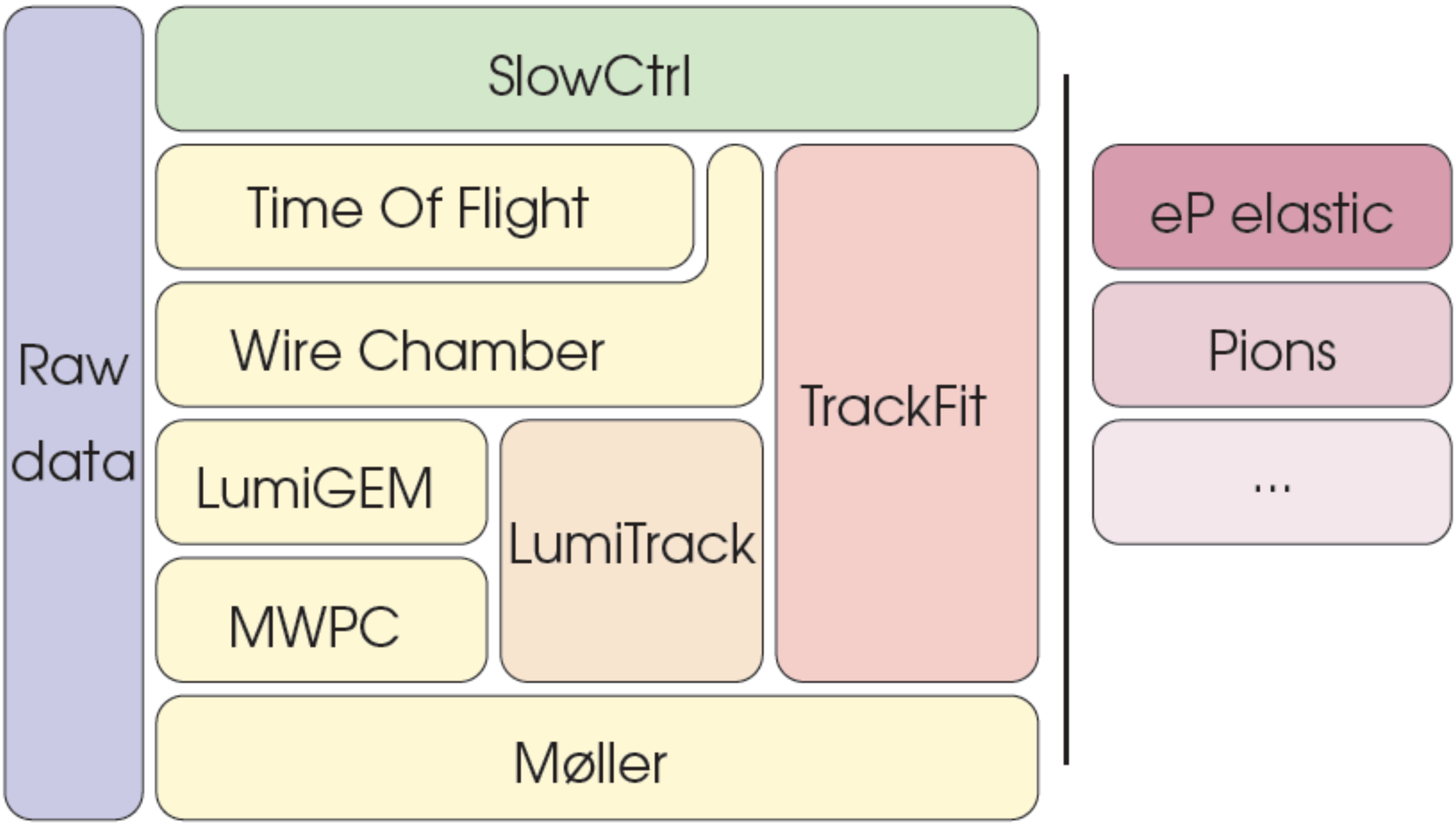

Radiative corrections of order α^3

- **Use MC framework to accurately implement all 'standard' RC and to extract effect from hard TPE**
- **Ensure consistency between different experiments**

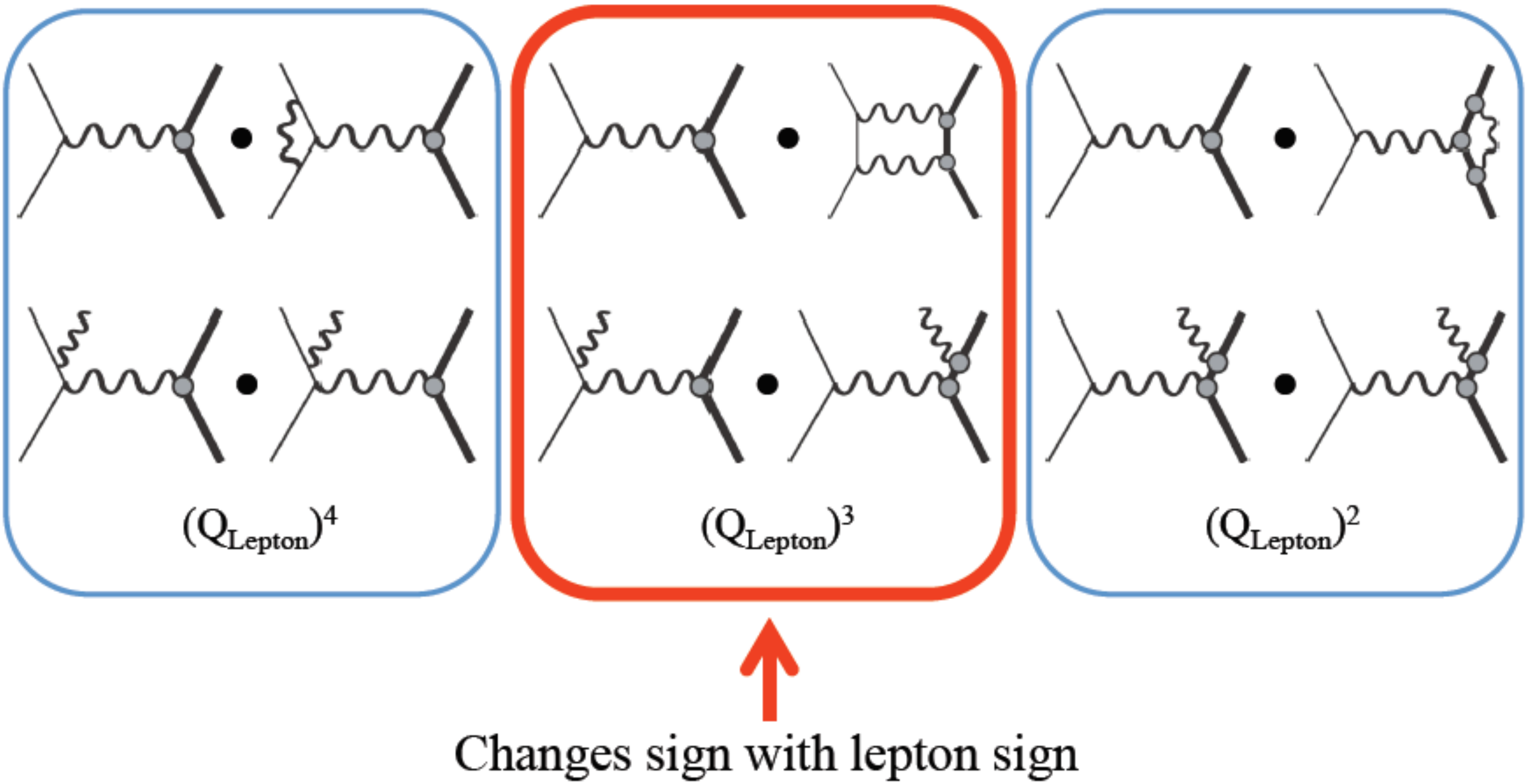

A. Schmidt, R. Russell, J. Bernauer (MIT)

MIT radiative generator

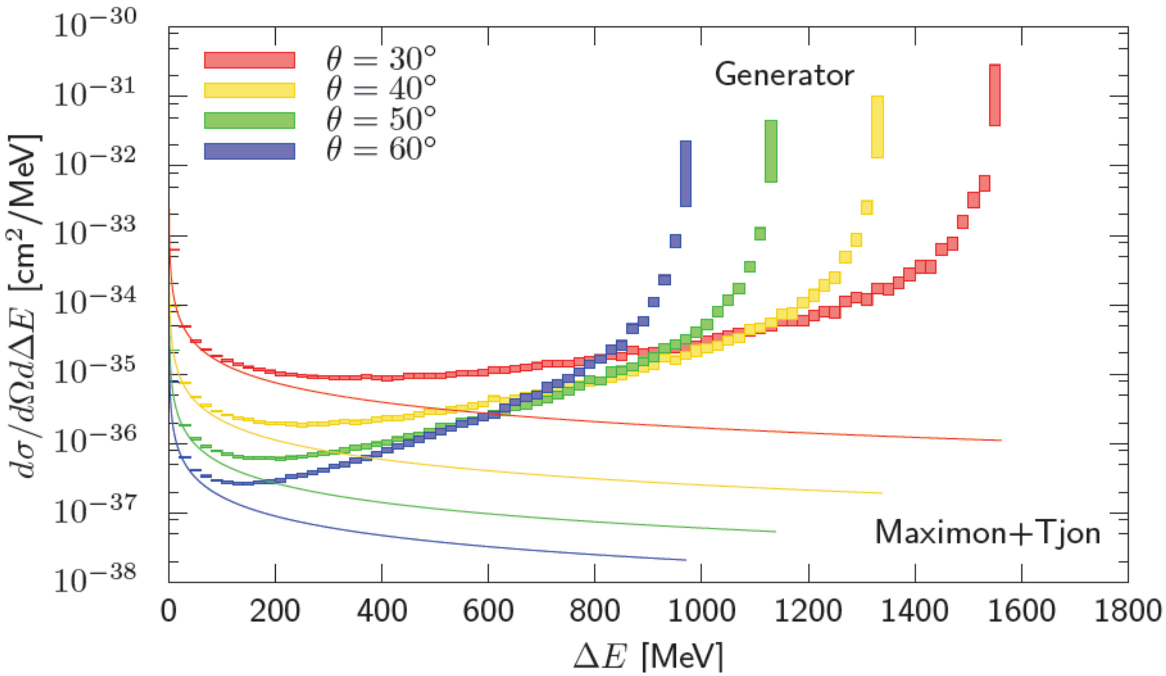

- Avoids approximations
- Agreement with Maximon&Tjon (soft photons) at low ΔE
- Excellent agreement with VEPP-3 generator

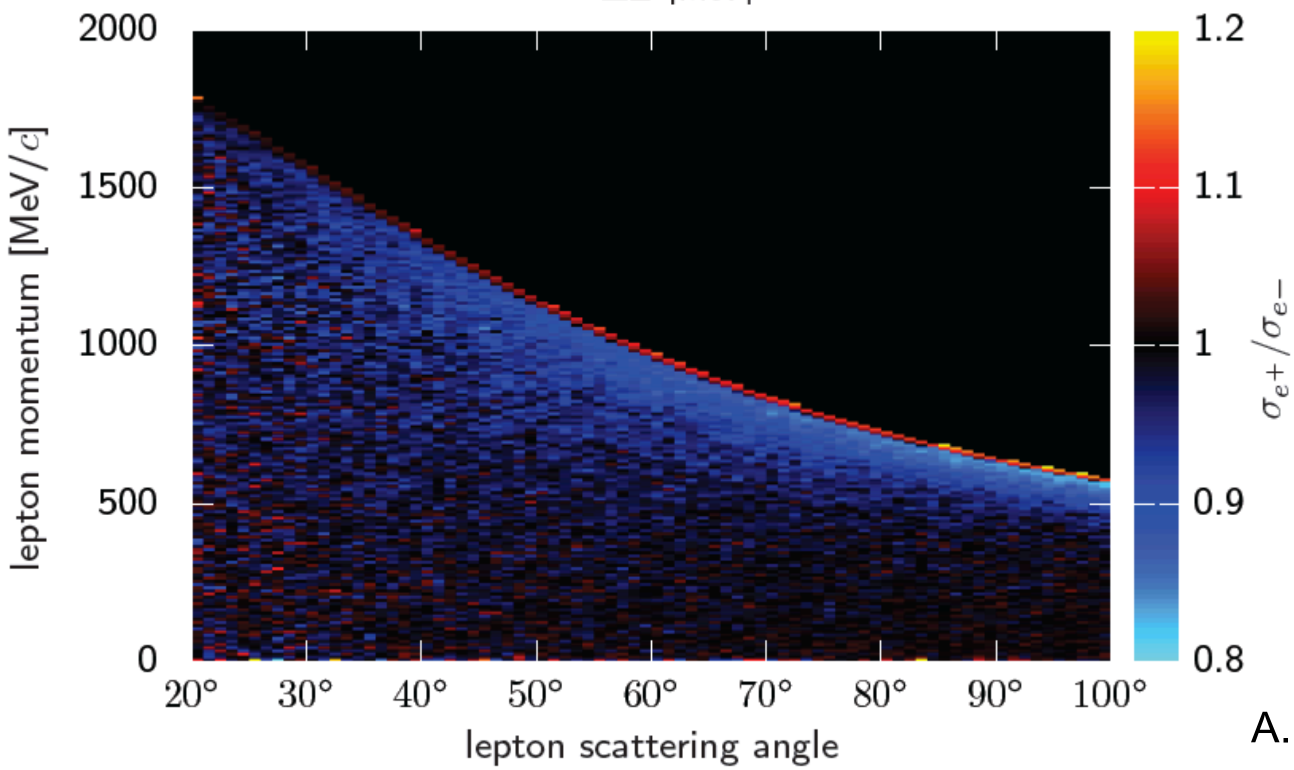

Effect on σ_{e+}/σ_{e-}

A. Schmidt, R. Russell, J. Bernauer (MIT)

MIT radiative generator

Baseline: Dipole F. F., Maximon Tjon rad. corrections

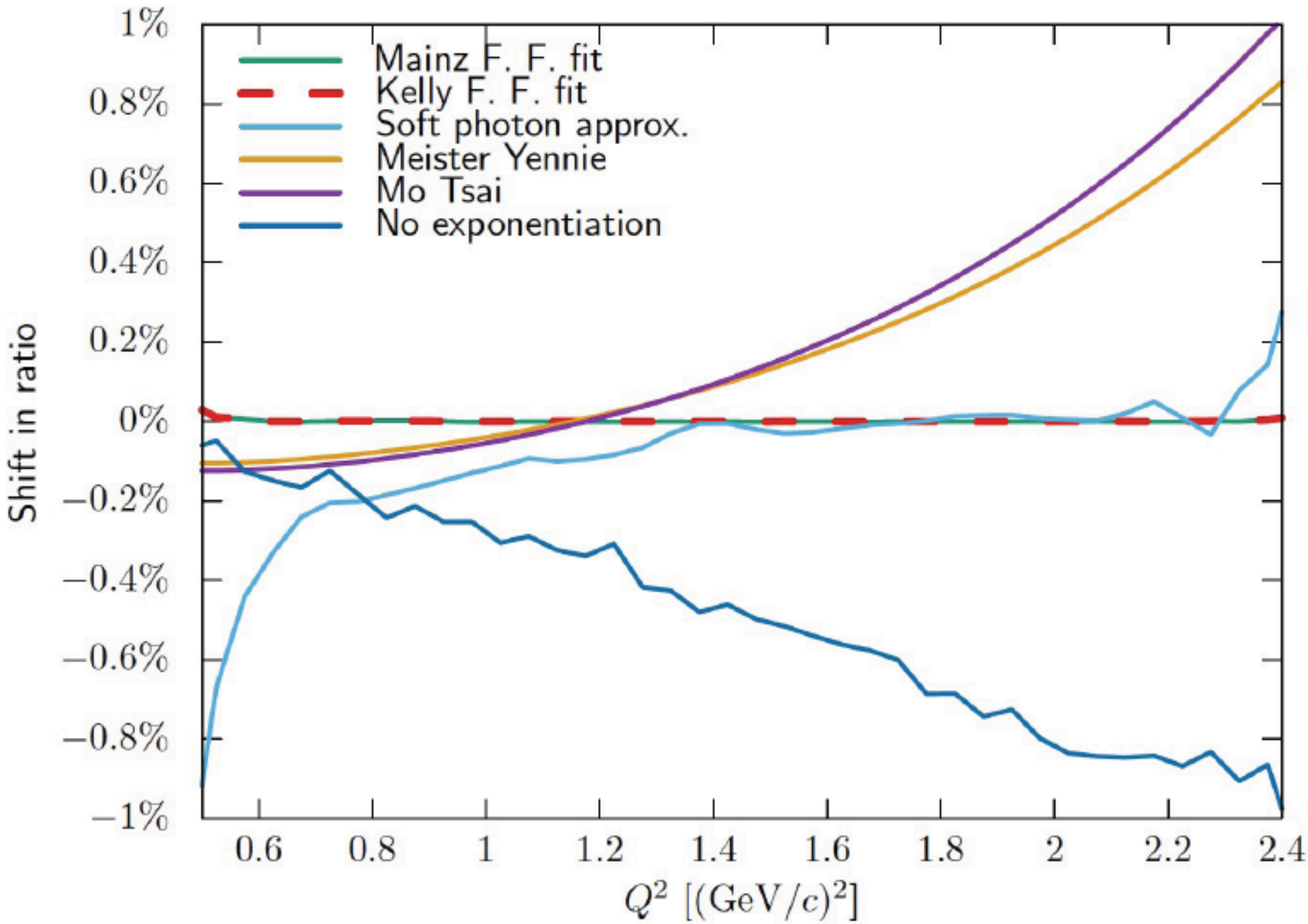

A. Schmidt, R. Russell, J. Bernauer (MIT)

Event selection

Based on 100 runs (~2% of the data)

Electron beam

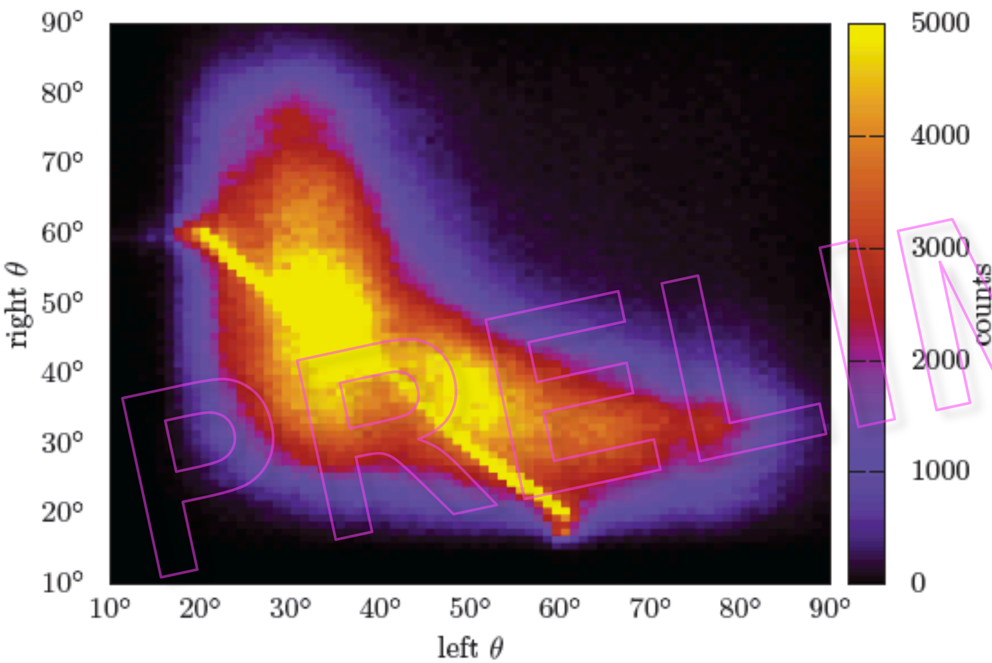

Positron beam

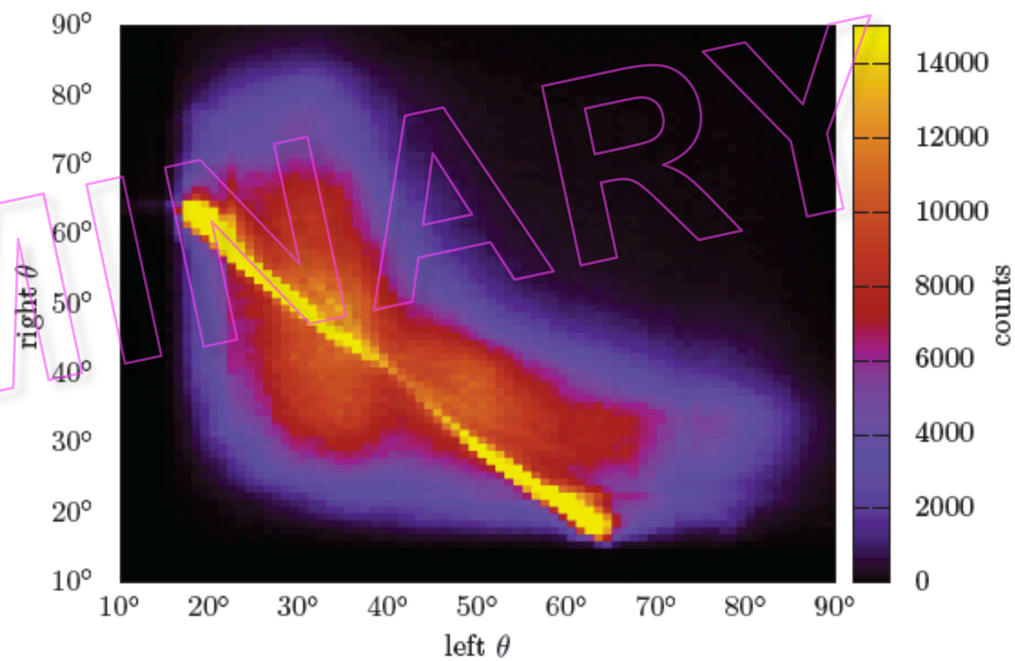

Polar angle in the right sector versus polar angle in left sector

Event selection

Based on 100 runs (~2% of the data)

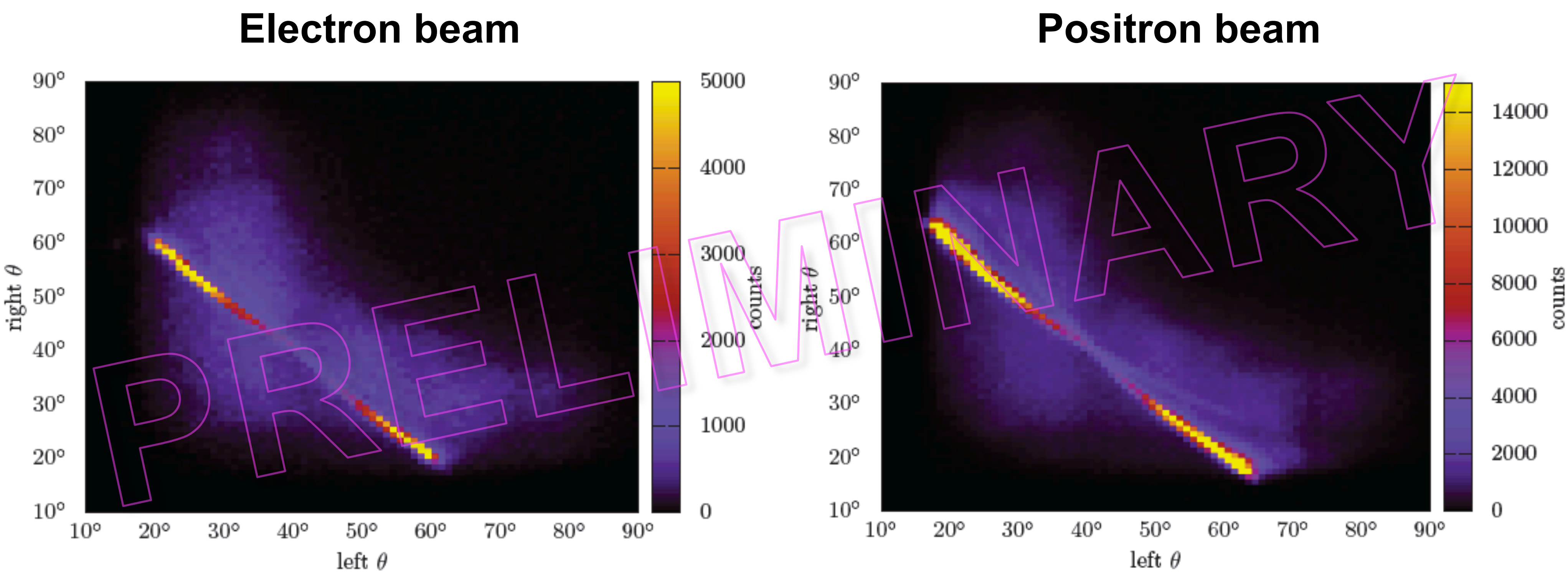

Polar angle in the right sector versus polar angle in left sector
Coplanarity cut ±5 degrees

A. Schmidt (MIT)

Event selection

Based on 100 runs (~2% of the data)

Electron beam

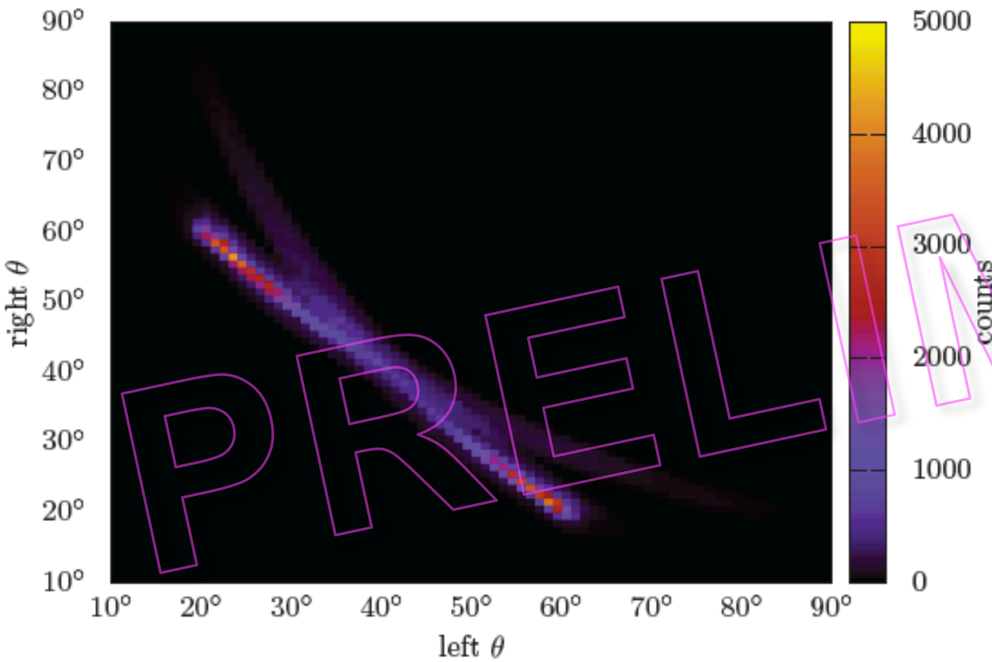

Positron beam

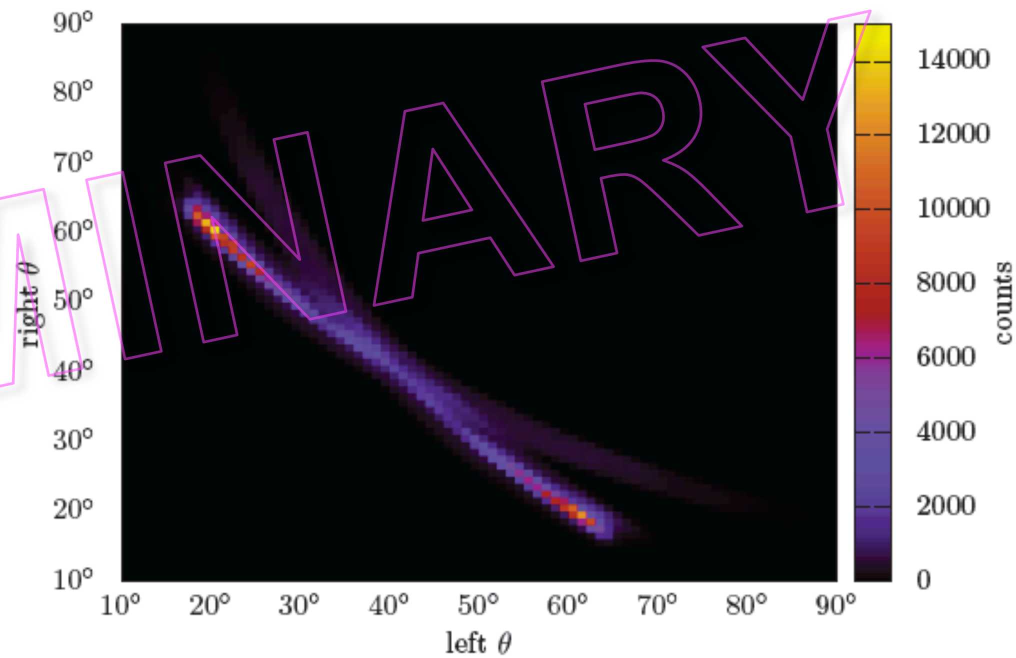

Polar angle in the right sector versus polar angle in left sector
Coplanarity cut ±5 degrees
Common vertex ±100 mm

Event selection

Based on 100 runs (~2% of the data)

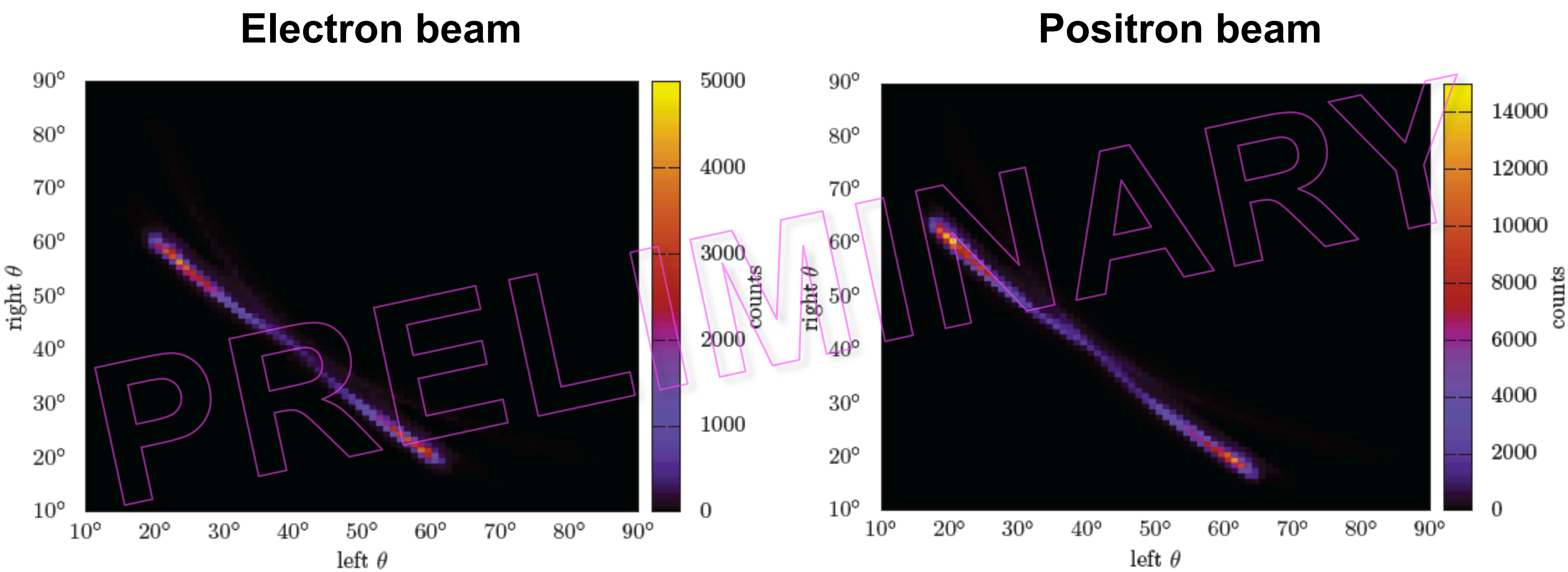

Polar angle in the right sector versus polar angle in left sector

Coplanarity cut ±5 degrees

Common vertex ±100 mm

Polar angle kinematic cut $|\theta_l - \theta_l(\theta_p)| < 5$ degrees

A. Schmidt (MIT)

Event selection

Based on 100 runs (~2% of the data)

Electron beam

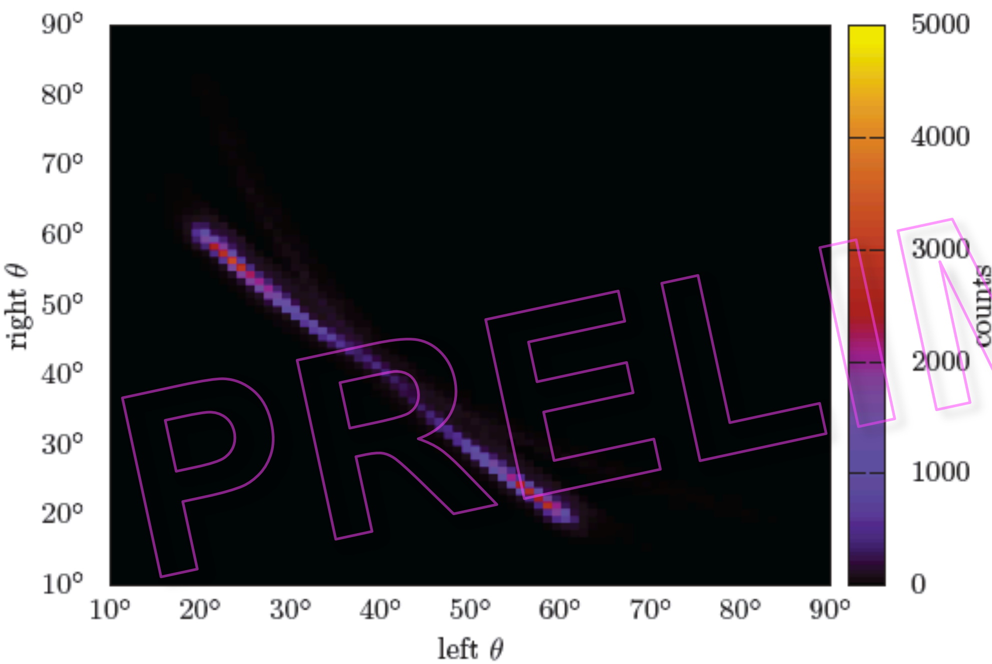

Positron beam

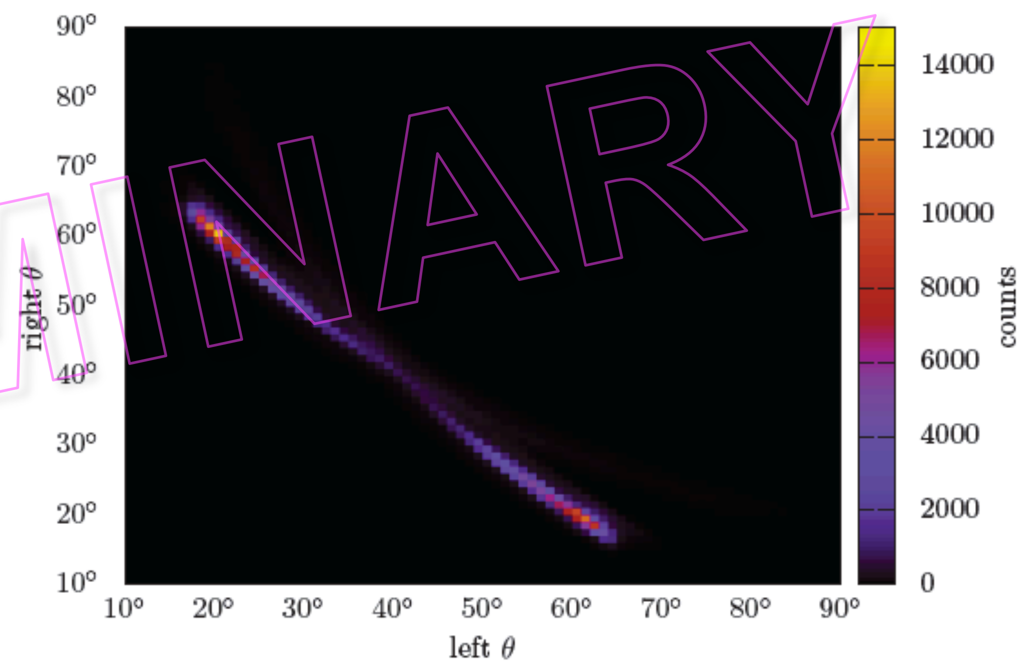

Polar angle in the right sector versus polar angle in left sector
Coplanarity cut ±5 degrees
Common vertex ±100 mm
Polar angle kinematic cut $|\theta_l - \theta_l(\theta_p)| < 5$ degrees
Momentum kinematic cut $|P_p - P_p(\theta_p)| < 400$ MeV/c

Toward final results

Data blinded

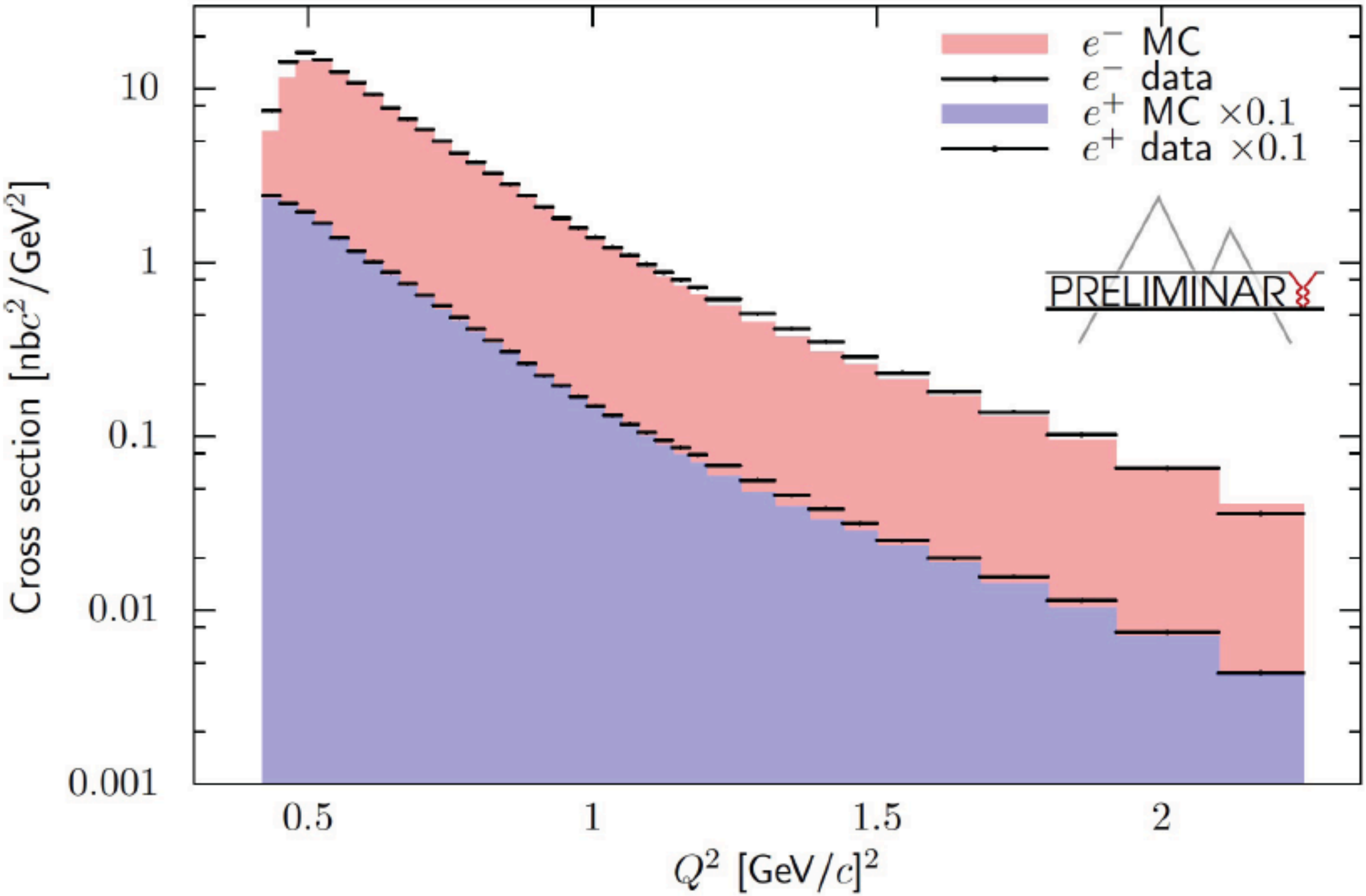

A. Schmidt (MIT)

OLYMPUS collaboration

~50 physicists from 13 institutions in 6 countries

Elected spokesmen / deputy:	**R. Milner / R. Beck**	**(2009–2011)**
	M.K. / A. Winnebeck	**(2011–2013)**
	D. Hasell / U. Schneekloth	**(2013–)**

- **Arizona State University:** TOF support, particle identification, magnetic shielding
- **DESY:** Modifications to DORIS accelerator and beamline, toroid support, infrastructure, installation
- **Hampton University:** GEM luminosity monitor
- **INFN Bari:** GEM electronics
- **INFN Ferrara:** Target
- **INFN Rome:** GEM electronics
- **MIT:** BLAST spectrometer, wire chambers, tracking upgrade, target and vacuum system, transportation to DESY, simulations, slow control, analysis framework
- **Petersburg Nuclear Physics Institute:** MWPC luminosity monitor
- **University of Bonn:** Trigger, data acquisition, and online monitor
- **University of Mainz:** Trigger, DAQ, Symmetric Moller monitor
- **University of Glasgow**: TOF scintillators
- **University of New Hampshire:** TOF scintillators
- **A. Alikhanyan National Laboratory (AANL), Yerevan:** TOF scintillators

Global analysis

Fit to unpolarized data

Fit including polarized data + TPE parameterization

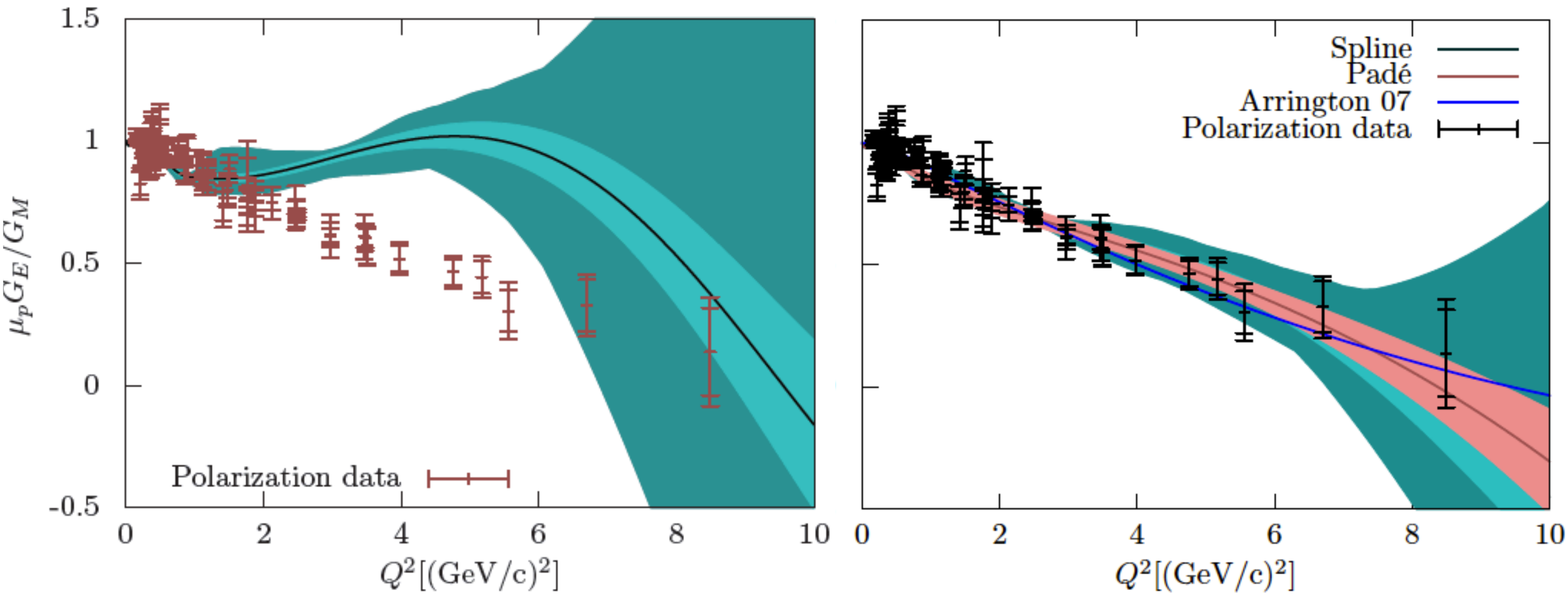

J.C. Bernauer *et al.*, PRC 90 (2014) 015206 [arXiv:1307.6227v2]

Summary and outlook

- The limits of OPE have been reached with the achieved precision
  - ➔ Large discrepancy between unpolarized and polarized data
  - ➔ Nucleon elastic form factors, particularly G_E^p under doubt

- The TPE hypothesis is suited to remove form factor discrepancy, however calculations of TPE are model-dependent

- Observables: ε dependence of polarization transfer, ε-nonlinearity of cross sections, single-spin asymmetries, e^+/e^- comparisons

- Positron/electron comparisons for a definitive test of TPE: VEPP-3, CLAS, OLYMPUS

- Broader Impact:
  - ➔ gamma-Z box in PVES; TPE effects in eA and inelastic scattering;
  - ➔ Proton radius puzzle: Size of TPE could be different for μp and ep, will be tested with MUSE@PSI (elastic $\{\mu,e\}^{\pm}p$ scattering)

- A comprehensive and rich program underway, expected to be conclusive in the near future

Backup

Wire chambers and TOF scintillators

- 2x18 TOFs for PID, timing and trigger
- 2 WCs for PID and tracking (z,θ,φ,p)
- WC and TOF refurbished from BLAST
  WC re-wired at DESY
  TOF rewrapped, efficiency tested
- Installed in OLYMPUS Apr-May 2011
- Stable operation

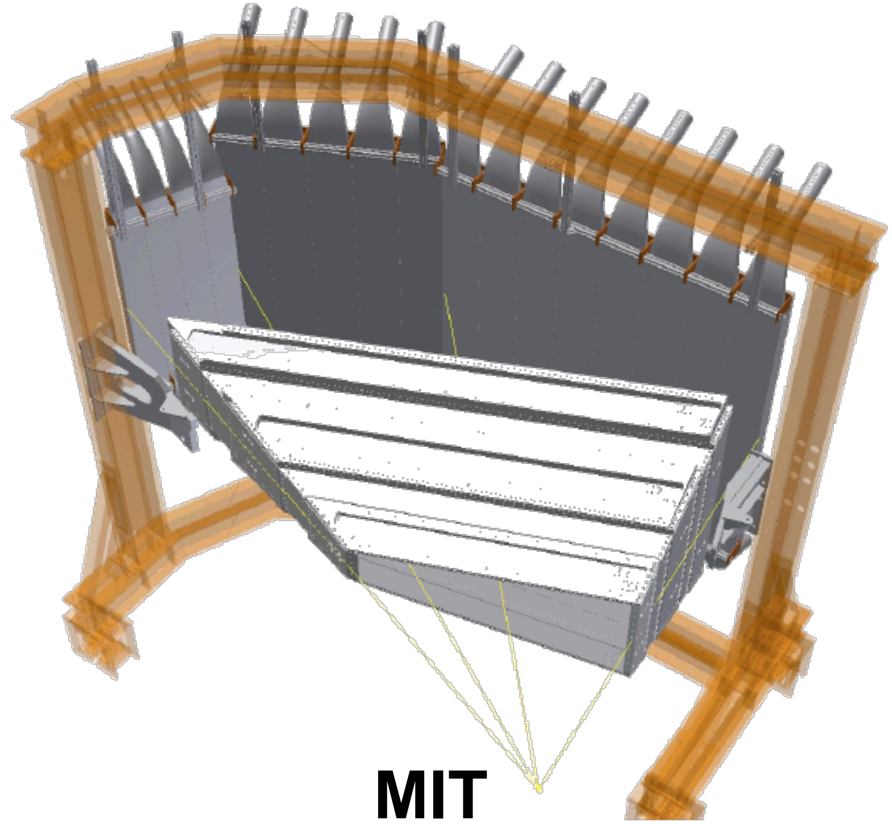

Glasgow, Yerevan, UNH, ASU

MIT

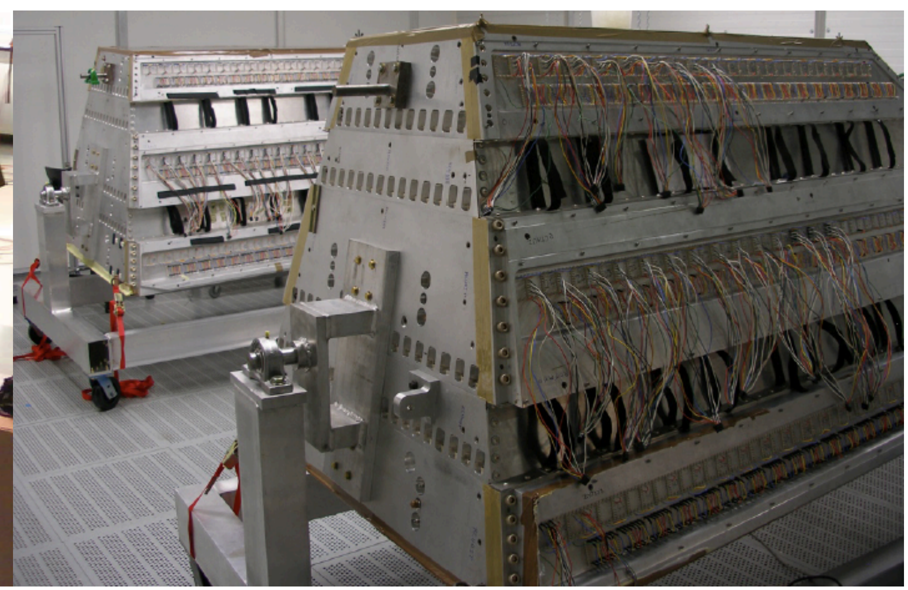

Luminosity monitors: GEM + MWPC

- Forward elastic scattering of lepton at 12°
  in coincidence with proton in main detector
- Two GEM + MWPC telescopes with
  interleaved elements operated independently
- SiPM scintillators for triggering and timing
- Sub-percent (relative) luminosity measurement
  per hour at 2.0 GeV
- High redundancy – alignment, efficiency
  Two independent groups (Hampton/INFN, PNPI)

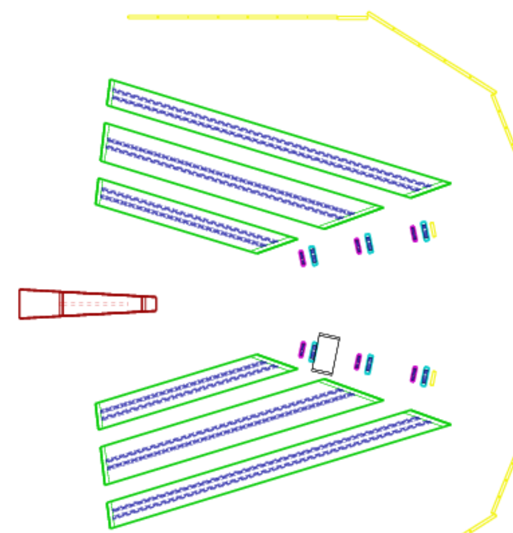

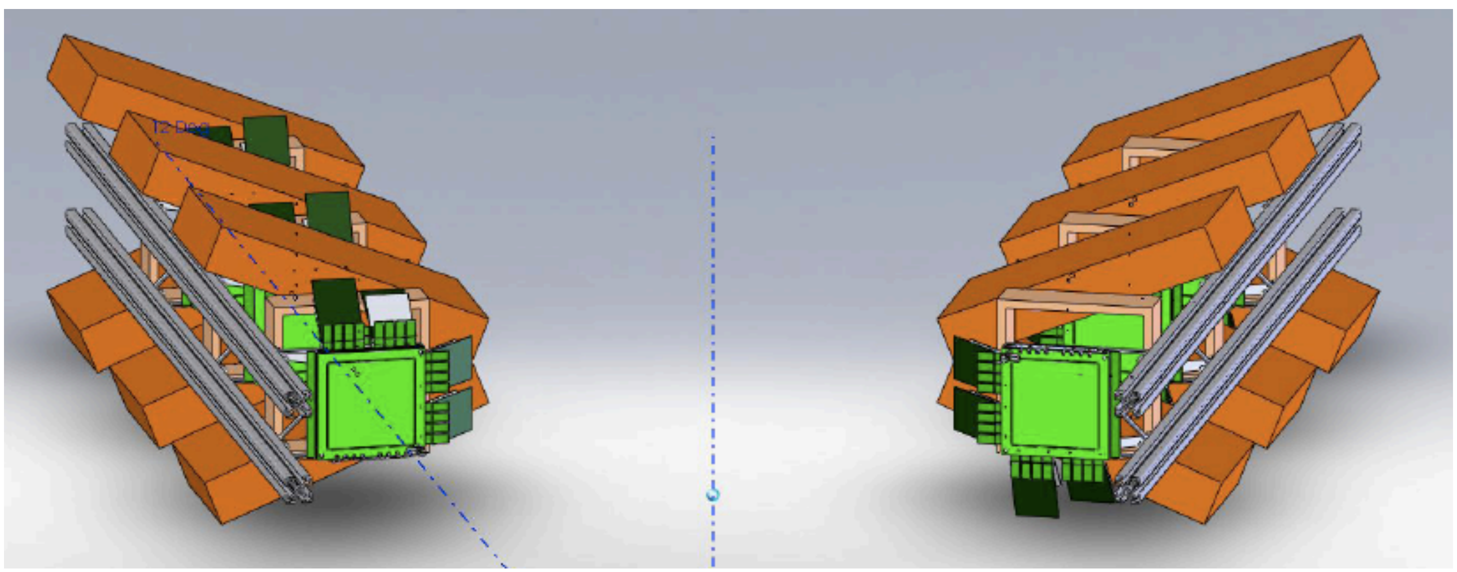

Designed to fit into forward cone

Luminosity monitors: GEM + MWPC

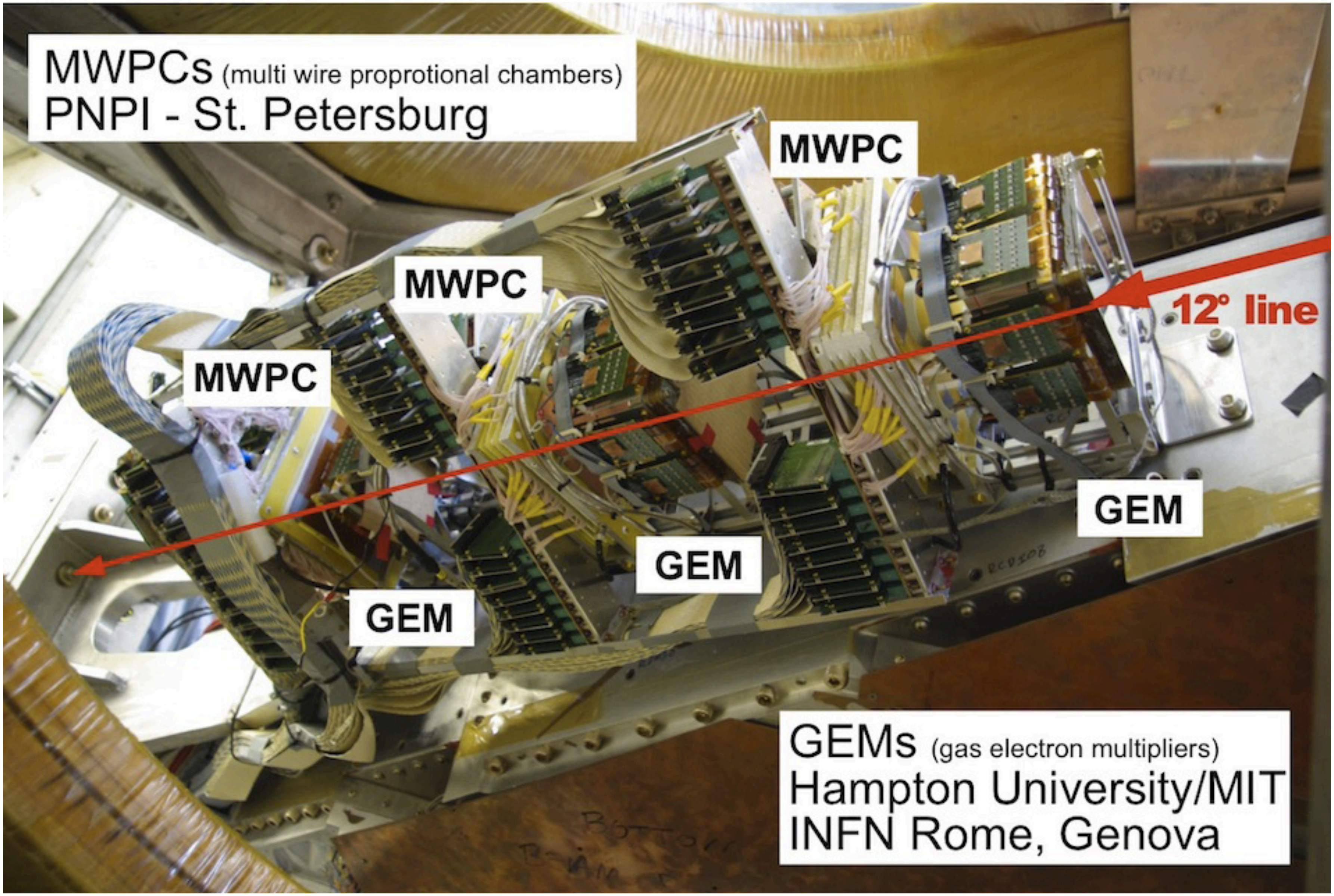

Telescopes of three GEMs and MWPCs interleaved
Mounted on wire chamber forward end plate
Extensively tested at DESY test beam facility

Symmetric Møller/Bhabha monitor

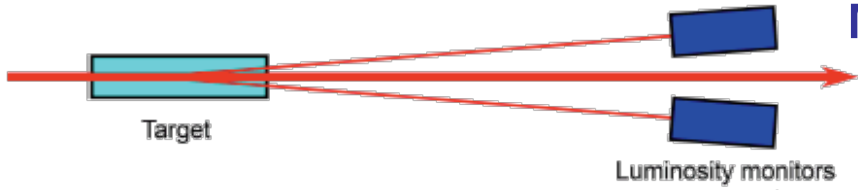

Mainz University

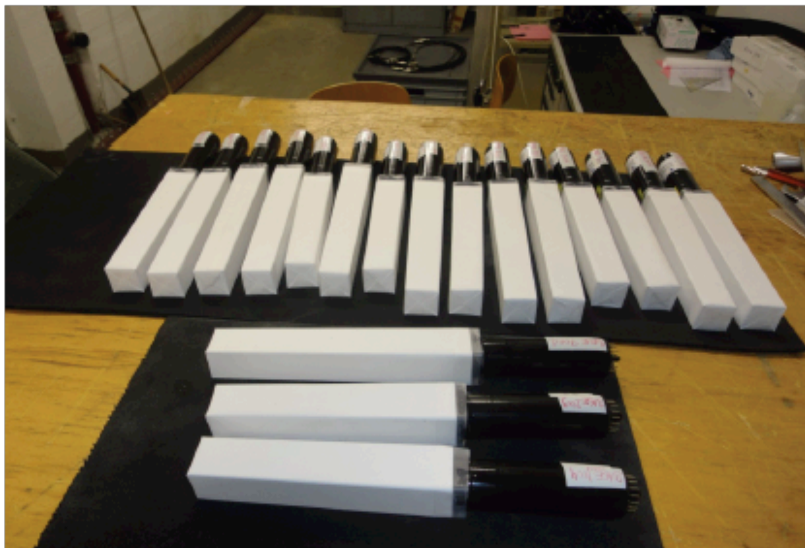

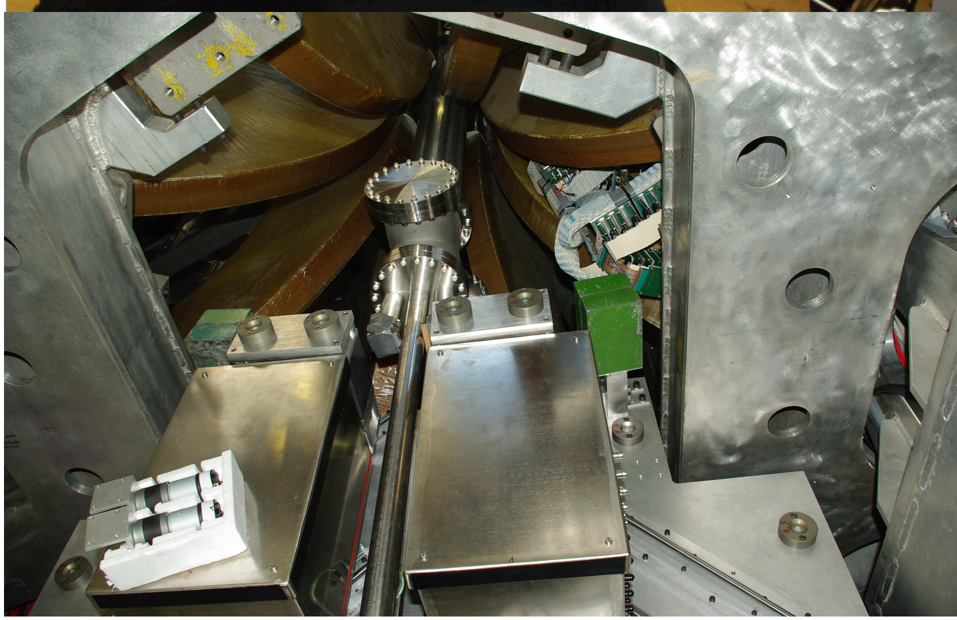

- Symm. angle 1.3^o @ 2.0 GeV
- Matrix of 3x3 PbF_2 crystals
- Tested at DESY and MAMI

Event display (3D)

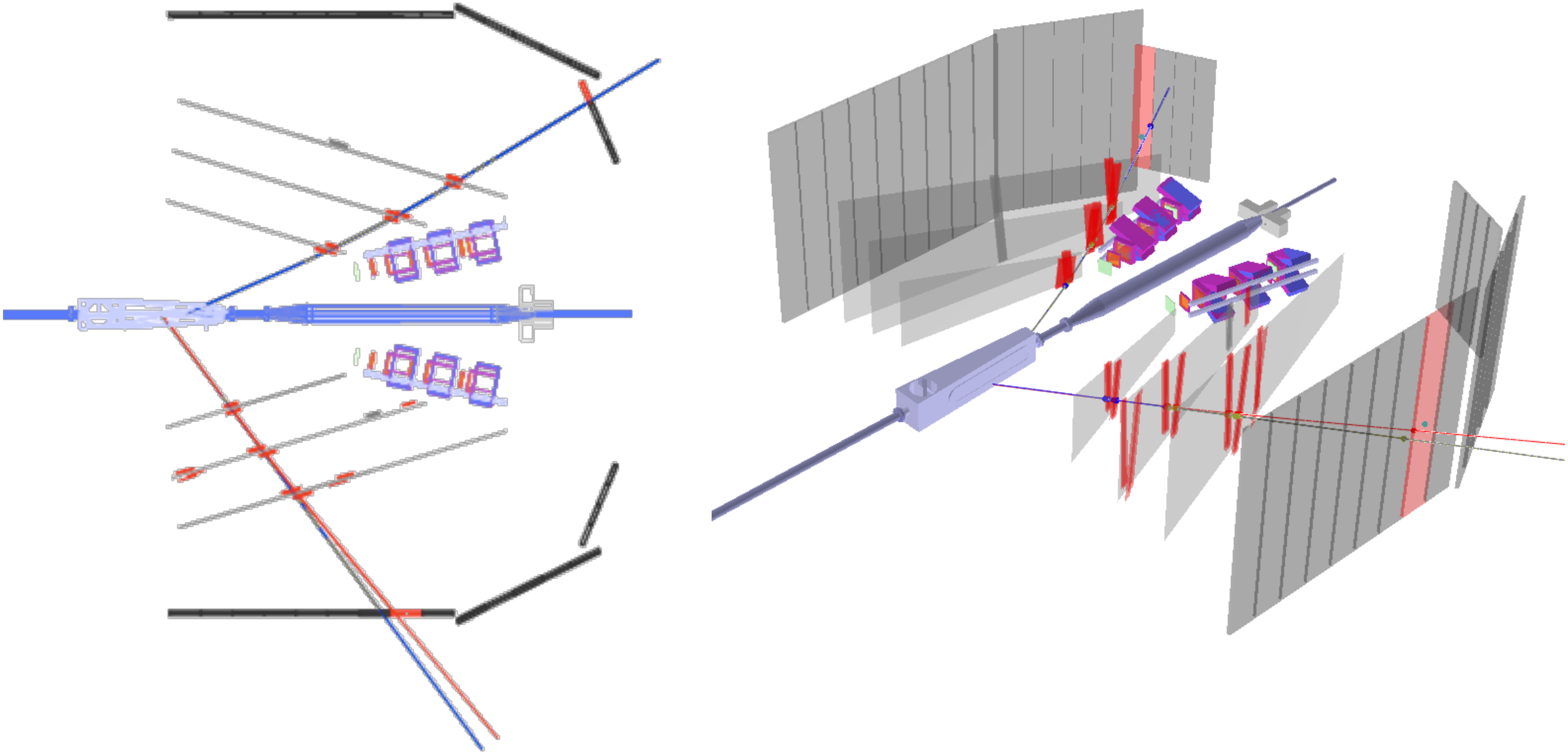

Run 4975, event 78

C. O'Connor (MIT)

Performance of DORIS

- DORIS top-up mode established
- Typically 65mA / 0.5 sccm
- Refills every ~2 minutes by few mA
- PETRA refills every 30 minutes